(2)

Marine Physical Laboratory

AD-A240 158

Acoustic Modem: December 20, 1989 Trip Report

A. Dotan, W. S. Hodgkiss, G. L. Edmonds, and J. C. Nickles

MPL Technical Memorandum 422
November 1990

91-10100

University of California, San Diego
Scripps Institution of Oceanography

UNCLASSIFIED

SECURITY CLASSIFICATION OF THIS PAGE

REPORT DOCUMENTATION PAGE

Form Approved OMB No. 0704-0188

1a. REPORT SECURITY CLASSIFICATION UNCLASSIFIED	1b. RESTRICTIVE MARKINGS
2a. SECURITY CLASSIFICATION AUTHORITY 2b. DECLASSIFICATION / DOWNGRADING SCHEDULE	3. DISTRIBUTION / AVAILABILITY OF REPORT Approved for public release; distribution unlimited.
4. PERFORMING ORGANIZATION REPORT NUMBER(S) MPL Technical Memorandum 422 [MPL-U-90/90]	5. MONITORING ORGANIZATION REPORT NUMBER(S)
6a. NAME OF PERFORMING ORGANIZATION University of California, San Diego 6b. OFFICE SYMBOL (If applicable) MPL	7a. NAME OF MONITORING ORGANIZATION Naval Research Laboratory
6c. ADDRESS (City, State, and ZIP Code) Marine Physical Laboratory Scripps Institution of Oceanography San Diego, California 92152	7b. ADDRESS (City, State, and ZIP Code) 4555 Overlook Avenue, S.W. Washington, D.C. 20375
8a. NAME OF FUNDING / SPONSORING ORGANIZATION Naval Research Laboratory 8b. OFFICE SYMBOL (If applicable) ONR	9. PROCUREMENT INSTRUMENT IDENTIFICATION NUMBER N00014-88-K-2040
8c. ADDRESS (City, State, and ZIP Code) 4555 Overlook Avenue, S.W. Washington, D.C. 20375	10. SOURCE OF FUNDING NUMBERS PROGRAM ELEMENT NO. | PROJECT NO. | TASK NO. | WORK UNIT ACCESSION NO.

11. TITLE (Include Security Classification)

Acoustic Modem: December 20, 1989 Trip Report

12. PERSONAL AUTHOR(S)

A. Dotan, W. S. Hodgkiss, G. L. Edmonds, and J. C. Nickles

13a. TYPE OF REPORT	13b. TIME COVERED	14. DATE OF REPORT (Year, Month, Day)	15. PAGE COUNT
tech memo	FROM ______ TO ______	November 1990	107

16. SUPPLEMENTARY NOTATION

17. COSATI CODES		
FIELD	GROUP	SUB-GROUP

18. SUBJECT TERMS (Continue on reverse if necessary and identify by block number)

acoustic modem, acoustic communication link, Swallow floats, sonobuoy

19. ABSTRACT (Continue on reverse if necessary and identify by block number)

An experiment was conducted on 20 December 1989 as part of a project investigating the design of an acoustic communication link between a Swallow float and a sonobuoy. The objective of the experiment was to measure the transmission characteristics of the acoustic channel at high frequency (10 to 20 kHz), including the nature of fading and multipath.

A conclusion from the analysis results, shows that in the frequency range of 10-20 kHz, the ocean is a nonminimum phase, slowly time-varying, frequency selective fading channel. The fading amplitude chracteristics changes between Rayliegh and Rayleigh-Rice distribution. The fading and the multipath phenomena are very strong in the ocean, and they must be considered in the design of an underwater acoustic communication system.

20. DISTRIBUTION / AVAILABILITY OF ABSTRACT ☐ UNCLASSIFIED/UNLIMITED ☒ SAME AS RPT. ☐ DTIC USERS	21. ABSTRACT SECURITY CLASSIFICATION UNCLASSIFIED
22a. NAME OF RESPONSIBLE INDIVIDUAL W. S. Hodgkiss	22b. TELEPHONE (Include Area Code) (619) 534-1798 22c. OFFICE SYMBOL MPL

DD Form 1473, JUN 86 Previous editions are obsolete. SECURITY CLASSIFICATION OF THIS PAGE

UNCLASSIFIED

Acoustic Modem: December 20 1989 Trip Report

A. Dotan, W.S. Hodgkiss, G.L Edmonds, and J.C. Nickles

Marine Physical Laboratory
Scripps Institute of Oceanography
San Diego, CA 92152

ABSTRACT

An experiment was conducted on 20 December 1989 as part of a project investigating the design of an acoustic communication link between a Swallow float and a sonobuoy. The objective of the experiment was to measure the transmission characteristics of the acoustic channel at high frequency (10 to 20 kHz), including the nature of fading and multipath.

A conclusion from the analysis results, shows that in the frequency range of 10-20 kHz, the ocean is a nonminimum phase, slowly time-varying, frequency selective fading channel. The fading amplitude chracteristics changes between Rayliegh and Rayleigh-Rice distribution. The fading and the multipath phenomena are very strong in the ocean, and they must be considered in the design of an underwater acoustic communication system.

Table of Contents

Table of Contents i
List of Figures ii
I Introduction 1
II Experiment Concept 1
II.1 signal set 4
II.2 Measuring Setup 7
II.3 XBT measurements 12
II.4 Log summary 13
II.4.1 Experiment Log 14
II.4.2 Digital tapes content 16
III Data analys 22
III.1 The channel multipath characteristics 22
III.2 The channel multipath characteristics 23
III.3 The channel multipath characteristics 24
III.4 The channel multipath characteristics 25
IV Real data analysis 104
References 107

List of Figures

Chapter II

Figure 2.1: Experiment Setup 2
Figure 2.2: Projector and Monitor Hydrophone Location 2
Figure 2.3: The frequency response of the AN/SSQ-57 sonobuoy 3
Figure 2.4: Time series and power spectrum of an 8 msec long, chirp waveform 5
Figure 2.5: Measuring Setup 8
Figure 2.6: Digitizing setup. 10
Figure 2.7: Antialaising filter frequency response. 11
Figure 2.8: XBT sound velocity profile. 12
Figure 2.9: XBT sound velocity profile compered with historical data

Chapter III

Figures 3.1-3.27: Waveforms and spectra of 27 eight msec chirps as was received by sonobuoy No 2 26

Figures 3.28-3.54: Waveforms and spectra of 27 eight msec chirps as was received by sonobuoy No 4 53-79

Figure 3.55: Time variation of channel direct path and first multipath character, first 20 msec.) as calculated from sonobuoy No 2 80

Figure 3.56: Time variaton of channel second third and forth multipath character, as calculated from sonobuoy No 2 (time slice between 370 and 530 msec) 81

Figure 3.57: Time variation of channel direct path and first multipath character, (5 msec interval) as calculated from sonobuoy No 4 82

Figure 3.58: Time variaton of channel second third and forth multipath character, as calculated from sonobuoy No 4 83

Figure 3.59: Time variaton of channel sixth multipath character, as calculated from sonobuoy No 4 (time slice between 370 and 530 msec) 84

Figure 3.60: Typical received 8 msec chirp waveform. 85

Figure 3.61: Typical channel multipath character 85

Figure 3.62: The square magnitude coherence function of the channel as a function of time, for waveforms received by sonobuoy No 2 86

Figure 3.63: The square magnitude coherence function of the channel as a function of time, for waveforms received by sonobuoy No 4 87

Figure 3.64: The spectra of 28 - 8 msec chirp waveform sequentially received by sonobuoy No 2 (one every 4 sec.) 88

Figure 3.65: The spectra of 28 - 8 msec chirp waveform sequentially received by sonobuy No 4 (one every 4 sec.) 89

Figure 3.66: Amplitude variation of nine tones received by sonobuoy No 2, 50 and 100 Hz apart 90
Figure 3.67: Amplitude variation of nine tones received by sonobuoy No 2, 250 and 500 Hz apart 91
Figure 3.68: Amplitude variation of nine tones received by sonobuoy No 2, 1kHz apart. 92
Figure 3.69: The correlation between the envelope of nine tones received by sonobuoy No 2 and the central tone for the five sets of tones. 93
Figure 3.70: Histograms of the envelopes of the 250 Hz spaced tones, received by sonobuoy No 2 94
Figure 3.71: Histograms of the envelopes of the 1 kHz spaced tones received by sonobuoy No 2 95
Figure 3.72: The histograms of the 15 kHz tone, at different time periods received by sonobuoy No 2 96
Figure 3.73: Amplitude variation of nine tones received by sonobuoy No 4, 50 and 100 Hz apart 97
Figure 3.74: Amplitude variation of nine tones received by sonobuoy No 4 250 and 500 Hz apart 98
Figure 3.75: Amplitude variation of nine tones received by sonobuoy No 4, 1kHz apart. 99
Figure 3.76: The correlation between the envelope of nine tones received by sonobuoy No 4 and the central tone for the five sets of tones. 100
Figure 3.77: Histograms of the envelopes of the 250 Hz spaced tones, received by sonobuoy No 4 101
Figure 3.78: Histograms of the envelopes of the 1 kHz spaced tones received by sonobuoy No 4 102
Figure 3.79: A simplified model of an underwater acoustic communication channel.

Chapter IV

Figure 4.1: Implemented DPSK receiver - block diagram 104
Figure 4.2: Power spectral density of the ambient noise (after bandpassing) 105
Figure 4.3: Comparison between theoretical and achieved bit error rate. 106

I Introduction

An experiment was conducted on 20 December 1989 as part of a project investigating the design of an acoustic communication link between a Swallow float and a sonobuoy. The experiment was located at $32^{\circ}40'$N and $117^{\circ}35.6'$W. During the experiment, the sea state was between zero and one and the wind speed was between 5 and 12 knots.

The objective of the experiment was to measure the transmission characteristics of the acoustic channel at high frequency (10 to 20 kHz), including the nature of fading and multipath.

II Experiment Concept.

The experiment plan was to transmit a set of waveforms from a transducer deployed deep in the ocean from a ship (R/V SPROUL) and receive the transmitted signal with four sonobuoys located 1 km apart and transmitting the received signal via a RF link back to the ship (see Figures 2.1 and 2.2). The transmitted and the received signals (from the sonobuoys) were recorded simultanously. In addition, a monitor hydrophone was deployed close to the projector and provided a replica of the waveforms which were transmitted through the water.

Figure 2.1 and Figure 2.2 show a schematic diagram of the experiment set up.

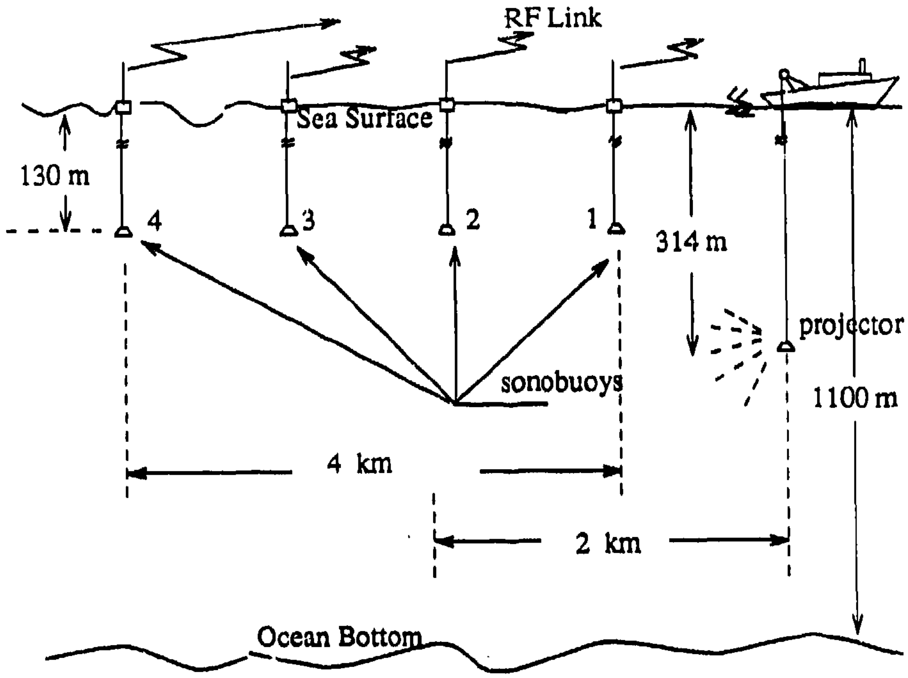

Figure 2.1. Experiment Setup.

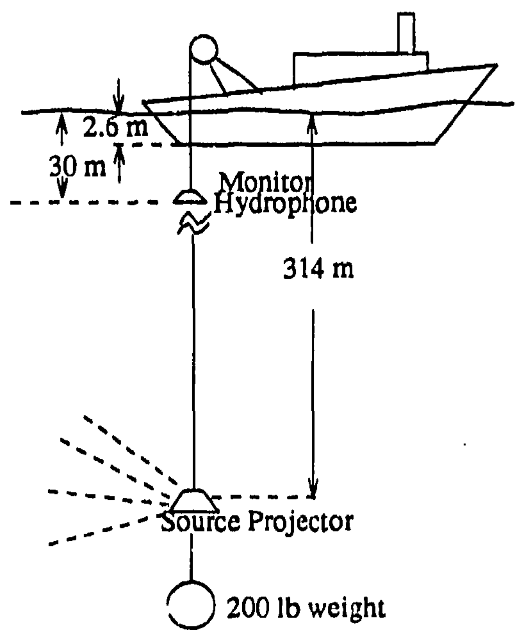

Figure 2.2. Projector and Monitor Hydrophone Location.

As a projector, we used a Sparton model 6130 free flooded ring transducer which transmitted a signal of source level of 182 DB/1μPa @ 1m. As receivers, we used the AN/SSQ-57 sonobuoys with frequency response shown in Figure 2.3.

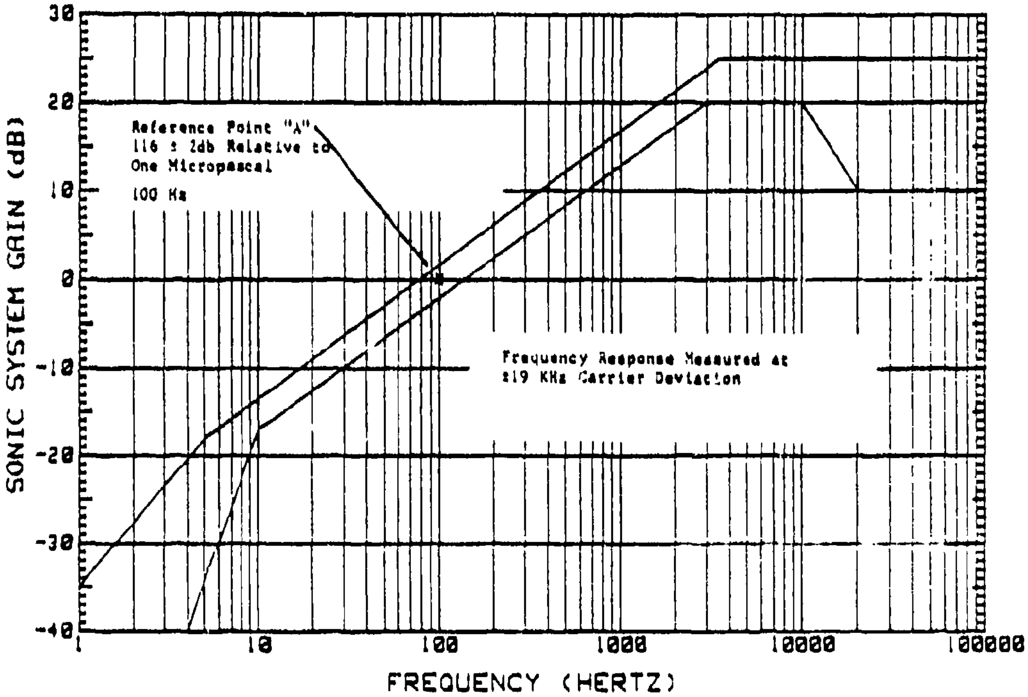

Figure 2.3. The frequency response of the AN/SSQ-57 sonobuoy.

II.1 Signal set

Three sets of waveforms were transmitted. The first set of waveforms was chosen such that it allowed to measure the multipath character of the channel. The second set of waveform was chosen such that it allowed to measure the channel fading characteristics. The third one was a set of different waveforms which simulated real data transmission.

The first set of waveforms was a set of spread spectrum waveforms implemented by chirp signals and by pseudo random sequense.

(1) Five different chirp waveforms were transmitted, 1 msec chirp with time-bandwidth product of 10, 2 msec chirp with time bandwidth of 20, 4 msec chirp with time bandwidth product of 40, 8 msec chirp with time bandwidth product of 80, and 16 msec chirp with time bandwidth product of 160. All these waveforms were designed such that they occupied a bandwidth of 10 kHz between 10 and 20 kHz. Figure 2.4 shows the 8 msec chirp and its power spectrum. Each waveform was transmitted once every four seconds for 2 minutes. The 8 msec chirp was transmitted for 10 minutes. A sync pulse was transmitting at the begining of each 2 or 10 min period and a10 sec break was done between different pulse length transmissions.

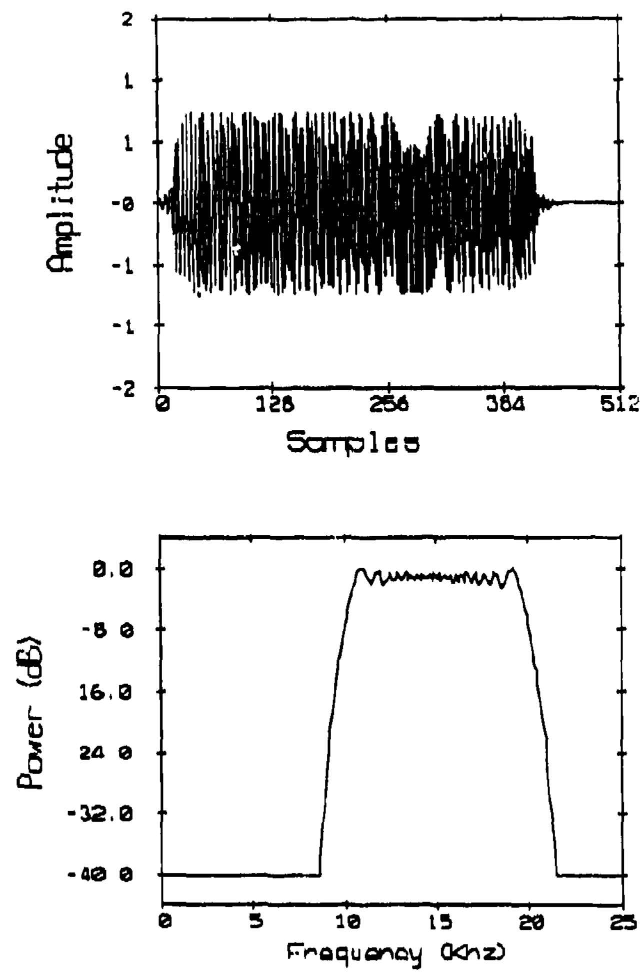

Figure 2.4. Time series and power spectrum of an 8 msec long chirp waveform.

(2) A maximum length pseudo random sequence of 127 digits modulated (on off shift keying) a 15 kHz carrier with rate of 3.75 kbit/sec. The sequence was transmitted once every 4 second for 2 minutes. A sync pulse was transmitted at the beginig of the 2 miutes transmission. The generator polynomial of the sequence was 0137 (octal), and the generated sequence was:

11000010 01001111 11101111 10001110 10101001 01011110 10011001

11001101

01100010 00101110 11001000 01111001 01101110 00001010 00110110

1000000

(3) 4 different maximum length pseudo random sequence of 127 digits each, modulated (on off shift keying) a 15 kHz carrier with rate of 3.75 kbit/sec. The 4 sequences were transmitted in a row one every 1 second for 10 minutes. A sync pulse (replacing 4 sec sequence of pings) was transmitted at the begining of every 2 min period. The four generator polynomials used were 0107, 0134, 0137, and 0151 (octal).

For 0107, the sequence generated is:

11001101 10001110 01110101 11000010 01100000 10101011 01001001

01001111

00100011 01010000 11111110 11101101 11101000 10110010 11111000

1000000

For 0134:

10011111 11000101 01011110 01100101 00010001 10000111 10111110

10110101

00110110 01110110 11101001 00101100 01110010 00010111 00000110

1000000

For 0137:

11000010 01001111 11101111 10001110 10101001 01011110 10011001

11001101

01100010 00101110 11001000 01111001 01101110 00001010 00110110

1000000

For 0151:

11110110 01100010 01001110 01111100 10000010 00110101 01001101
10100101

00001011 00001100 10111111 10101101 11011110 00111010 00101011
1000000

The second set of waveforms was a set of nine tones equally spaced, transmitted for 2 minutes. This set of tones was retransmitted five times, where each time the space between the tones was changed (50, 100, 250, 500 and 1000 Hz appart). The fifth tone was always centered at 15 kHz.

The third set was a of combinations of chirp pulses. Any transmission of a particular type of waveform sequence was made in blocks of 8 seconds (7.9 second on and 0.1 second off) with total duration of 2 minutes (15 blocks). the pulses were transmitted coherently. An 8 seconds break was between sequence type, and a sync pulse was transmitted at the begining of each 2 minutes sequence.

II.2 Measuring Setup

Figure 2.5 gives a schematic block diagram of the measuring setup used in the experiment.

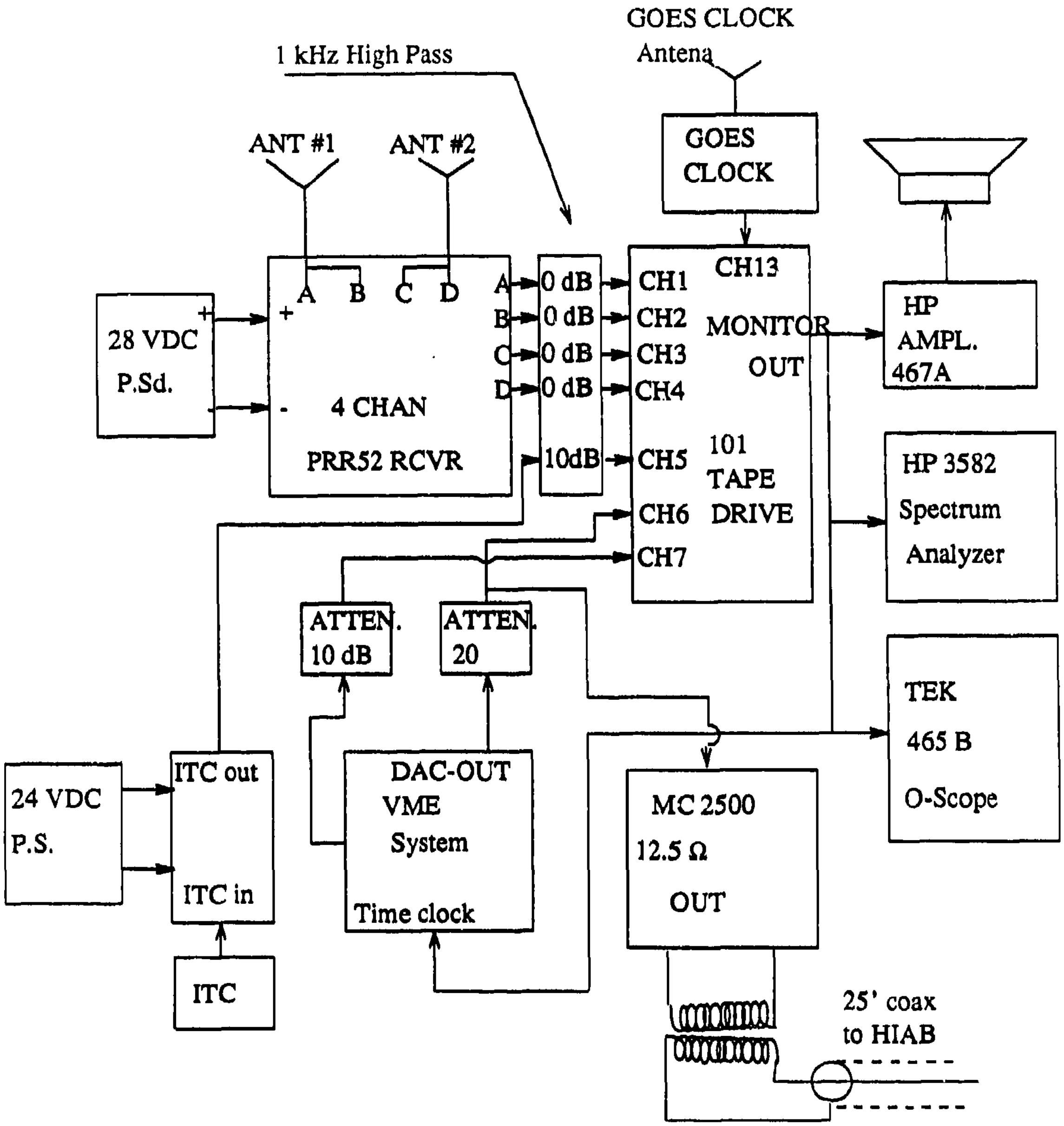

Figure 2.5. Measuring setup

The right hand side of the block diagram describes the waveform generator, power amplifier, and transmitted signal monitoring. The left hand side describes the receiving part including the 4 channel FM receiver, GOES clock, Honeywell 101 tape

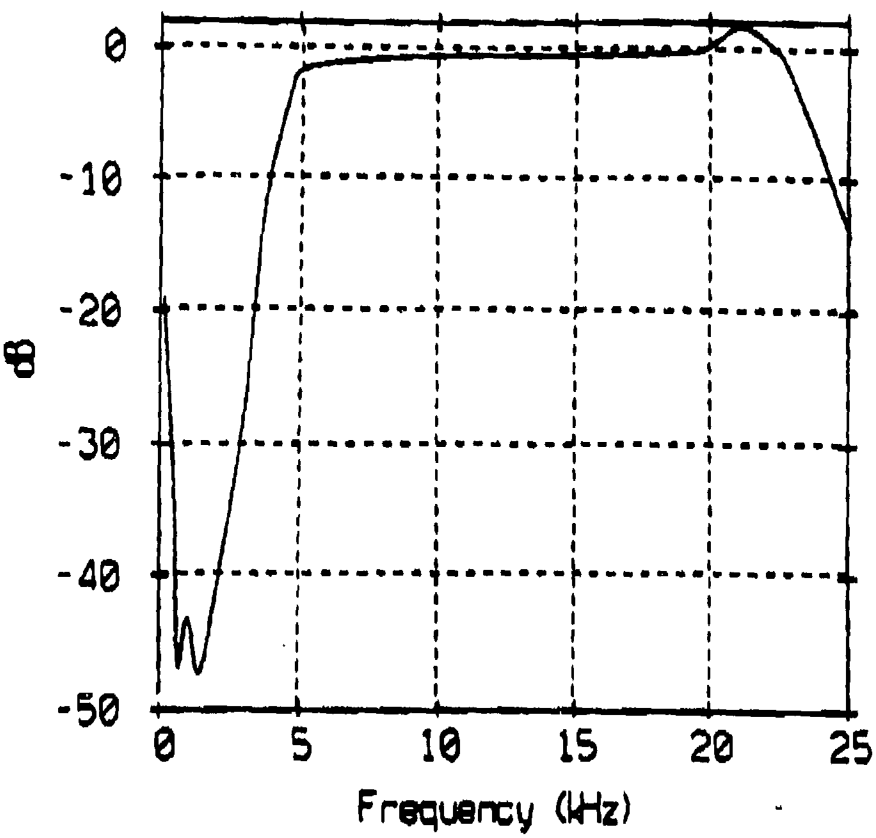

Figure 2.6. Antialaising filter frequency response.

II.3 XBT measurements

Expendable bathythermograph (XBT) measurment was made from the R/V SPROUL at the begining of the experiment. The Sippican model T-4 XBT was used. This temperature measurement along with historical salinity data archived by the National Oceanographic Data Center[1] was used with an equation relating temperature, salinity and depth to sound speed[2] Figure 2.7 shows the sound speed profile as calculated from the XBT data.

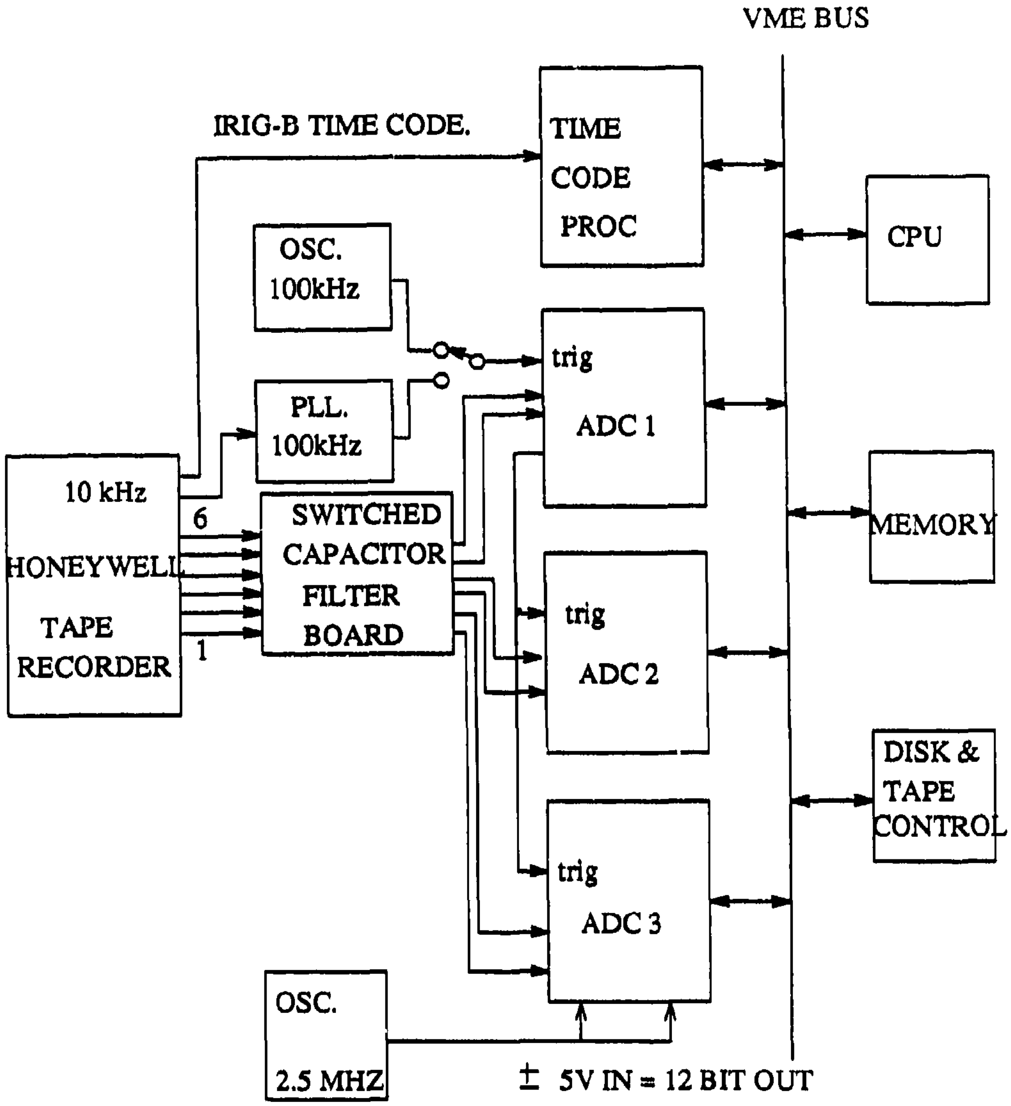

Figure 2.6. Digitizing setup.

The digitizer was calibrated such that 1 Volt at the output of the tape recorder corresponds to 1 volts at the input to the analog to digital converter (ADC). Figure 2.7 gives the frequency response of the antialaising filter that was used.

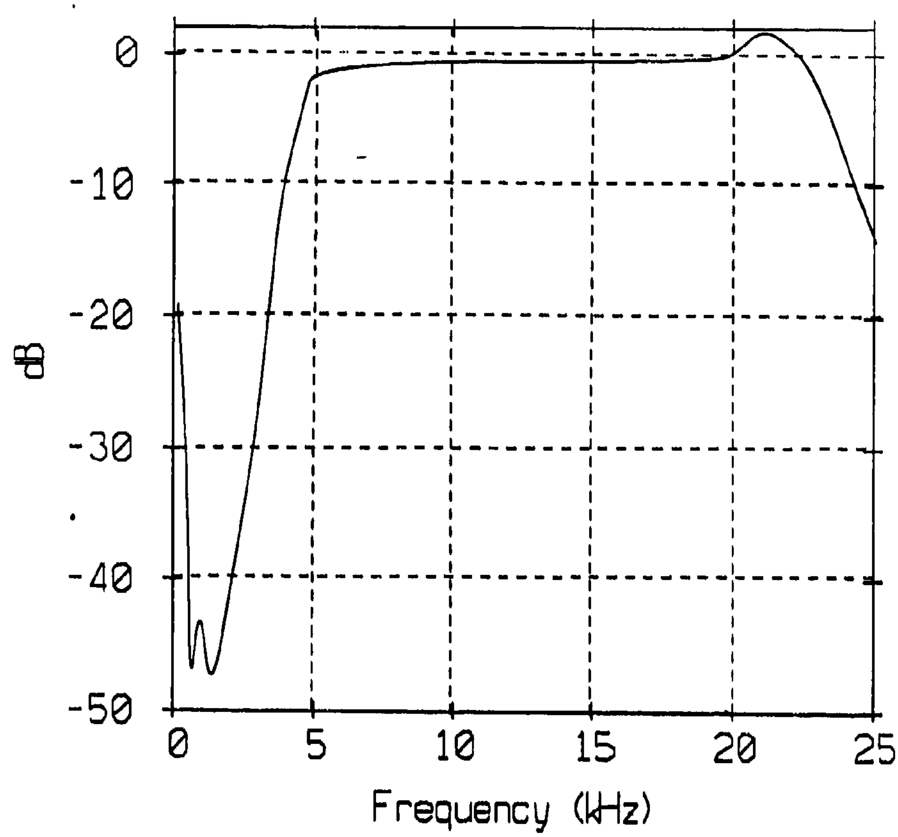

Figure 2.7. Antialaising filter frequency response.

II.3 XBT measurements

An expendable bathythermograph (XBT) measurment was made from the R/V SPROUL at the begining of the experiment. The Sippican model T-4 XBT was used. This temperature measurement along with historical salinity data archived by the National Oceanographic Data Center[1] was used with an equation relating temperature, salinity and depth to sound speed[4] where derived.

Figure 2.8 shows the sound speed profile as calculated from the XBT data.

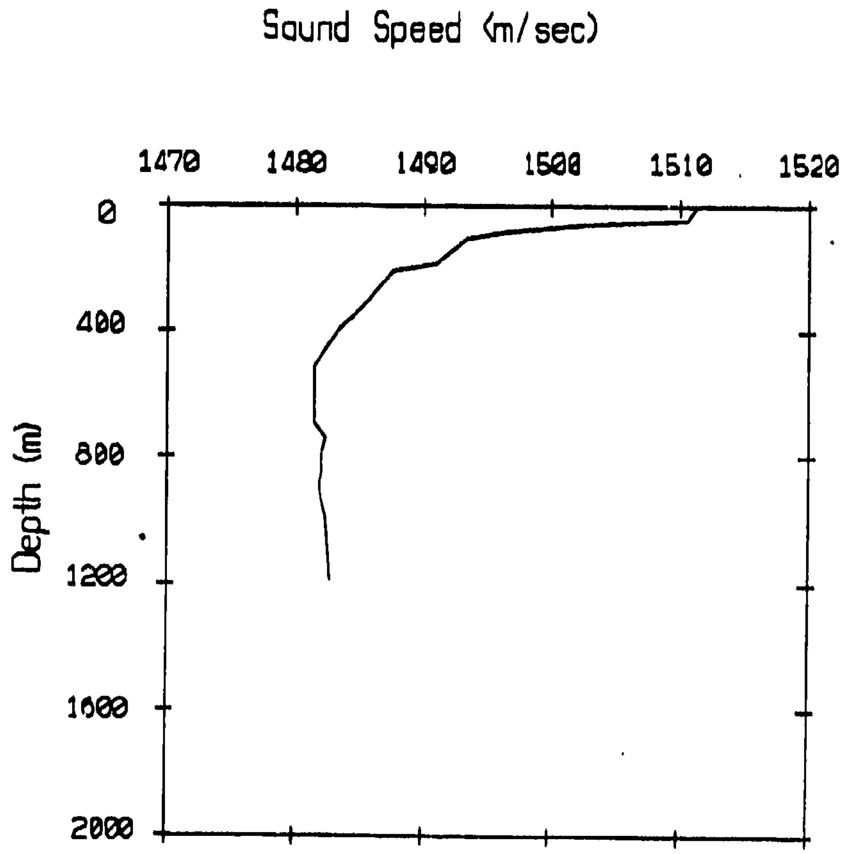

Figure 2.8. XBT sound speed profile.

Figure 2.9 compares the sound speed profile calculated from the XBT data with a sound profile based on historical data.

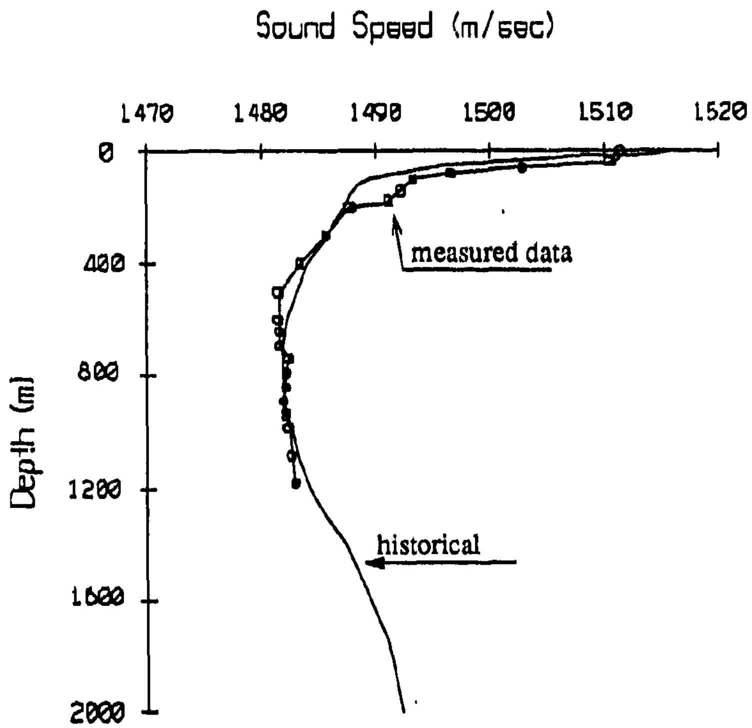

Figure 2.9. XBT sound speed profile compered with historical data

II.4 Log summary.

In this section two lists are enclosed. The first is the experiment log as was written in the log book during the experiment and the second is the contents of each of the digital tapes.

II.4.1 Experiment log

20 December 1989, Acoustic Modem Experiment No 2, (R/V SPROUL)

10:53	Arriving on station
11:03	Launch 1-st sonobuoy at 32°40.06′N 117°35.93W (channel #2) looks good.
11:21	Second sonobuoy launched, at 32°40.49′N 117°35.89W. Range to buoy 1 500 msec.
11:39	Third sonobuoy launched, does not work, hydrophone has become detached.
11:46	Launch last sosnobouy, looks good.
12:30	Water depth is 600 fathom, 32°42.08′N 117°35.38W. 1.4 sec, 2.1 sec, 3.3 sec time difference between transmitted signal and received echoes.
12:55	XBT probe launched.
13:27	32°41.40′N 117°35.05W, On station, deploy source.
14:02	Monitor hydrophone at 163.7 meters, source at 174.4 meters.
14:35	Range: 2.5 sec to #1, 2.25 sec to #2 2.0 sec to #4.
14:35:43	Start transmitting, 120 volts p-p at stereopower amp. Monitor hydrophone weak & noisy.
14:38	Rev engine.
15:04	Stop transmitting 1 min before end of 10 minutes sequence of 4 mls (1 mls/sec).
15:07	Range: 3.05 sec to #1, 2.75 sec to #2, 2.25 sec to #4.
15:14:47	New tape. Start transmitting 9 tones 50 Hz apart.
15:26:32	Add 10 dB gain to monitor hydrophone.
15:29:40	Transmitter power failure during PRN up chirps. Tape recorder stop.

15:40:47	Start PRN up chirps (1 msec) again.
15:46:30	Transmitter power failure.
15:58	Tape running, PRN up chirp last 2 minutes sequence.
16:02	Took 10 dB back out of monitor hydrophone gain.
16:10	Position $32^{0}42.00'N$ $117^{0}33.90W$.
	New tape.
	Start transmitting 4-phase PRN up chirp.
16:14	Range: #1 is 3.7 sec
	#4 is 3.1 sec
	Add 6 dB to monitr hydrophone channel.
16:28:15	Start transmitting 4-phase PRN up chirp.
16:45	Back transmitting, start up/down chirp, 180^{0} PRN.
	Sonobuoy #1 has died.
17:01	Channel #1 is back.
17:04	End of thape #3.
17:07	Range to #4 is 3.5 sec
	#2 is 3.7 sec
	New Tape.
	Start transmitting up/down chirp selected by PRN.
	Sonobuoy receiver A (Rf channel 2) is intermittant.
	Switch receiver C to RF chan 2. Now have first sonobuoy(Rf chan2) on Tape track 1 & 3.
17:24	Start Tape #4.
17:54	Stop Tape #4.
18:07	Start Tape #5.
	2 msec up/down chirp PRN phase flips.
18:29	Continuing Tape #5.

Start 1 msec up chirp 0° phase.

18:35	Stop Tape #5.
	4.1 sec travel time to chan 4 (on tape) buoy.
	No other buoy ranges obtained.
18:45	Start tape #6.
	Resume transmitting 1 msec up chirps 0°,180°.
	PRN phase.
18:54	32°41.74'N 117°32.92W.
19:14	Stop Tape #6.
	Start Tape #7.
19:25:37	Start transmitting 4 phase up/down PRN chirp.
19:38	Stop Tape #7.
19:41	End of experiment.
	32°41.86'N 117°32.68W.

II.4.2 Contents of Digital tapes

The digitized data was recorded in SIO format. Each tape contains 2 min long files. The enclosed list gives the starting time and the content of each file.

::::::::::::::::::::::::::

Digital tape number 1

::::::::::::::::::::::::::

354 14:35:43.486856 Start channel probe, 1 msec chirps

354 14:37:43.486929 Start channel probe, 2 msec chirps

354 14:39:43.486989 Start channel probe, 4 msec chirps

354 14:41:43.487048 Start channel probe, 8 msec chirps

354 14:43:43.487083 Start channel probe, 8 msec chirps

354 14:45:43.487124 Start channel probe, 8 msec chirps

354 14:47:43.487162 Start channel probe, 8 msec chirps

354 14:49:43.487207 Start channel probe, 8 msec chirps

354 14:51:43.487255 Start channel probe, 16 msec chirps

354 14:53:43.487300 Start channel probe, single mls

354 14:55:43.487335 Start channel probe, multiple mls

354 14:57:43.487383 Start channel probe, multiple mls

354 14:59:43.487427 Start channel probe, multiple mls

354 15:01:43.487454 Start channel probe, multiple mls

::::::::::::::::::::::::::::::::

Digital tape number 2

::::::::::::::::::::::::::::::::

354 15:14:33.817220 Start multiple tones, sep. 50 Hz

354 15:16:33.817264 Start multiple tones, sep. 100 Hz

354 15:18:33.817302 Start multiple tones, sep. 250 Hz

354 15:20:33.817346 Start multiple tones, sep. 500 Hz

354 15:22:33.817392 Start multiple tones, sep. 1000 Hz

354 15:24:33.817451 Start 1 msec up-chirps, fixed phase

354 15:26:33.817527 Start 1 msec up-chirps, fixed 180 degree shift

354 15:40:47.669677 Start 1 msec up-chirps, biphase coded prn

354 15:42:47.669773 Start 1 msec up-chirps, biphase coded prn

354 15:44:47.669896 Start 1 msec up-chirps, biphase coded prn

354 16:00:51.380761 Start 1 msec up-chirps, biphase coded prn

354 16:02:51.380854 Start 1 msec up-chirps, fixed 90 degree shift

354 16:04:51.380946 Start 1 msec up-chirps, quadphase coded prn

::::::::::::::::::::::::::

Digital tape number 3

::::::::::::::::::::::::::

354 16:28:16.400295 Start 1 msec up-chirps, quadphase coded prn

354 16:30:16.400359 Start 1 msec alt-chirps, fixed phase

354 16:32:16.400433 Start 1 msec alt-chirps, fixed 180 degree shift

354 16:34:16.400539 Start 1 msec alt-chirps, biphase coded prn

354 16:36:16.400646 Start 1 msec alt-chirps, biphase coded prn

354 16:46:00.877604 Start 1 msec alt-chirps, biphase coded prn

354 16:48:00.877658 Start 1 msec alt-chirps, biphase coded prn

354 16:50:00.877737 Start 1 msec alt-chirps, biphase coded prn

354 16:52:00.877821 Start 1 msec alt-chirps, biphase coded prn

354 16:54:00.877919 Start 1 msec alt-chirps, fixed 90 degree shift

354 16:56:00.878041 Start 1 msec alt-chirps, quadphase coded prn

354 16:58:00.878187 Start 1 msec up/down coded chirps

354 17:00:00.878345 Start 1 msec up/down coded chirps

354 17:02:00.878510 Start 1 msec up/down coded chirps

::::::::::::::::::::::::::

Digital tape number 4

::::::::::::::::::::::::::

354 17:24:23.138786 Start 1 msec up/down coded chirps

354 17:26:23.138871 Start 1 msec up/down coded chirps

354 17:28:23.138974 Start 2 msec up-chirps, fixed phase

354 17:30:23.138990 Start 2 msec up-chirps, fixed 180 degree shift

354 17:32:23.139099 Start 2 msec up-chirps, biphase coded prn

354 17:34:23.139197 Start 2 msec up-chirps, biphase coded prn

354 17:36:23.139325 Start 2 msec up-chirps, biphase coded prn

354 17:38:23.139504 Start 2 msec up-chirps, biphase coded prn

354 17:40:23.139654 Start 2 msec up-chirps, biphase coded prn

354 17:42:23.139825 Start 2 msec up-chirps, fixed 90 degree shift

354 17:44:23.139987 Start 2 msec up-chirps, quadphase coded prn

354 17:46:23.140150 Start 2 msec alt-chirps, fixed phase

354 17:48:23.140343 Start 2 msec alt-chirps, fixed 180 degree shift

354 17:50:23.140522 Start 2 msec alt-chirps, biphase coded prn

::::::::::::::::::::::::::

Digital tape number 5

::::::::::::::::::::::::::

354 18:06:59.718626 Start 2 msec alt-chirps, biphase coded prn

354 18:08:59.718750 Start 2 msec alt-chirps, biphase coded prn

354 18:10:59.718860 Start 2 msec alt-chirps, biphase coded prn

354 18:12:59.718962 Start 2 msec alt-chirps, biphase coded prn

354 18:14:59.719058 Start 2 msec alt-chirps, fixed 90 degree shift

354 18:16:59.719181 Start 2 msec alt-chirps, quadphase coded prn

354 18:18:59.719343 Start 2 msec up/down coded chirps

354 18:20:59.719509 Start 2 msec up/down coded chirps

354 18:22:59.719670 Start 2 msec up/down coded chirps

354 18:24:59.719851 Start 2 msec up/down coded chirps

354 18:26:59.720047 Start 2 msec up/down coded chirps

354 18:29:02.791139 Start 1 msec up-chirps, fixed phase

354 18:31:02.791343 Start 1 msec up-chirps, fixed 180 degree shift

354 18:33:02.791564 Start 1 msec up-chirps, biphase coded prn

::::::::::::::::::::::::::

Digital tape number 6

::::::::::::::::::::::::::

354 18:45:34.913526 Start 1 msec up-chirps, biphase coded prn

354 18:47:34.913671 Start 1 msec up-chirps, biphase coded prn

354 18:49:34.913825 Start 1 msec up-chirps, biphase coded prn

354 18:51:34.913977 Start 1 msec up-chirps, biphase coded prn

354 18:53:34.914127 Start 1 msec up-chirps, fixed 90 degree shift

354 18:55:34.914289 Start 1 msec up-chirps, quadphase coded prn

354 18:57:34.914445 Start 1 msec alt-chirps, fixed phase

354 18:59:34.914609 Start 1 msec alt-chirps, fixed 180 degree shift

354 19:01:34.914805 Start 1 msec alt-chirps, biphase coded prn

354 19:03:34.914992 Start 1 msec alt-chirps, biphase coded prn

354 19:05:34.915184 Start 1 msec alt-chirps, biphase coded prn

354 19:07:34.915385 Start 1 msec alt-chirps, biphase coded prn

354 19:09:34.915571 Start 1 msec alt-chirps, biphase coded prn

354 19:11:34.915778 Start 1 msec alt-chirps, fixed 90 degree shift

::::::::::::::::::::::::::

Digital tape number 7

::::::::::::::::::::::::::

354 19:25:38.611052 Start 1 msec alt-chirps, quadphase coded prn

354 19:27:38.611174 Start 1 msec up/down coded chirps

354 19:29:38.611319 Start 1 msec up/down coded chirps

354 19:31:38.611471 Start 1 msec up/down coded chirps

354 19:33:38.611617 Start 1 msec up/down coded chirps

354 19:35:38.611760 Start 1 msec up/down coded chirps

III Channel character - experimental results

The measured channel parameters were: (1) the channel multipath character, (2) the coherence function as a function of time. (indicates the nature of the time-varying character of the acoustic channel), and (3) histograms of amplitude variation at each frequency commponent of the waveforms (enable us to measure the statistics of the fading and the correlation between two frequency componnents).

III.1 The channel multipath characteristcs

The waveforms that were received by the sonobouys were distorted replicas of the transmitted signal plus many other delayed replicas that result from the multipaths. Figures 3.1 - 3.54 show a set of 27, 8 msec chirp waveforms as were recieved by sonobuoys No 2 and No 4. Figures 3.1 - 3.27 correspond to sonobuoy No 2 and Figures 3.28 - 3.54 correspond to sonobuoy No 4. These plots show the direct path and the first multipath received signals only. The multipath characteristics of the channel are calculated by correlating the received and the transmitted waveforms and envelope-detecting the result. Figure 3.55 and Figure 3.56 show the multipath characteristics of the channel between the transmitter and sonobuoy No 2, calculated from a sequence of a 27 chirp pulses. (Corrections for the relative drift between the receiver and transmitter have been done). Figure 3.55 shows the direct path and the first multipath and Figure 3.56 shows the second and the third multipath. Figures 3.57-3.59 show the multipath characteristics between sonobuoy No 4 and the transmitter, calculated from the same 27 chirp pulses. Figure 3.57 shows the direct path and the first multipath. Figure 3.58 shows the second third and fourth multipath and Figure 3.59 shows the fifth multipath. Figure 3.60 and Figure 3.61 give a detailed look at on the first multipath of one of the received 8 msec chirp signals. Typically, the chanel multipath characteristcs are caracterized by the received signal from the direct path being much weaker than the signal received from the first multipath (caused by reflection from the sea surface) (see Figures 3.55 and 3.57). The other multipaths having larger delay are caused by reflection from the sea bottom or from multiple reflections (bottom and surface) and are much weaker than the first multipath.

The underwater acoustic channel is a time-varying channel and hence, the channel multipath character also varies with time. Figures 3.55-3.59 illustrate the time variation of the channel multipath character. Careful inspection of the first 20 msec (Figure 3.55 and Figure 3.57) shows not only that the multipath intensity changes with time but that the multipaths die and rebuild during a long time of inspection. Another interesting property of the channel multipath character is that each multipath consits of a group of many close multipaths (micromultipath effect). This effect is more dominant, as the number of reflections (from bottom as well as from surface) become larger (see Figures 3.56, 3.58 and 3.59).

III.2 Time variation properties of the channel

One of the characteristics of an underwater acoustic channel is its time-varying property. The squared magnitude coherence (SMC) is a good measure of the correlation between the channel character in two different time intervals[2]. A spread spectrum waveform between 10 and 20 kHz (8 msec chirp) was transmitted every 4 seconds and the squared magnitude coherence function between the first received waveform and the rest of the waveforms was calculated. Figures 3.62 and 3.63 show the the calculated SMC of the waveforms received by sonobuoye No 2 and No 4. Sonobuoy No 4 was allocated further from the trransmitter then sonobuoy No 2, the received waveforms were much noisy and hence the SMC is lower then in sonobuoy No 2. From the calculated SMC (Figures 3.62 and 3.63) it is observed that for most frequency components, the channel properties are rearly time invariant and the coherence is very high (almost 1). An exception is in the frequency range between 13 and 16 kHz (normalized frequencies of 0.26 and 0.32), where the coherence becomes smaller as the time difference becomes larger. As a result, one can conclude that the rate of variation of the channel character is much lower than the bit rate (seconds compared with miliseconds) and that the channel can be assumed to be very slowly time-varying. A different way to show the rate of variation of the channel character as the function of time is to look at the spectrum variation of the received signal as a function of time (see Figure 3.64 and 3.65). The spectrum has small variation in a time interval of some tens of seconds which shows again that the channel is very slow time-varying. Figures 3.64 and 3.65 shows the specura of a set of chirp waveforms received by sonobuoys 2 and 4 respectively.

III.3 The frequency selectivity properties of the channel

Another characteristic feature of a communication channel is its frequency selectivity. This parameter was measured by transmitting a set of tones and calculating the correlation between the envelopes of the tones.

The envelope variation of each frequency component as was received by sonobuoy No 2 is presented in Figures 3.66, 3.76, 3.68. Figure 3.66 presents the envelope variation of each frequency component for tones seperated 50 and 100 Hz apart and Figure 3.67 for 250 and 500 Hz appart. Figure 3.68 gives the envelope variation when the tones are seperated 1000 Hz apart. The correlation coefficient of the envelope variation between the nine tone groups was calculated with respect to the center tone (15 kHz) (see Figure 3.72). The statistical distribution of the amplitude of each tone was calculated.

Figures 3.73 and 3.74 present the histograms of the envelope of the tones when the tones are 250 Hz and 1000 Hz apart.

Figures 3.73-3.78 are the same as Figures 3.66-3.72 but for the waveforms recieved by sonobuoy No 4.

Inspection of the Figures shows that the correlation of the fading phenomena between two frequencies is time dependent. The correlation between the same two frequencies obtains different values at different time intervals. As an example, the correlation between signals at 15 and 15.1 kHz is -0.039 in one case (tones 50 Hz apart, Figure 3.66) and 0.1111 in the second (tones 100 Hz apart). The correlation between two tones 500 Hz apart (15 and 15.5 kHz) is 0.15564 in one time interval and -0.0452 in other time interval. A second feature of the data is that not only the correlation function is time-varying, but the statistics of the envelope are also time-varying. Figure 3.72 gives the histogram of the envelope of the central tone (at 15 kHz) at five different time intervals of 65 seconds length and 120 seconds apart. From Figure 3.72, one can see that at each different time interval the statistics of the envelope change between a Rayleigh-like distribution and a Rayleigh-Rice like distribution[5]. The Rayleigh-like distribution exists when no specular multipath component exists, and the Rayleigh-Rice like distribution appears when a strong specullar multipath component exists.

III.4 Channel modeling

The analysis of the three at-sea experiments shows that the acoustic communication channel is a time-varying frequency selective channel, which suffers from strong multipath effects. A simplified model of this complicated channel is a sum of independent channels each having a different transfer function and a different delay depending on the delay caused by the multipath (see Figure 3.79). The channel is assumed to be a frequency selective Rayleigh fading channel with low correlation between two frequencies if they differ by 50-100 Hz.

The equivalent lowpass multipath character of the channel can be described as

$$h_c(\tau,t) = h_0(\tau,t) + \sum_{l=1}^{m} h_l(\tau - TD_l, t) \tag{3.1}$$

where

$$h_l(\tau,t) = \begin{cases} f_l(\tau,t) & \tau \ll TD_l \\ 0 & else \end{cases}$$

$h_0(\tau,t)$ is the direct path and $h_l(\tau,t)$, $l = 1 \cdots n$ are the delayed (with delay of TD_l) pathss caused by the multipaths.

A more simplified model for the channel can be described as

$$h_c(\tau,t) = \alpha_0 \, \delta(\tau) + \sum_{l=1}^{m} \alpha_l \, \delta(\tau - TD_l). \tag{3.2}$$

As seen from Figures 3.57, 3.60 and 3.61, one of the multipath signal is much stronger than the direct path. This result was also verified experimantally and explained by Lord and Plemons (see their Figures)[3]. For cases where an α_l exsits such that $\alpha_l > \alpha_0$, the transfer function of the channel is a non minimum phase transfer function. A necessary condition for a function to be a minimum phase is that $\sum_{l=1}^{m} |\alpha_l| < |\alpha_0|$

144543.1.ch2 , pulse No1

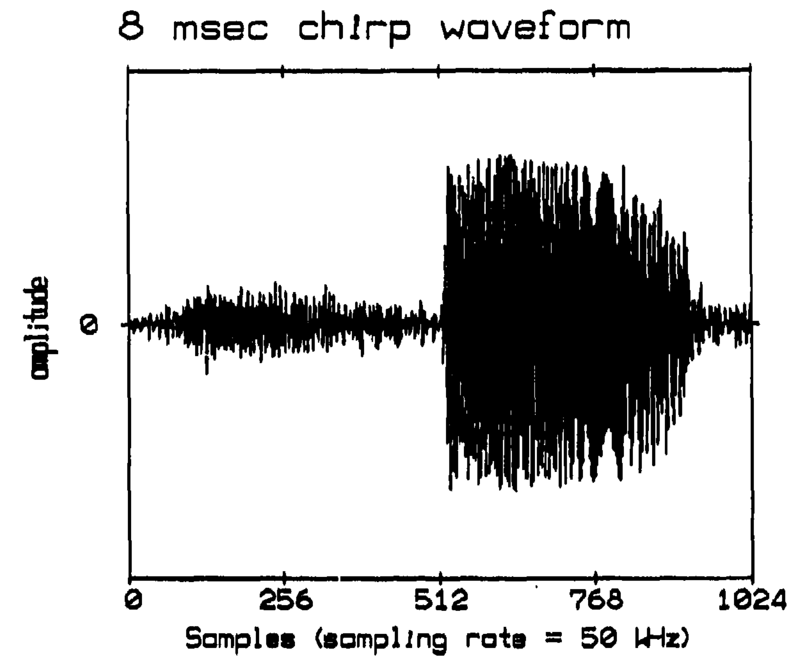

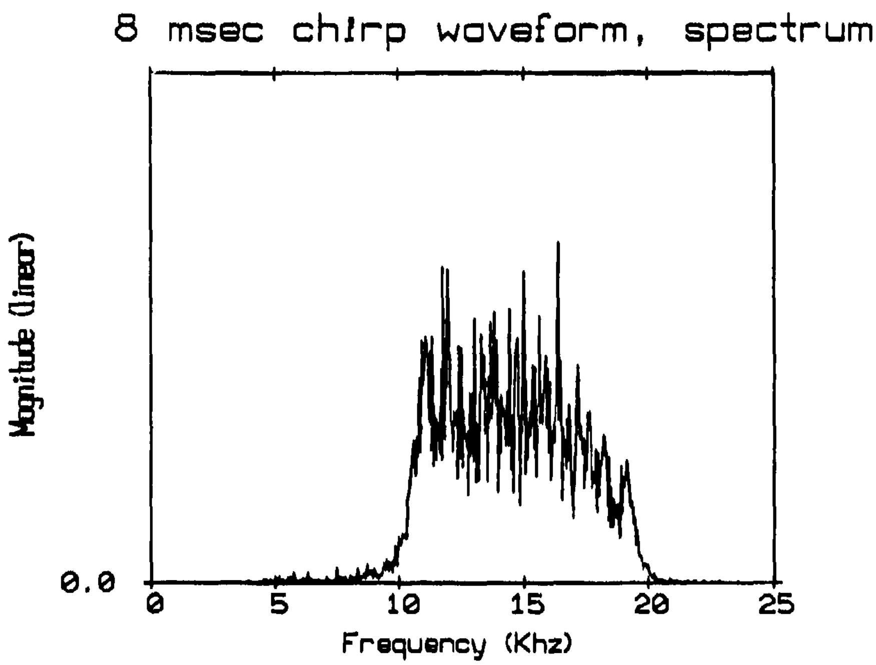

Figures 3.1-3.27. Waveforms and spectra of 27 eight msec chirps as was received by sonobuoy No 2.

144543.1.ch2 , pulse No2

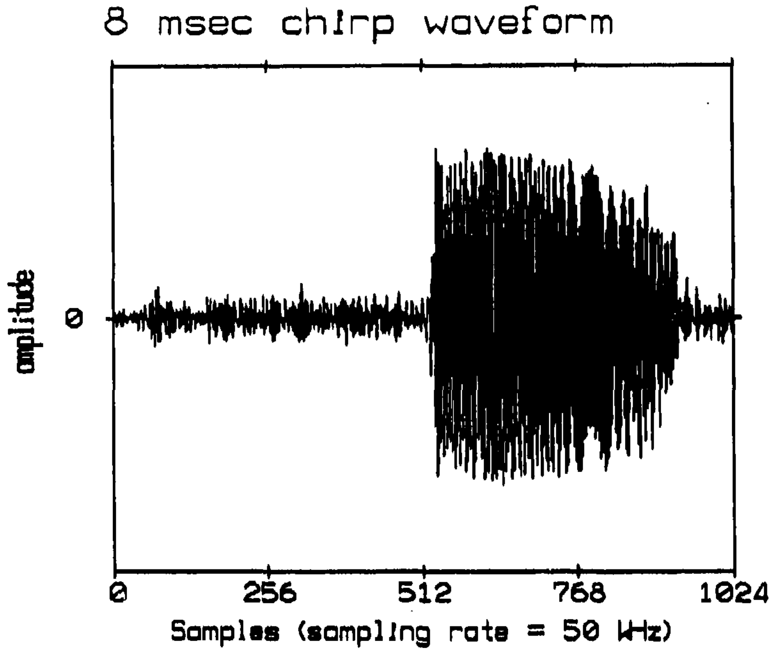

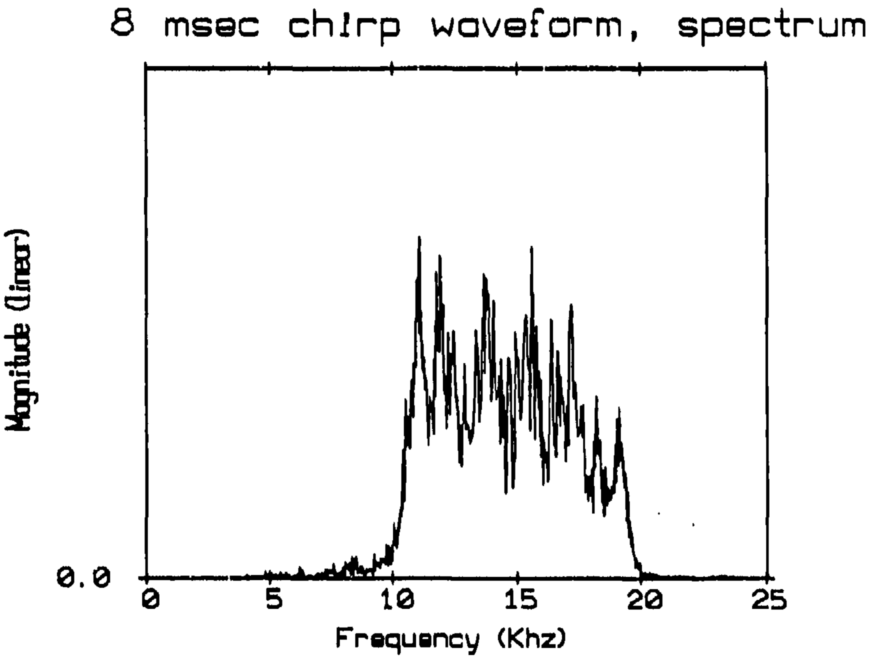

144543.1.ch2 , pulse No3

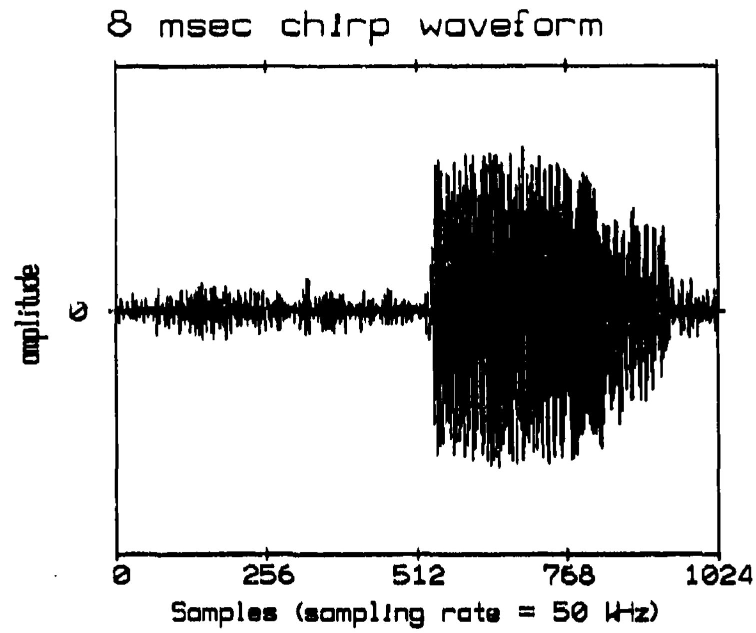

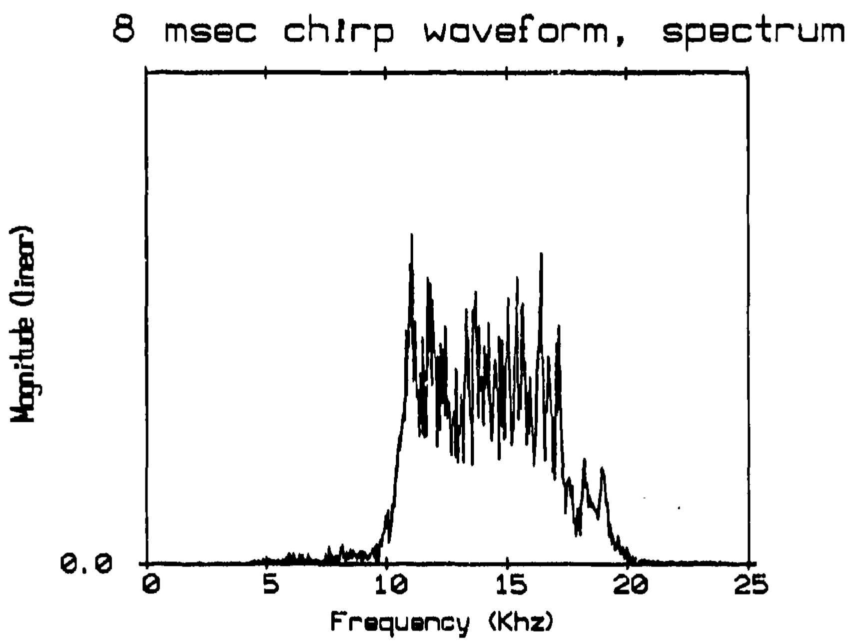

144543.1.ch2 , pulse No4

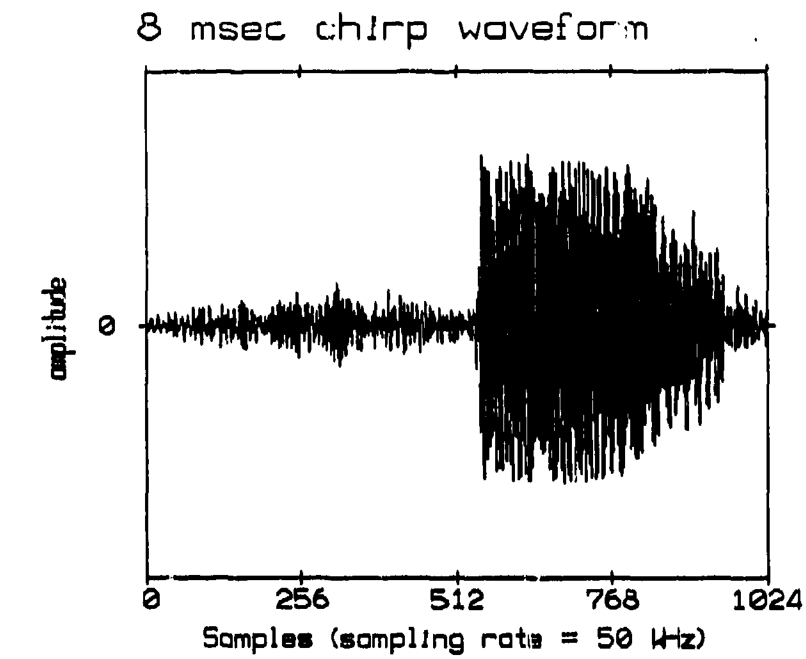

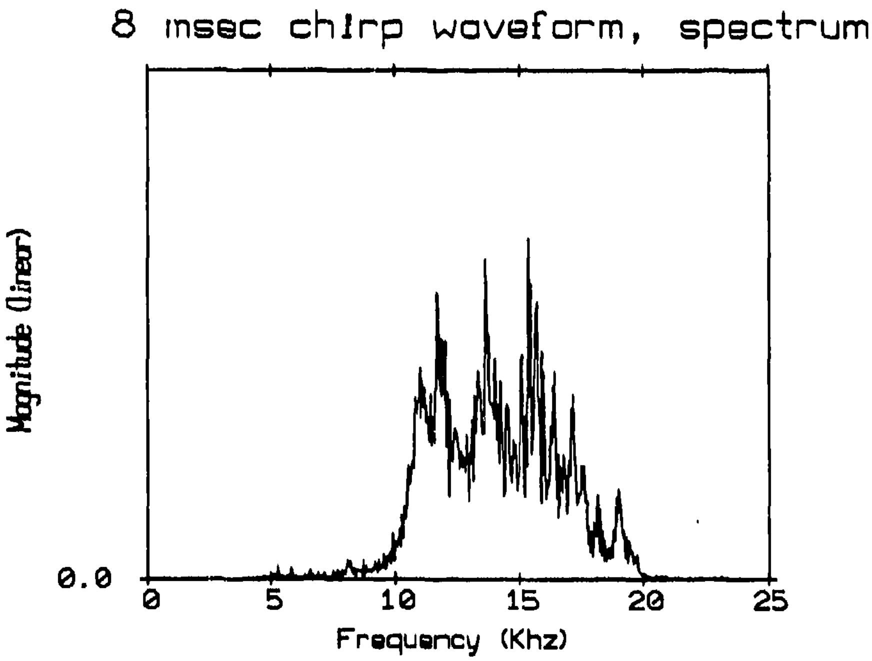

144543.1.ch2 , pulse No5

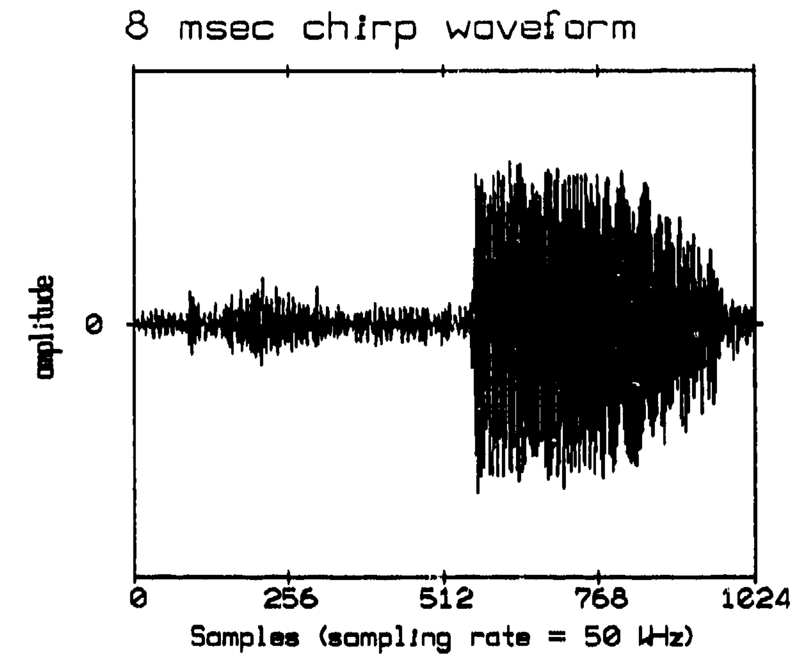

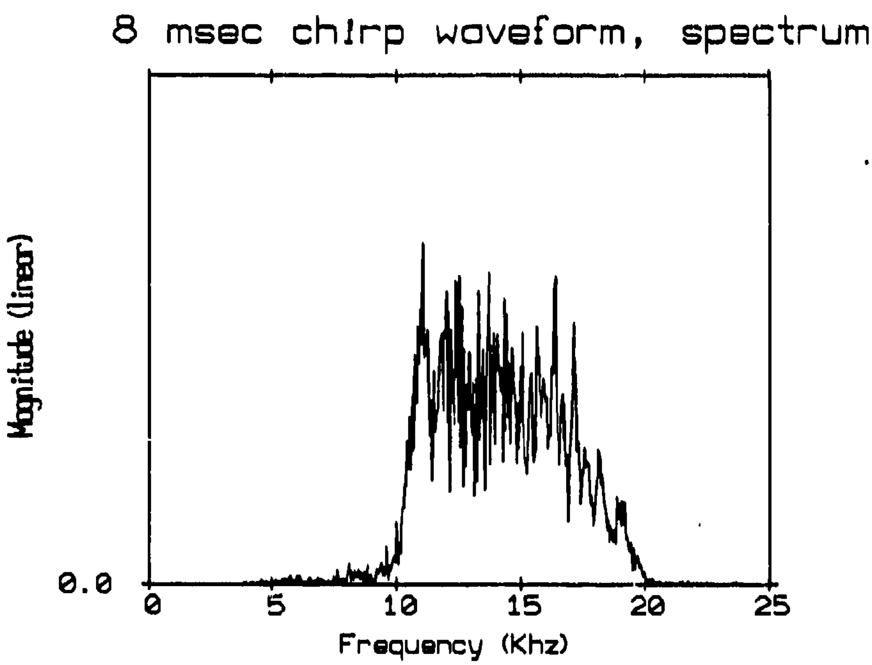

144543.1.ch2 , pulse No6

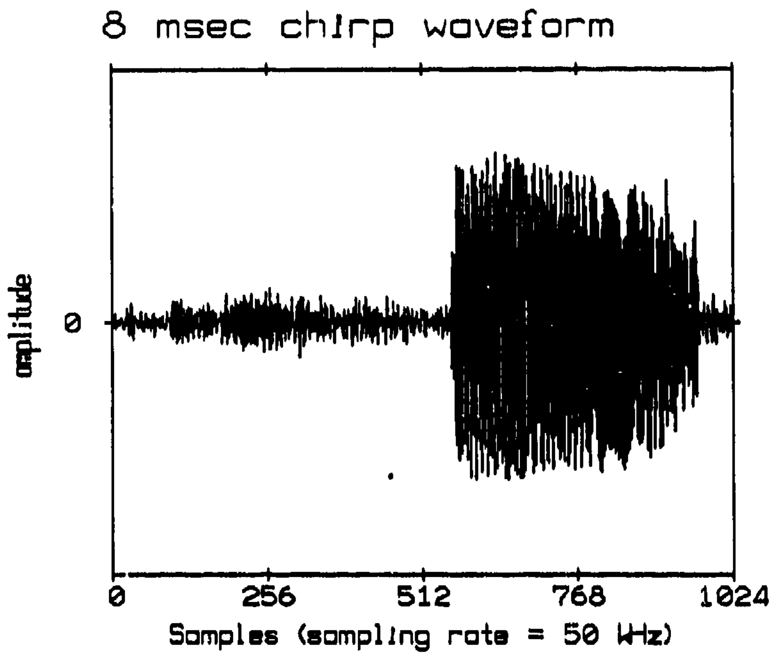

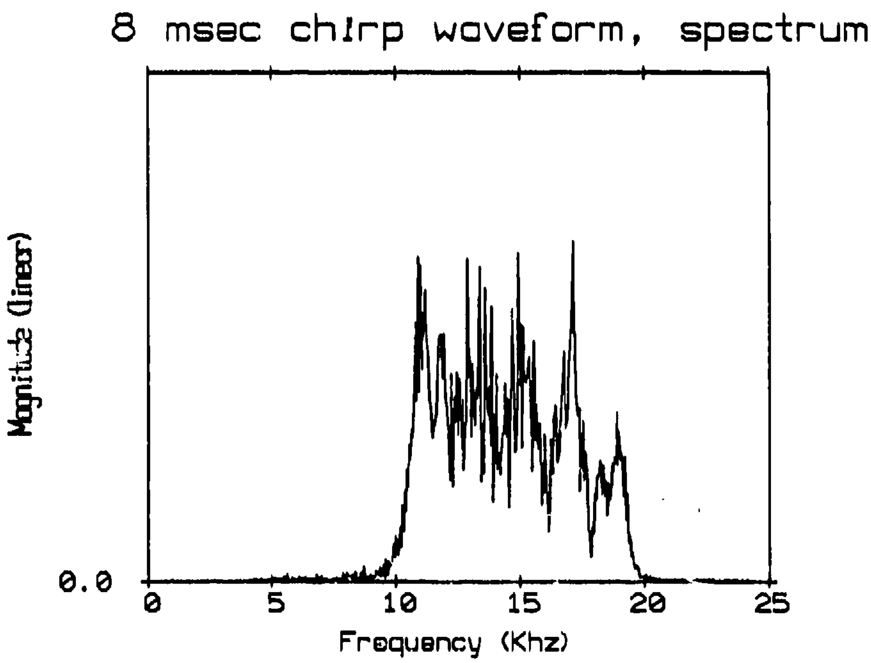

144543.1.ch2 , pulse No7

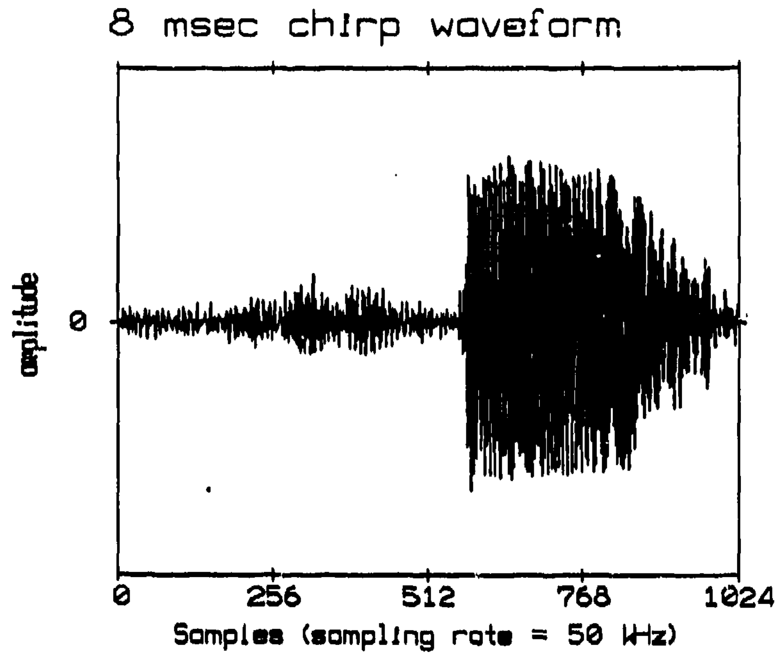

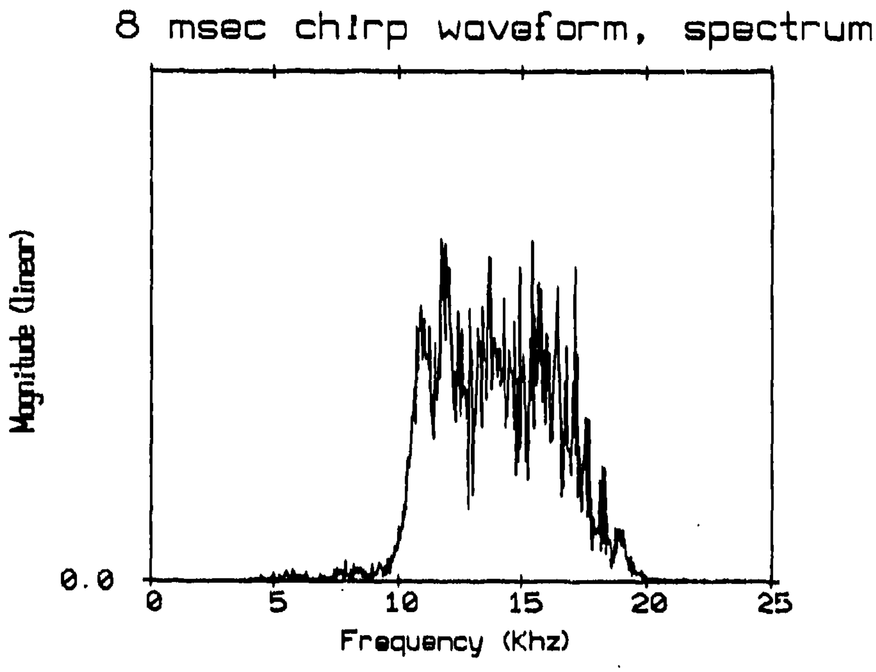

144543.1.ch2 , pulse No8

8 msec chirp waveform

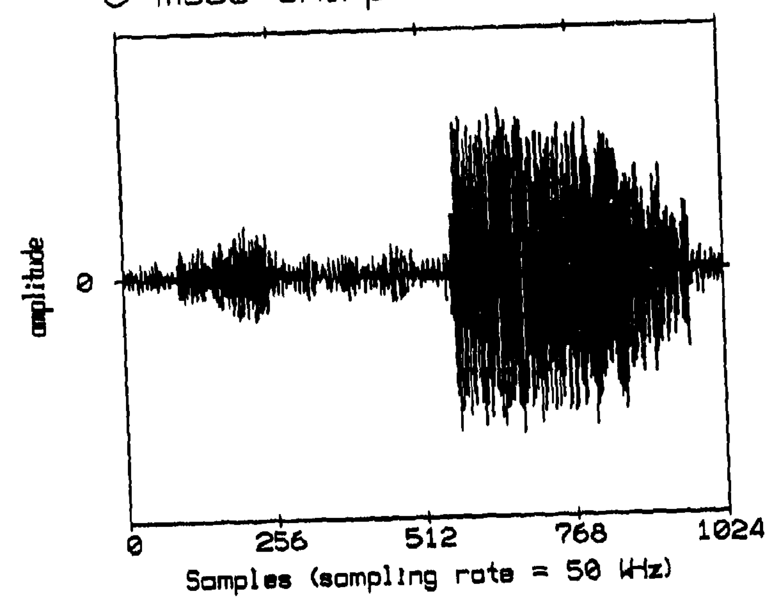

8 msec chirp waveform, spectrum

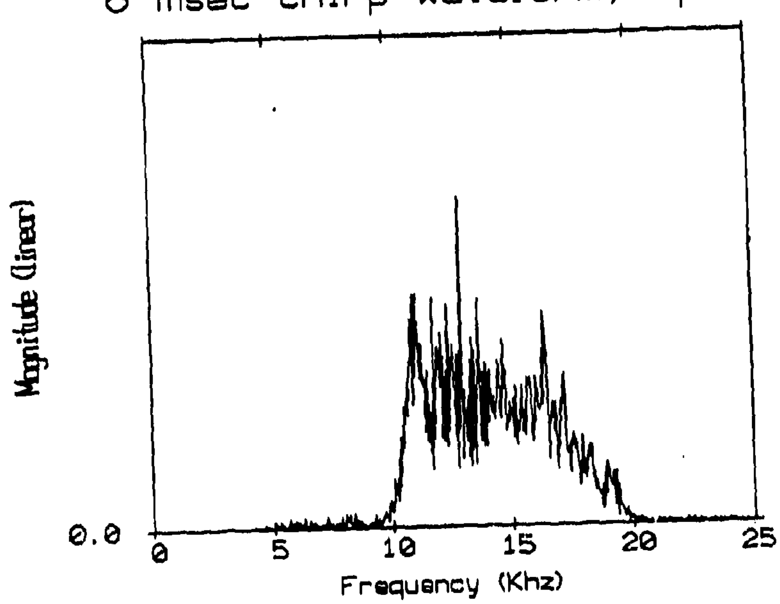

144543.1.ch2 , pulse No9

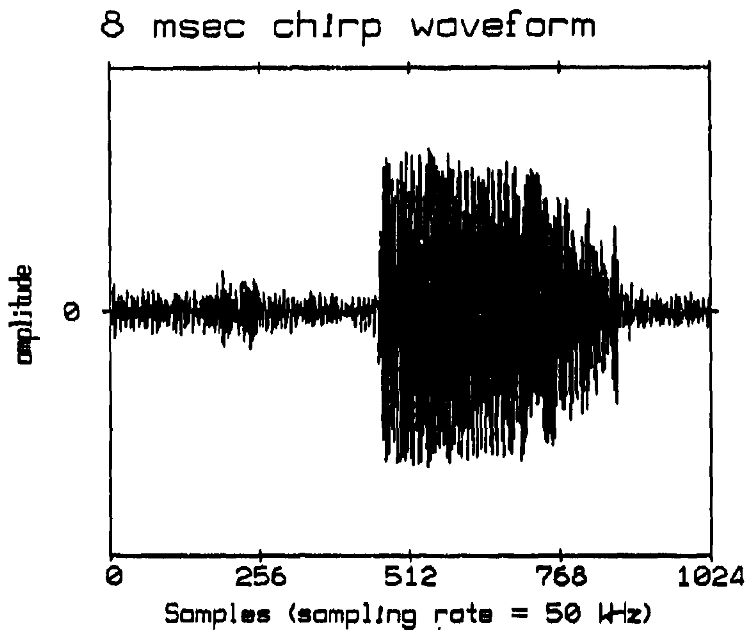

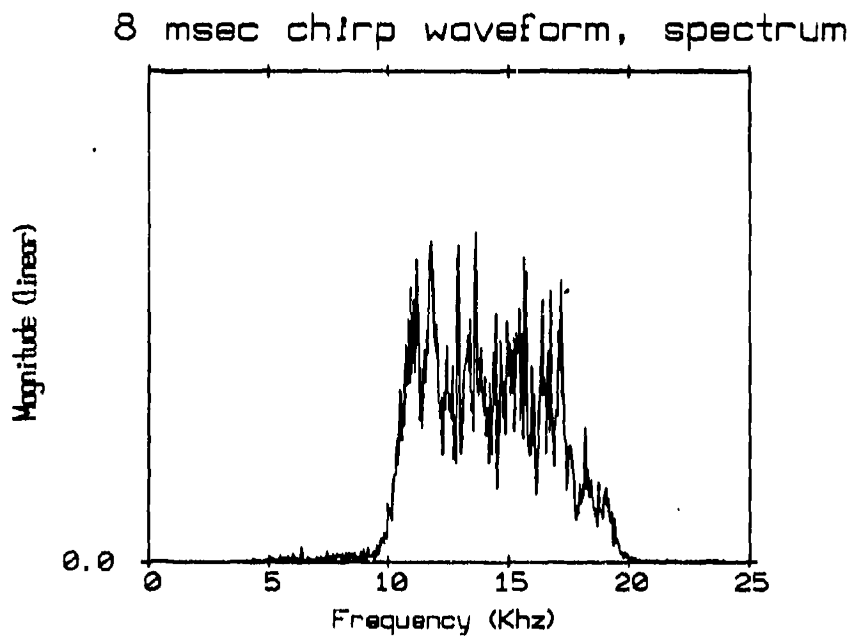

144543.1.ch2 , pulse No10

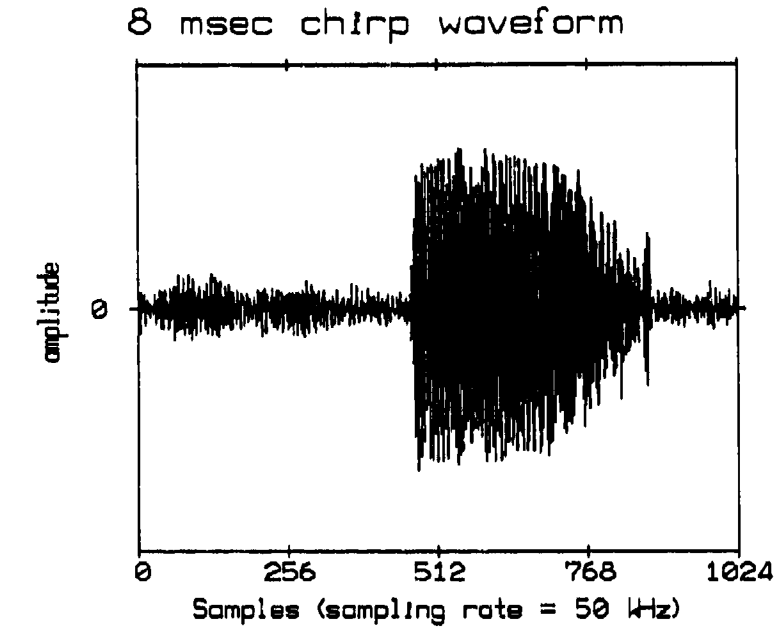

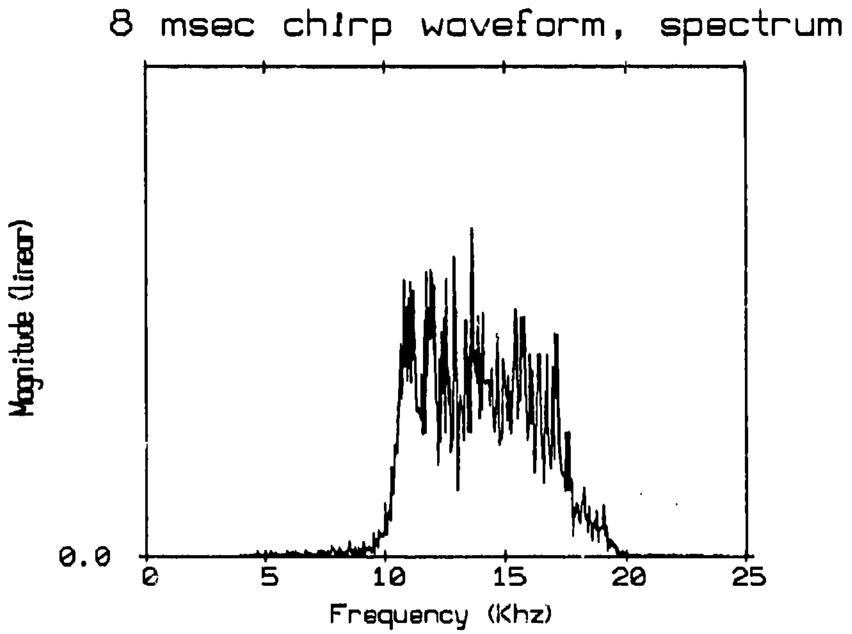

144543.1.ch2 , pulse No11

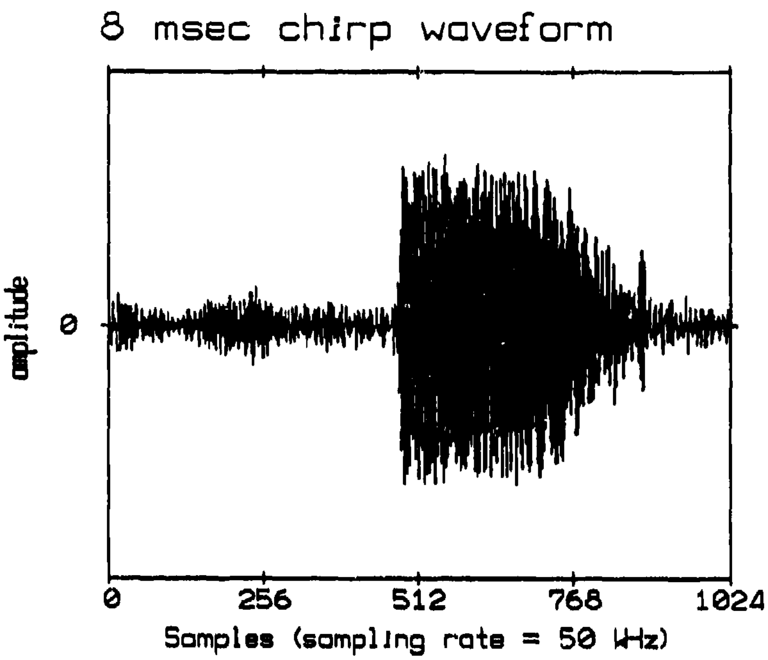

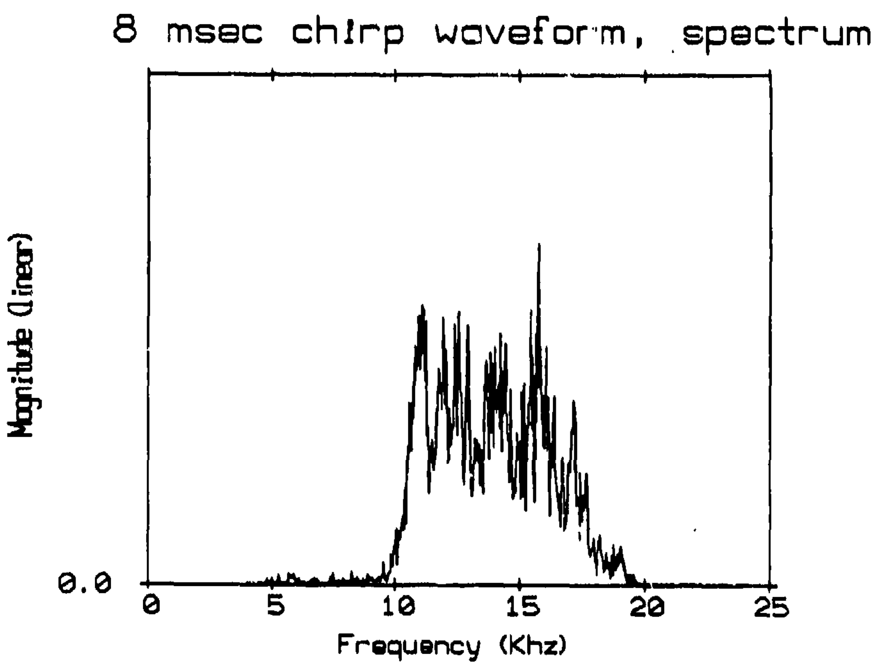

144543.1.ch2 , pulse No12

8 msec chirp waveform

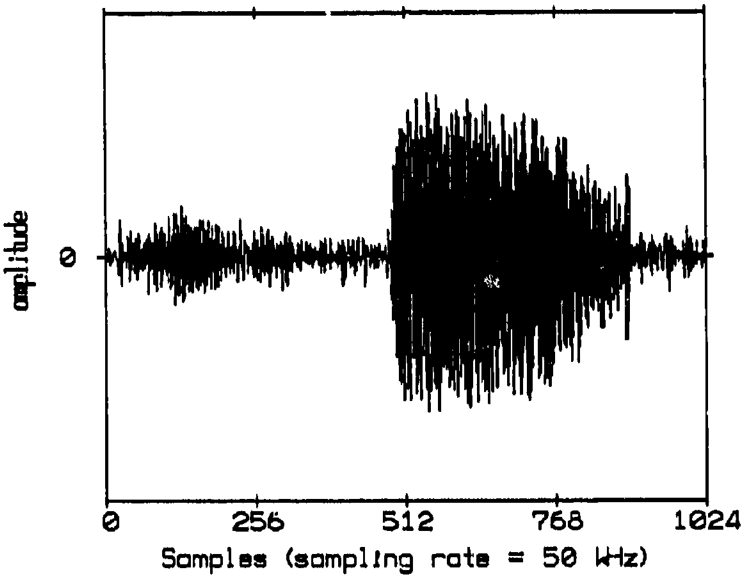

8 msec chirp waveform, spectrum

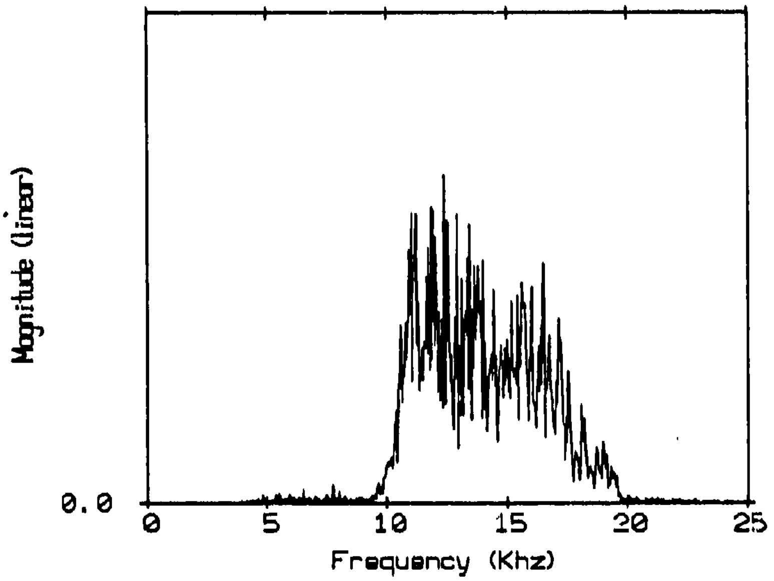

144543.1.ch2 , pulse No13

8 msec chirp waveform

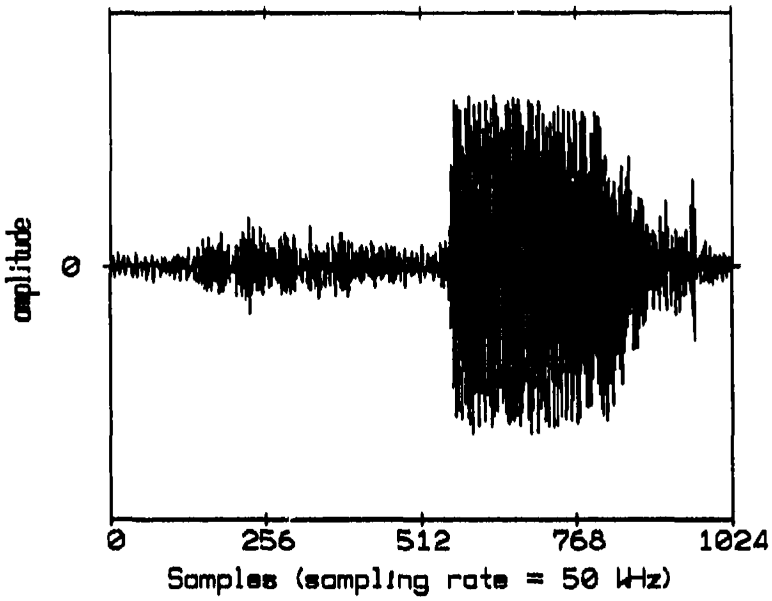

8 msec chirp waveform, spectrum

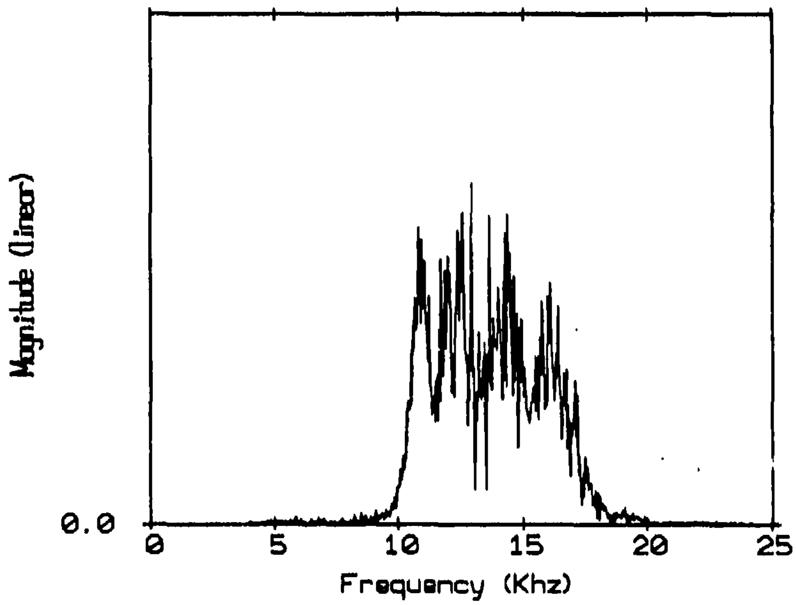

144543.1.ch2 , pulse No14

8 msec chirp waveform

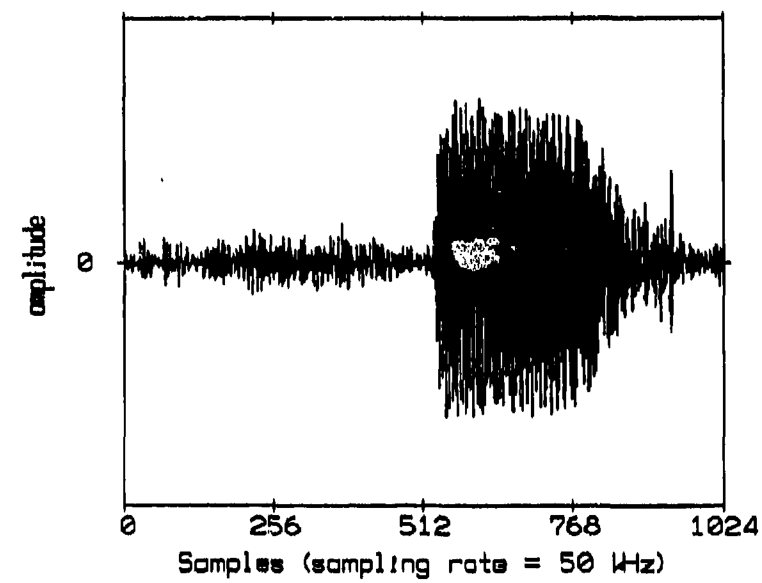

8 msec chirp waveform, spectrum

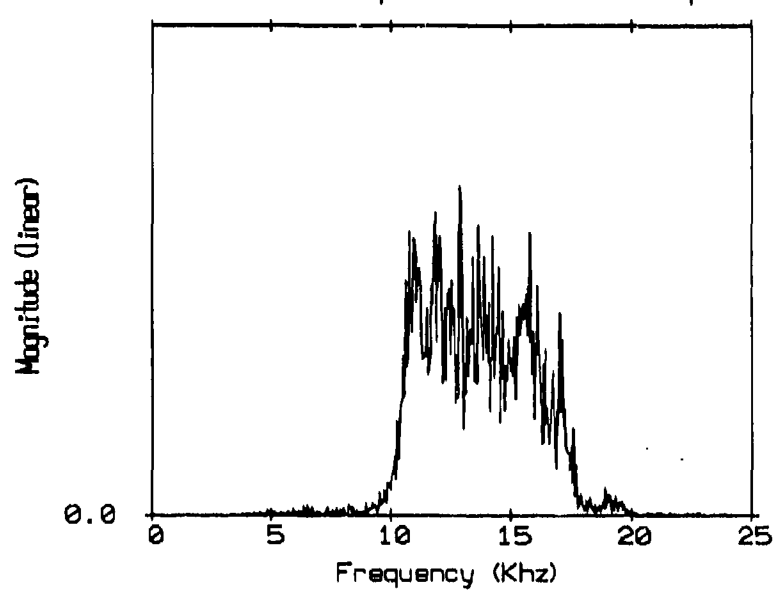

144543.1.ch2 , pulse No15

8 msec chirp waveform

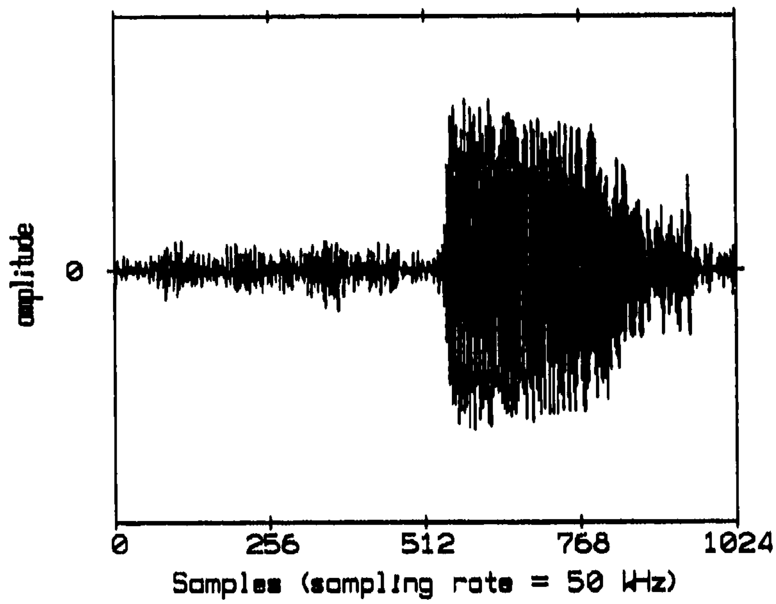

8 msec chirp waveform, spectrum

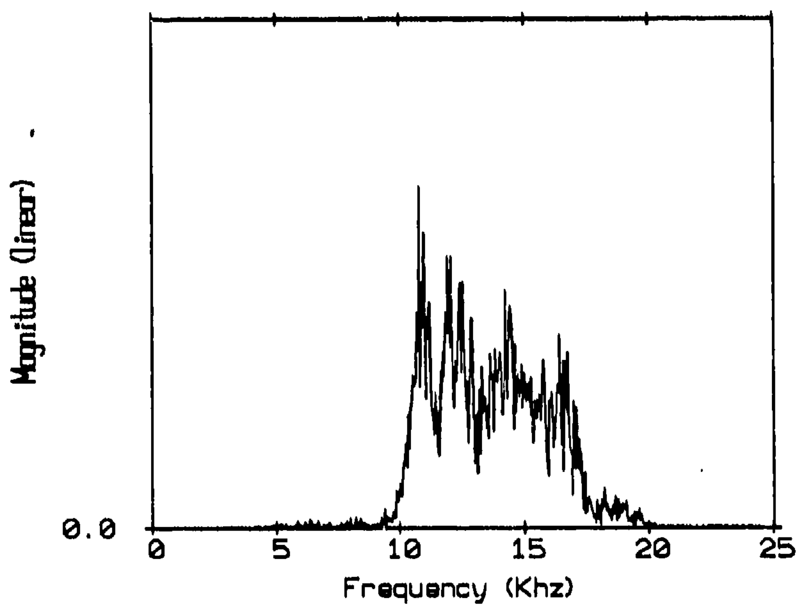

144543.1.ch2 , pulse No16

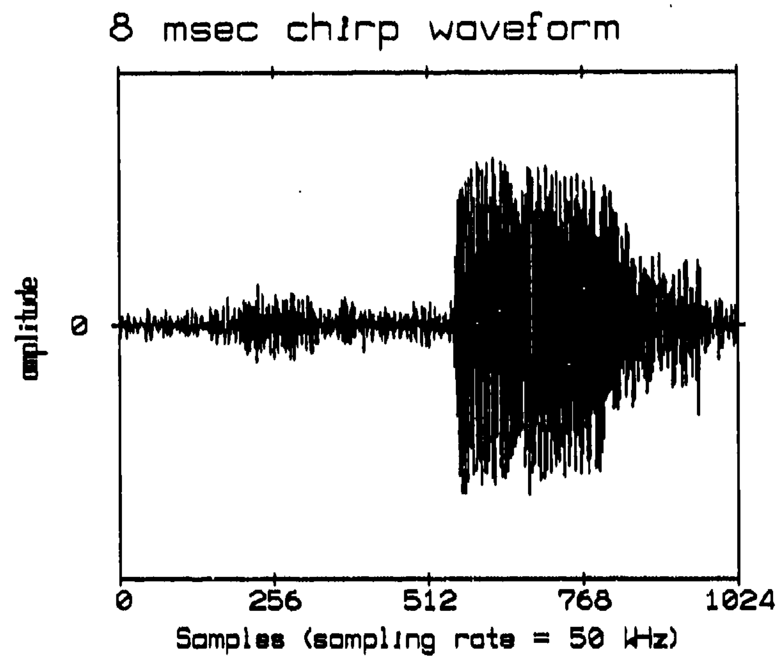

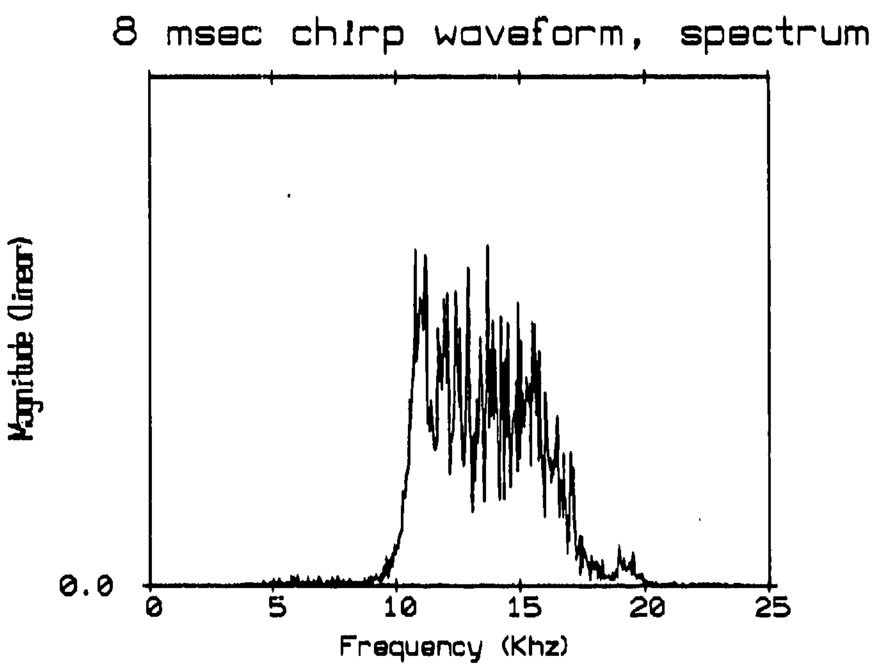

144543.1.ch2 , pulse No17

8 msec chirp waveform

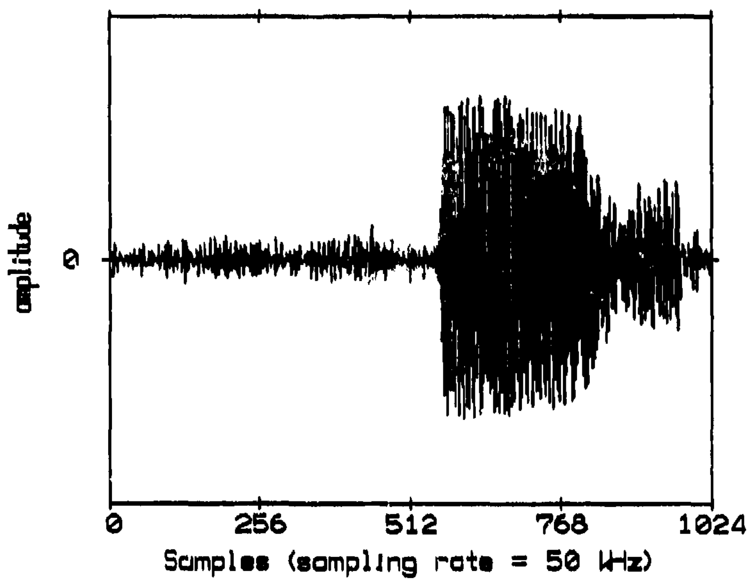

8 msec chirp waveform, spectrum

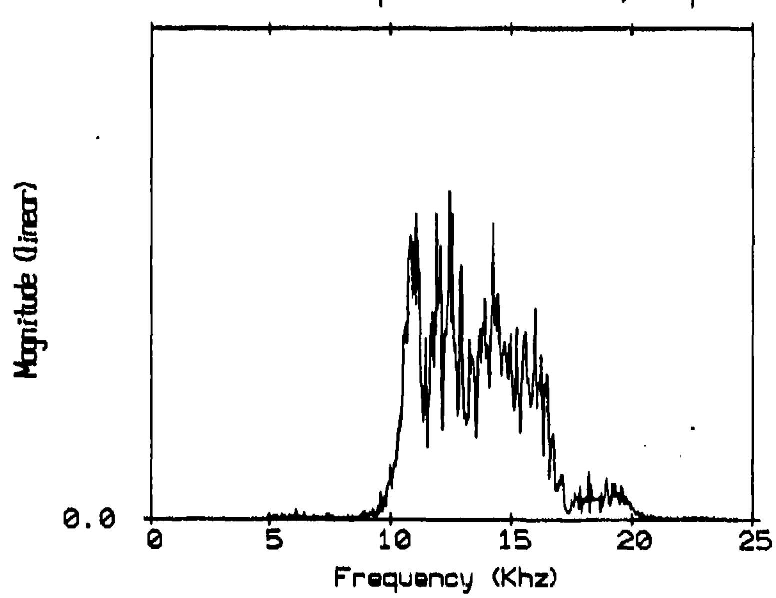

144543.1.ch2 , pulse No18

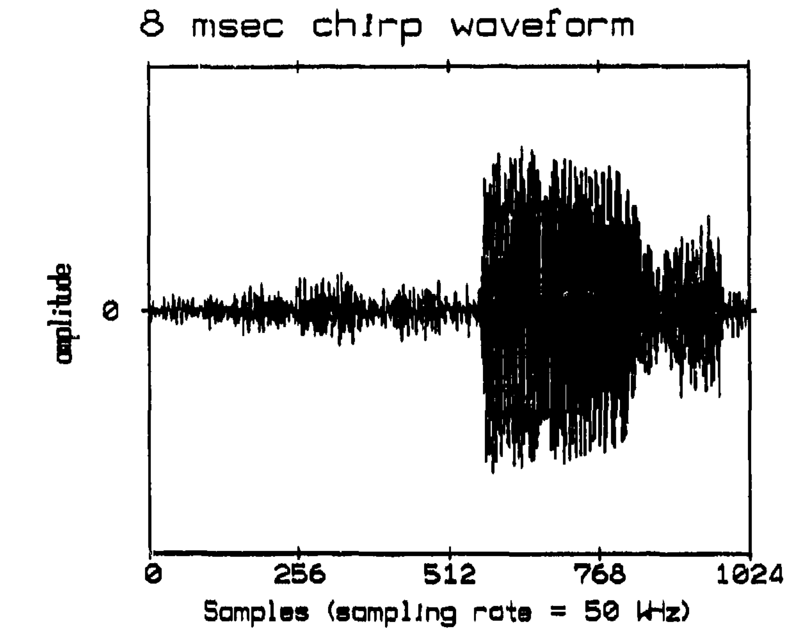

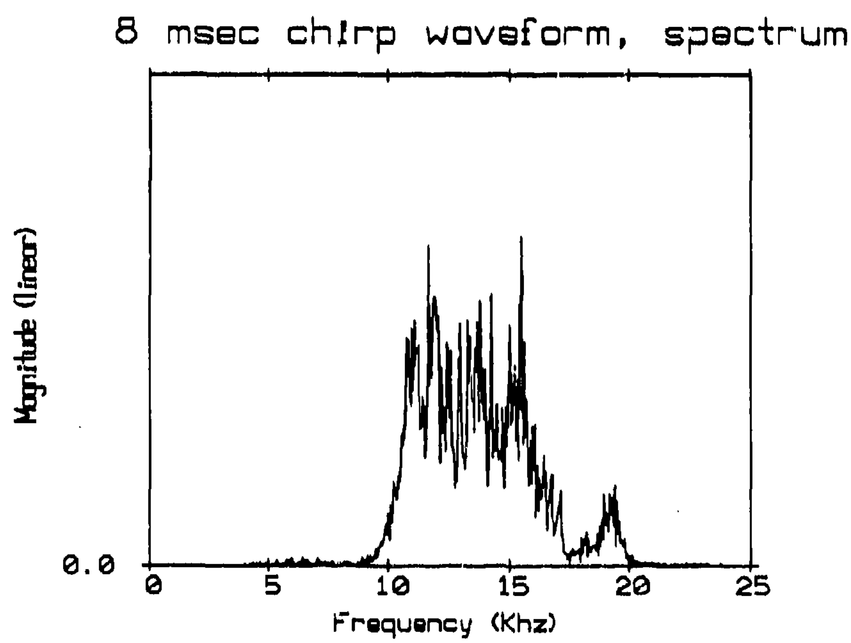

144543.1.ch2 , pulse No19

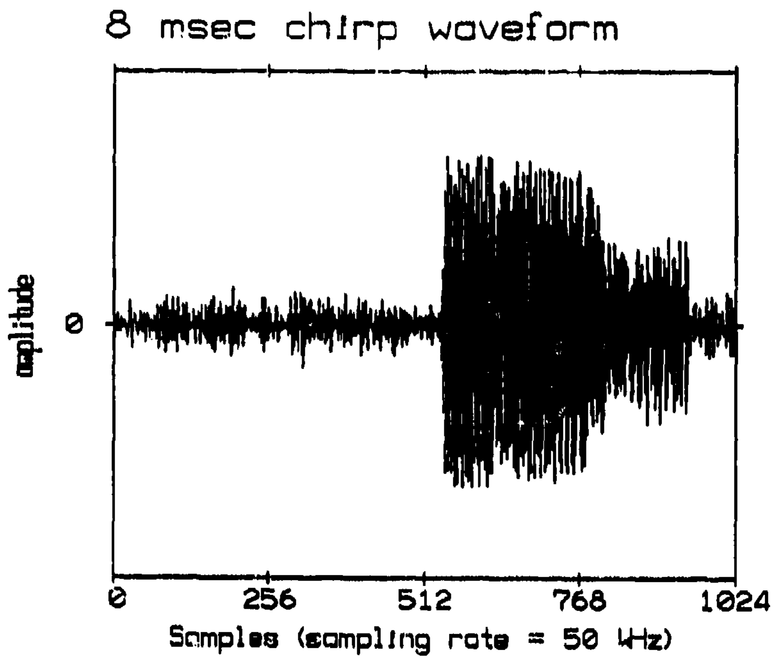

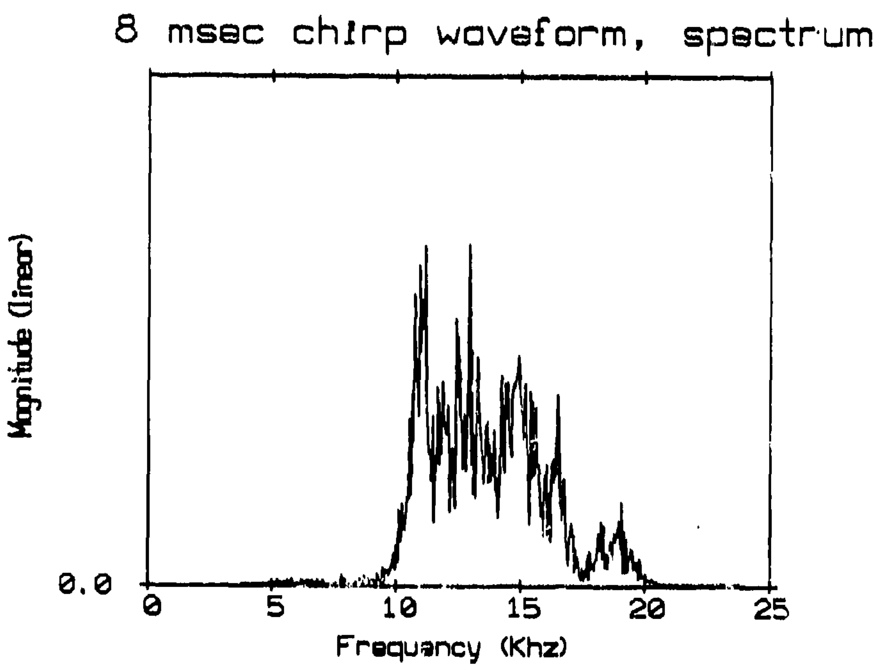

144543.1.ch2 , pulse No20

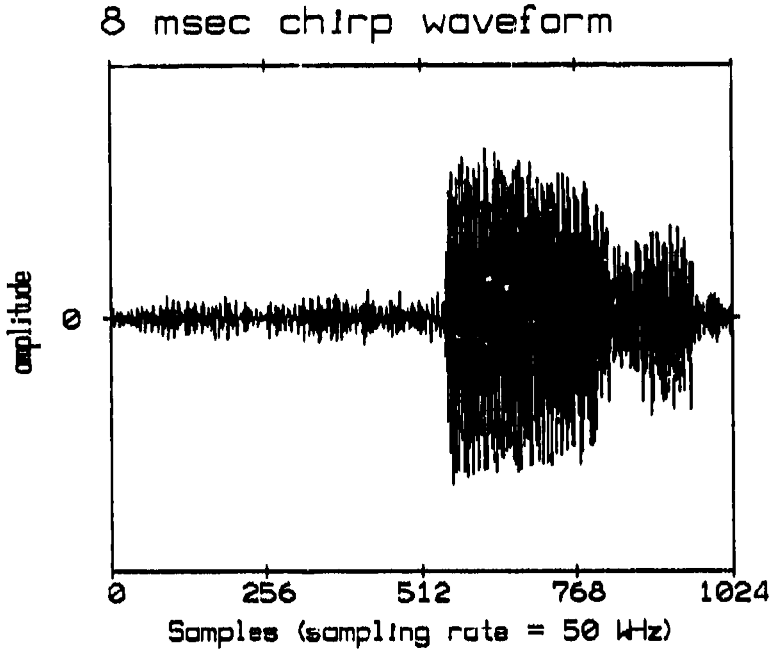

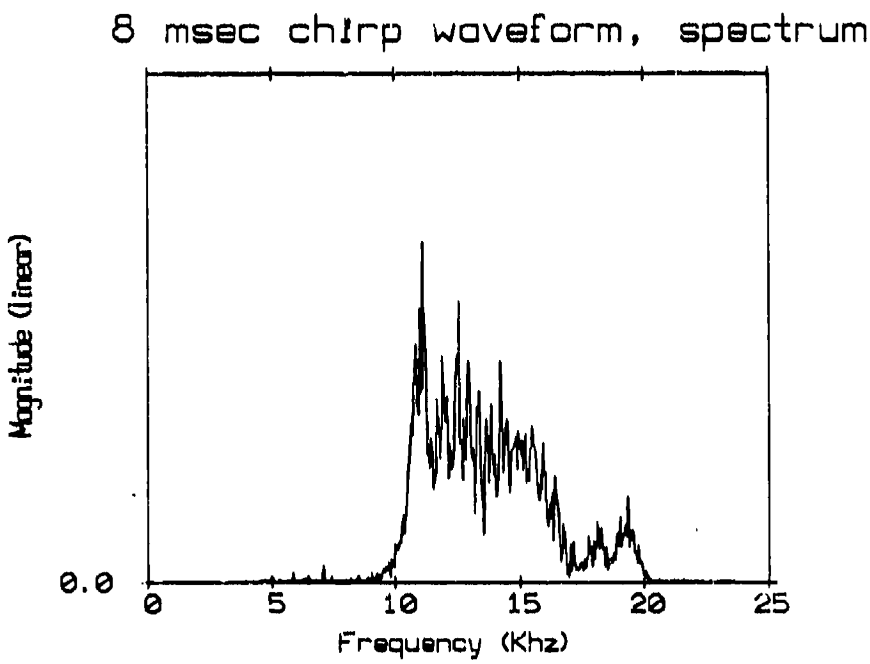

144543.1.ch2 , pulse No21

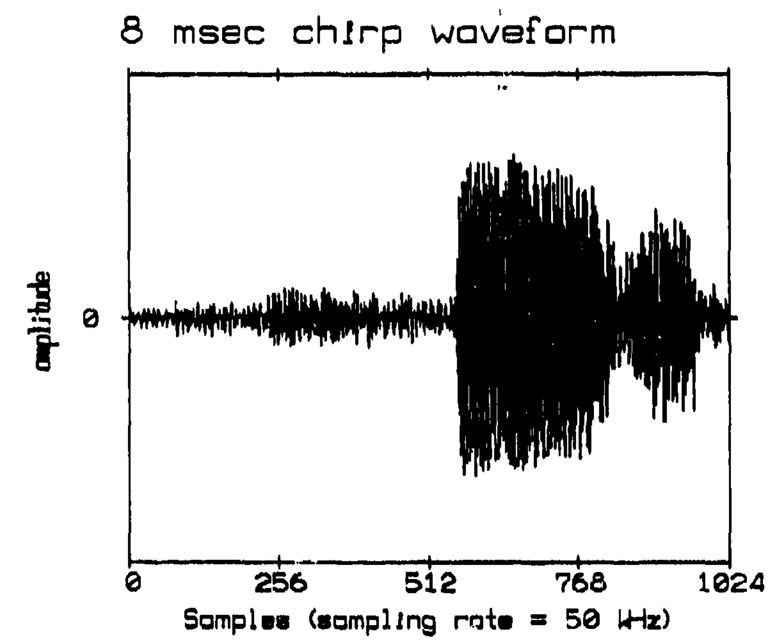

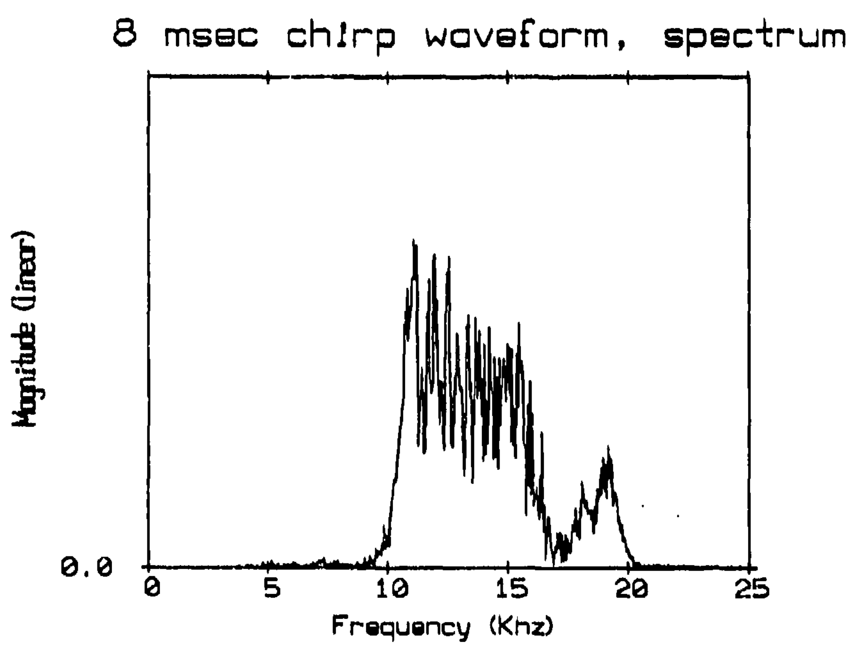

144543.1.ch2 , pulse No22

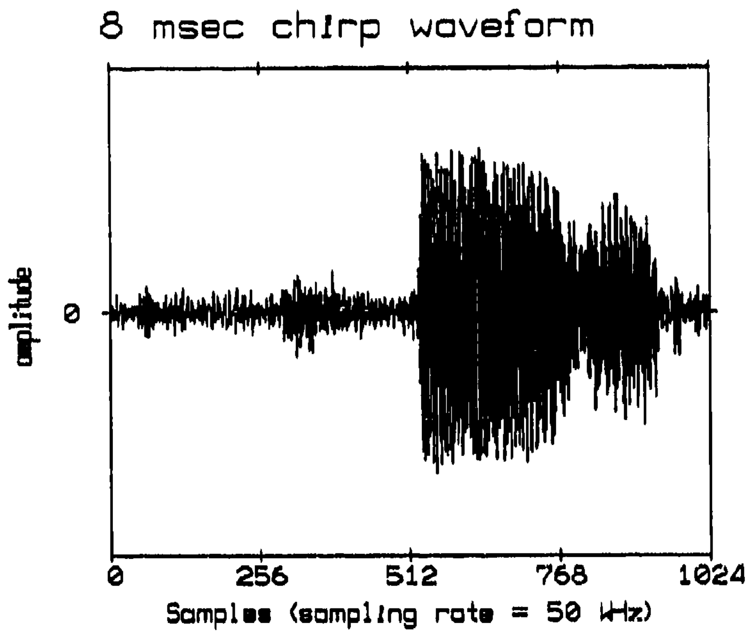

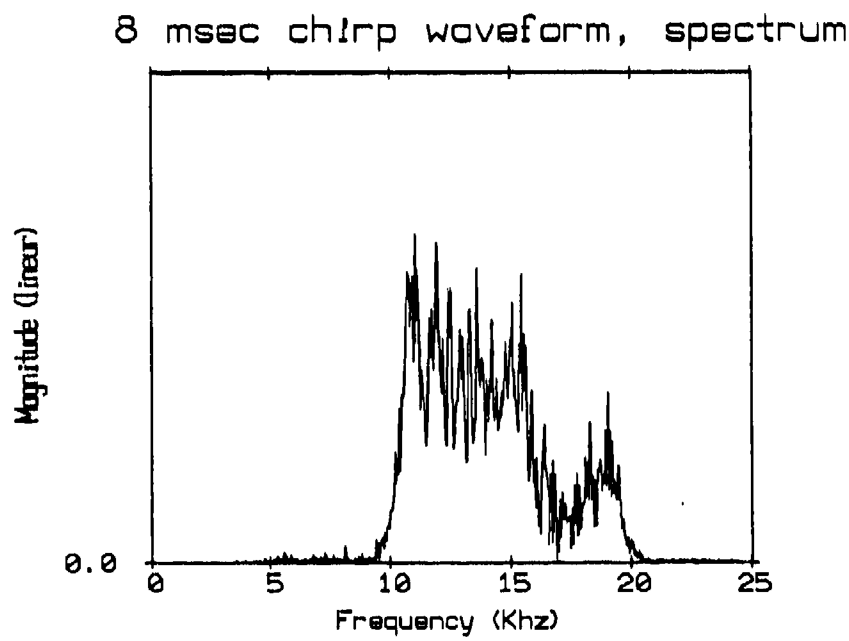

144543.1.ch2 , pulse No23

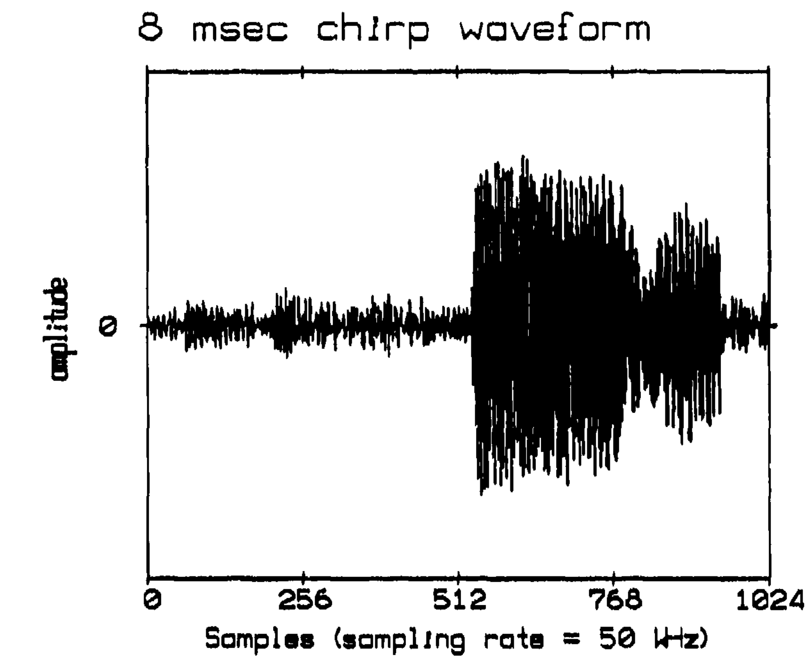

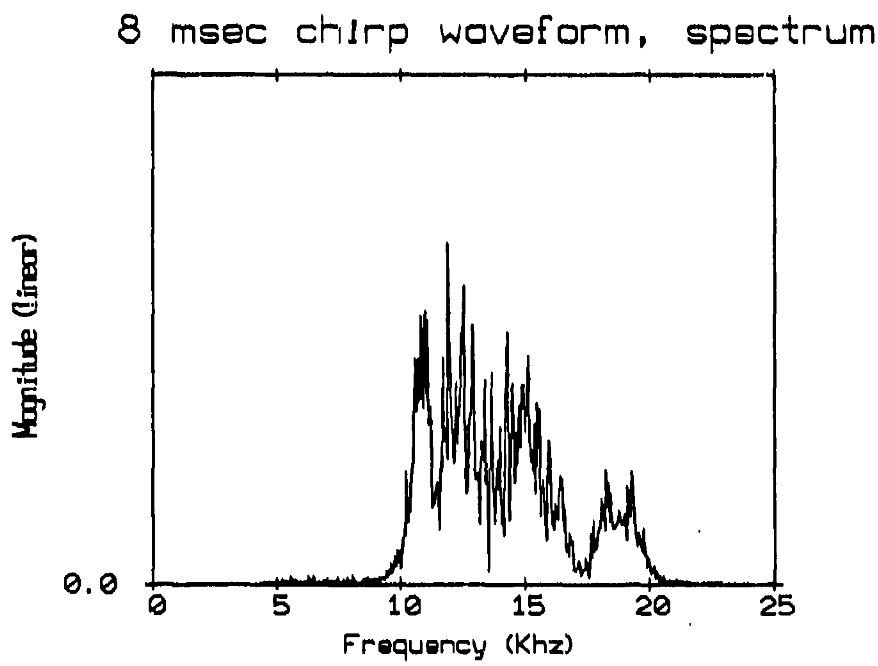

144543.1.ch2 , pulse No24

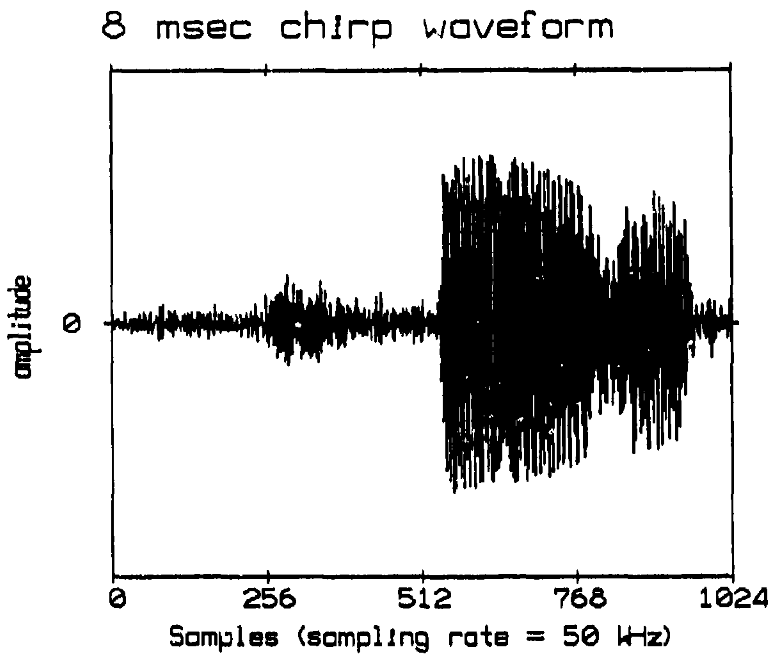

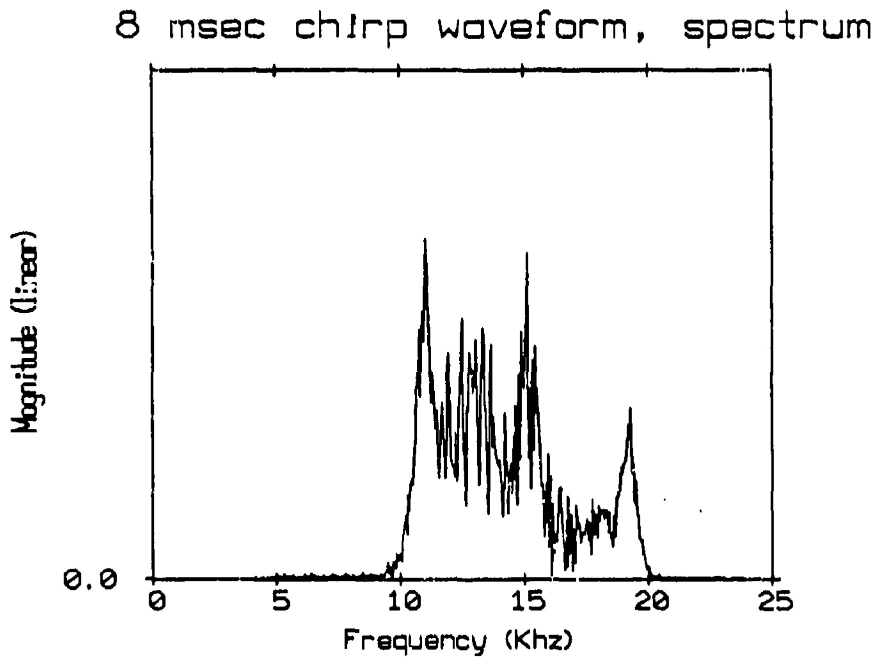

144543.1.ch2 , pulse No25

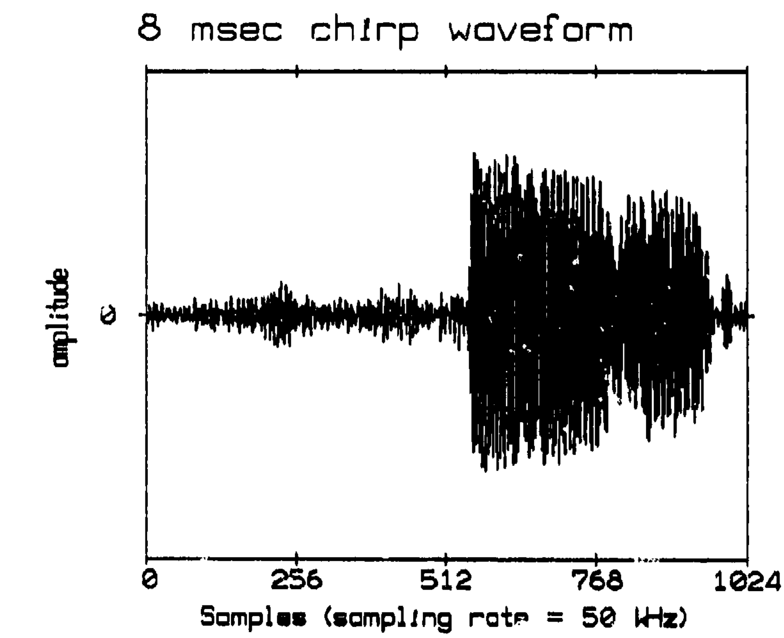

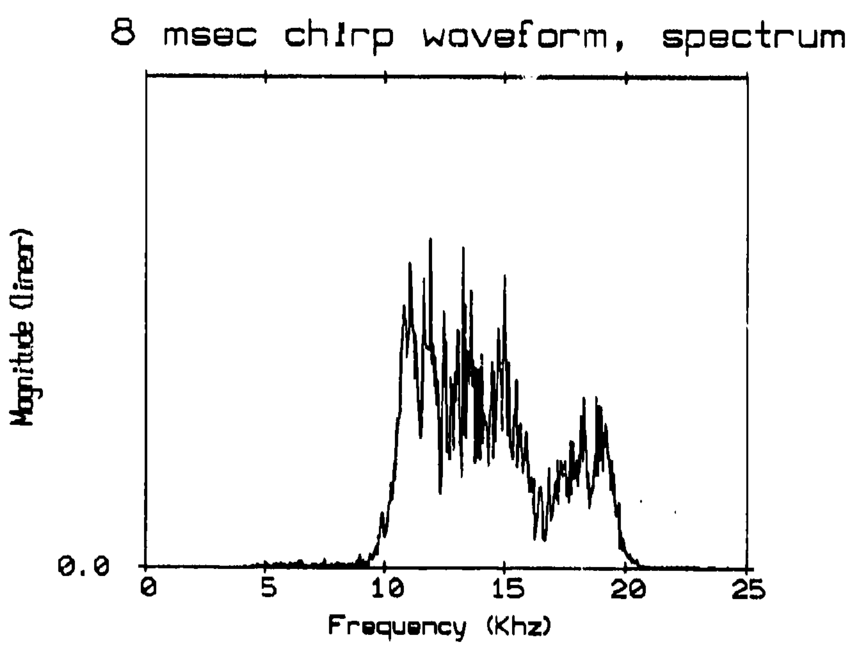

144543.1.ch2 , pulse No26

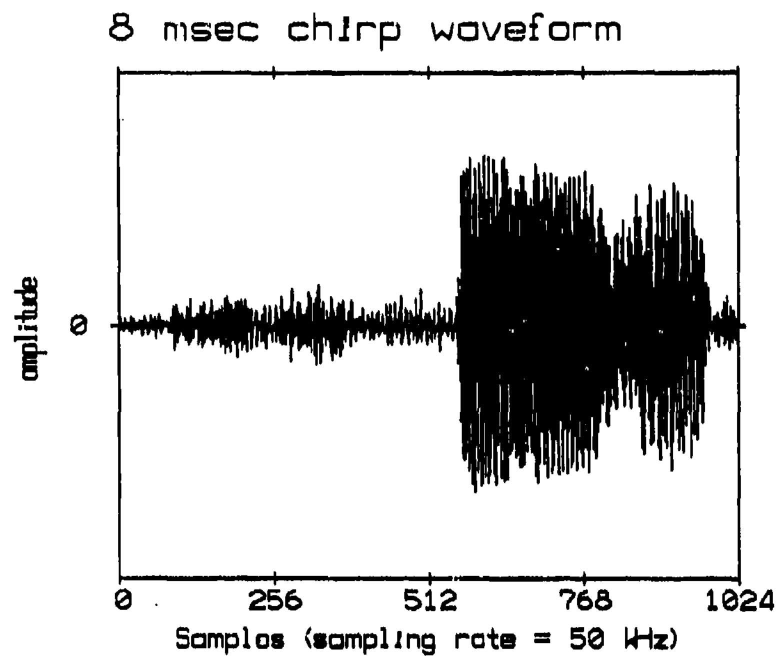

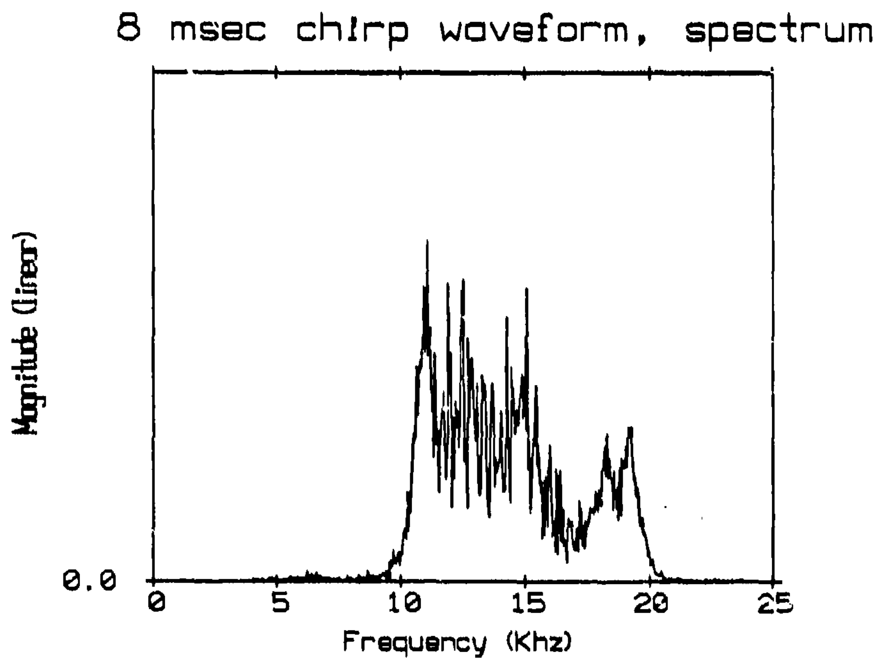

144543.1.ch2 , pulse No27

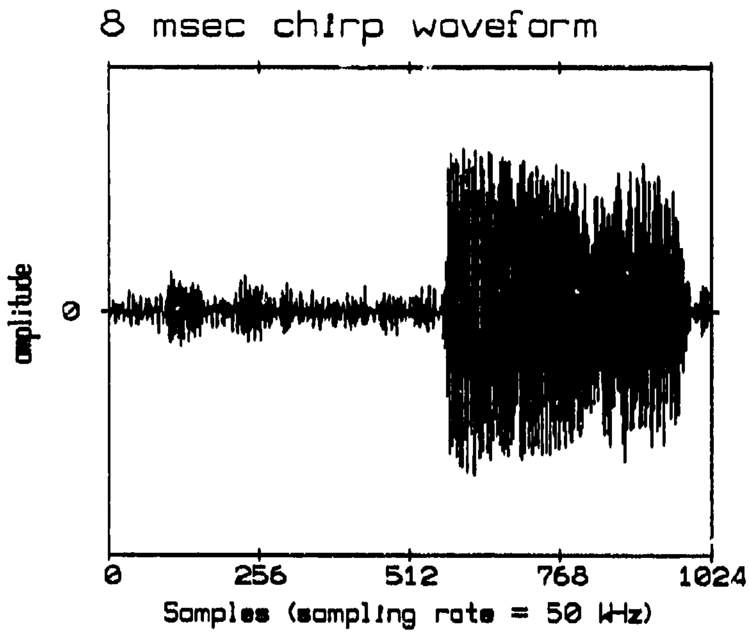

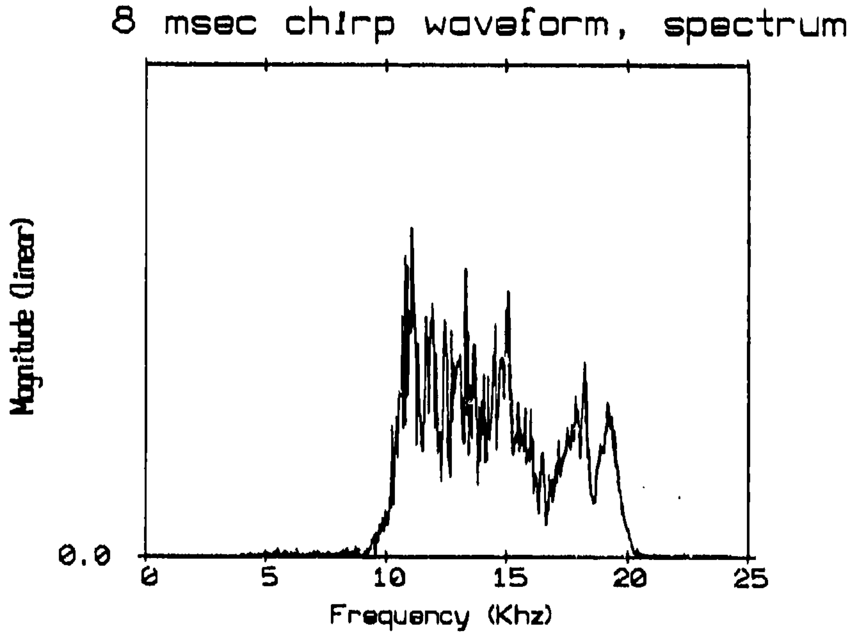

144543.1.ch4 , pulse No1

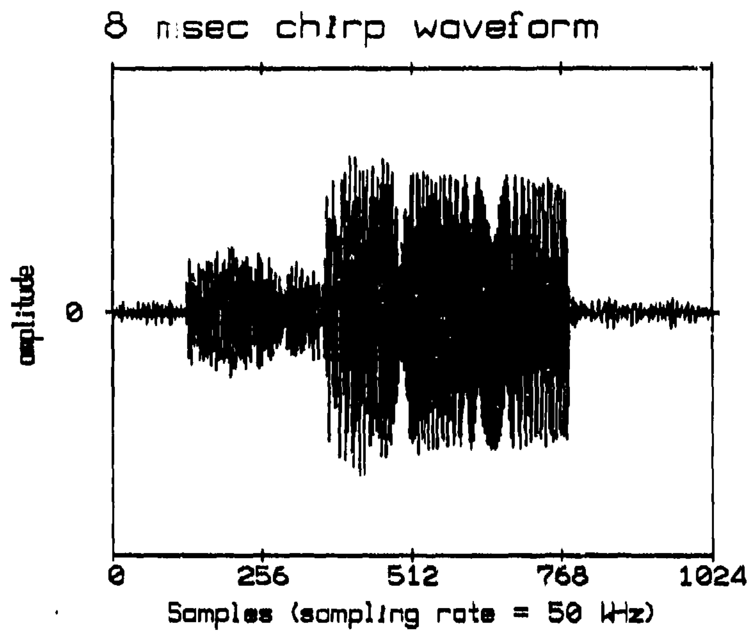

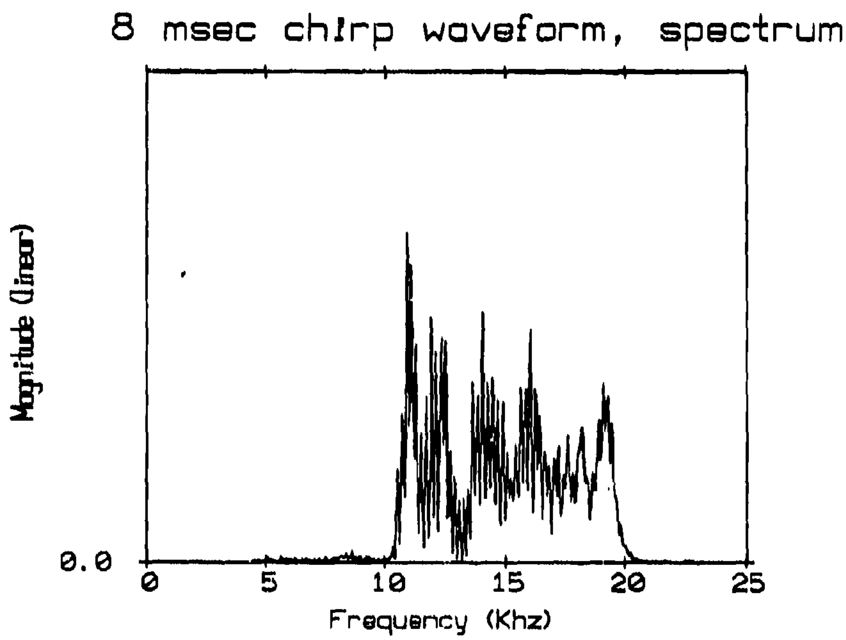

Figures 3.28-3.54. Waveforms and spectra of 27 eight msec chirps as was received by sonobuoy No 4.

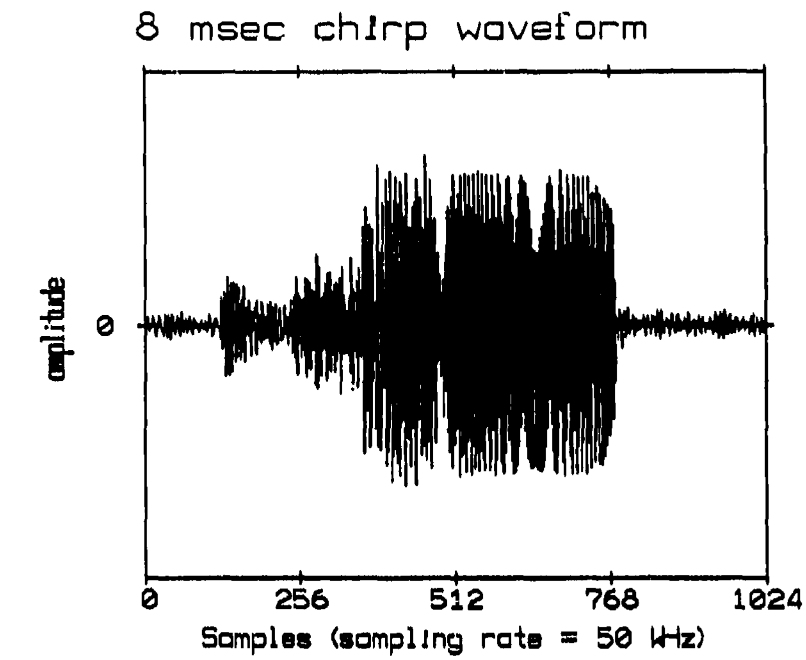

8 msec chirp waveform
amplitude
0
0
256
512
768
1024
Samples (sampling rate = 50 kHz)

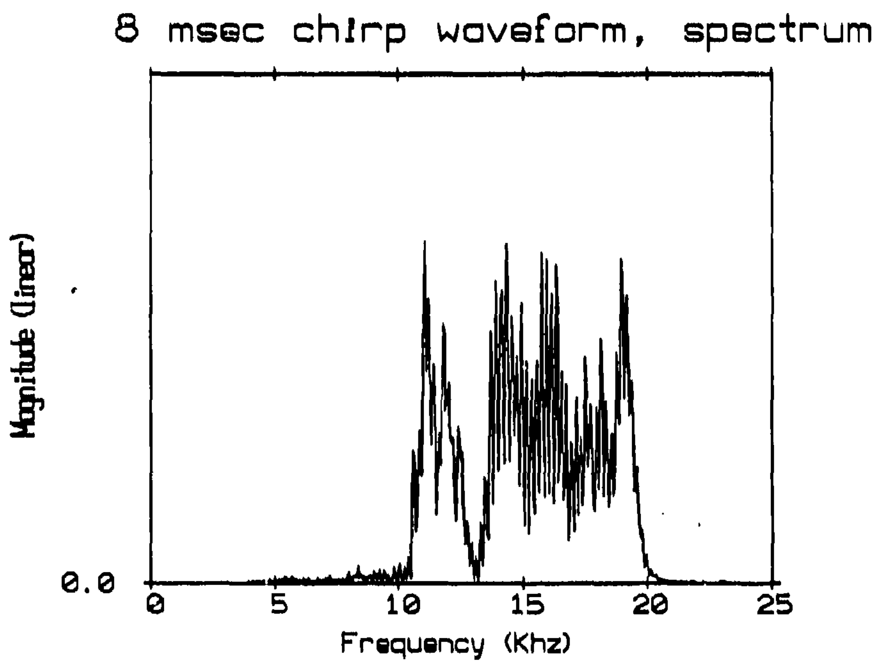

8 msec chirp waveform, spectrum
Magnitude (linear)
0.0
0
5
10
15
20
25
Frequency (Khz)

144543.1.ch4 , pulse No3

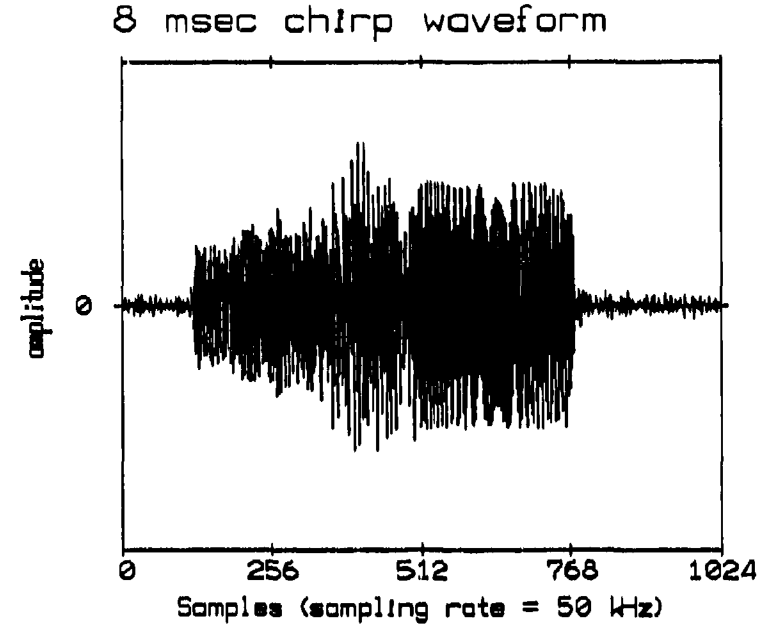

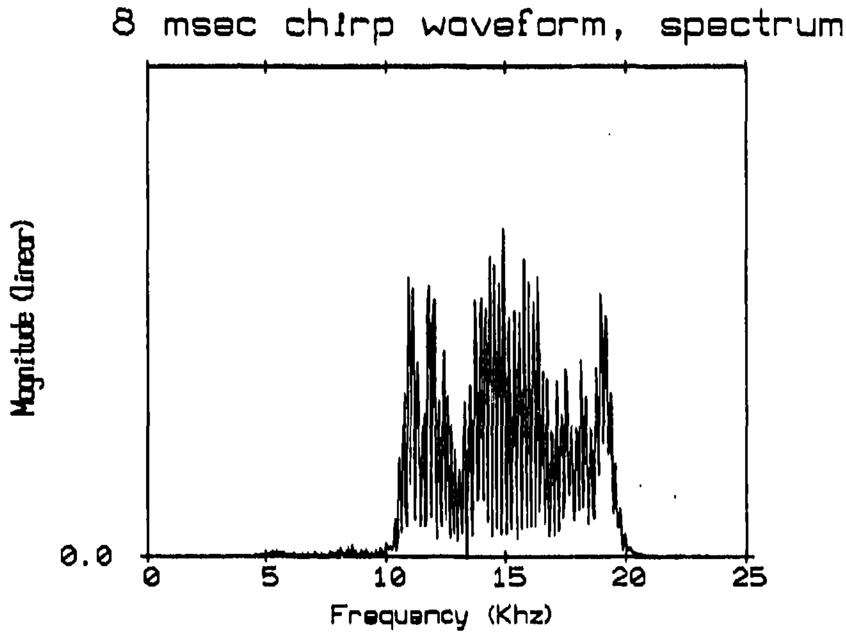

144543.1.ch4 , pulse No4

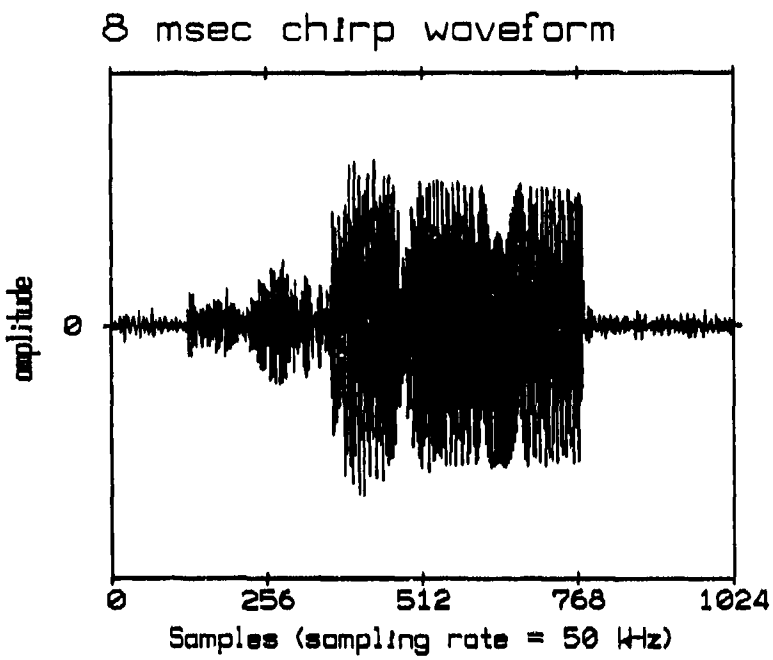

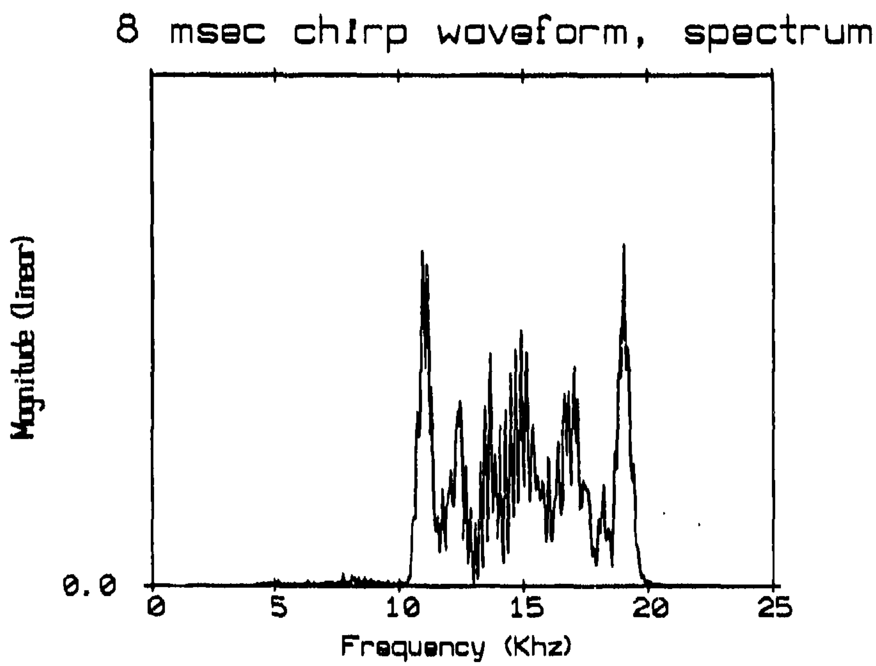

144543.1.ch4 , pulse No5

8 msec chirp waveform

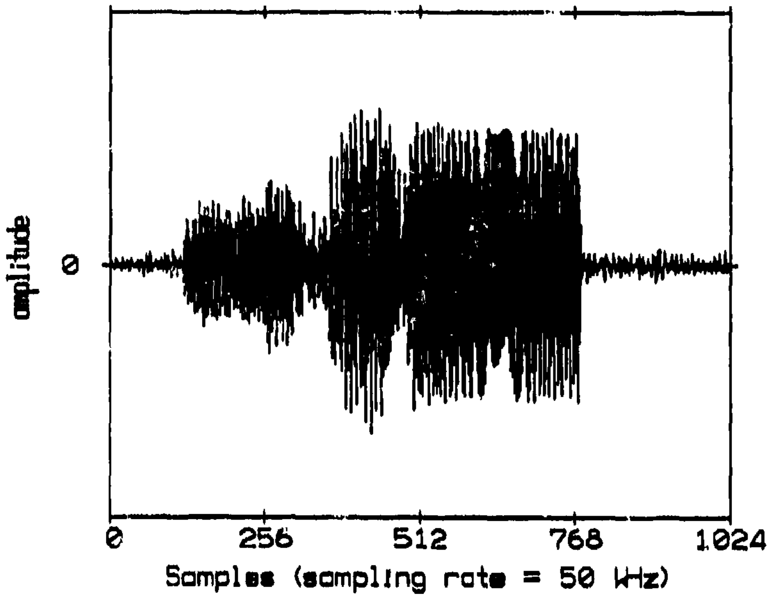

8 msec chirp waveform, spectrum

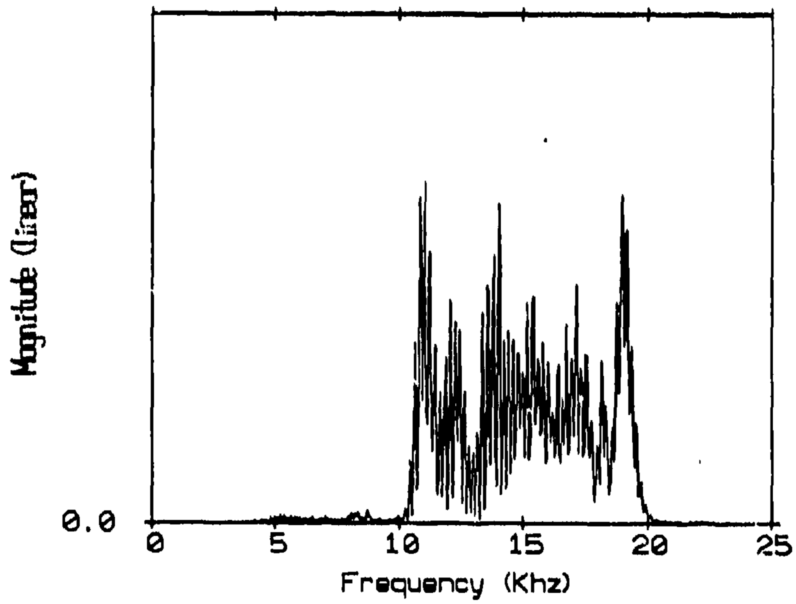

144543.1.ch4 , pulse No6

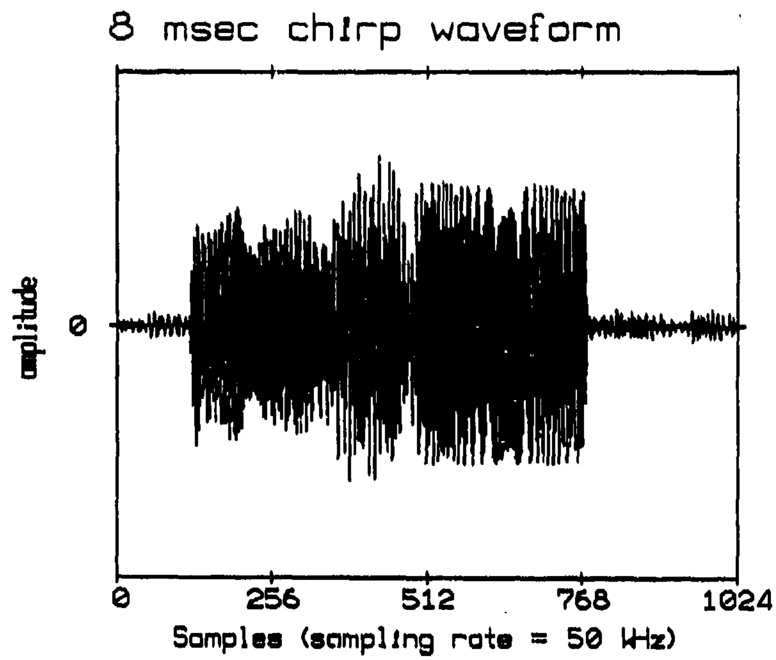

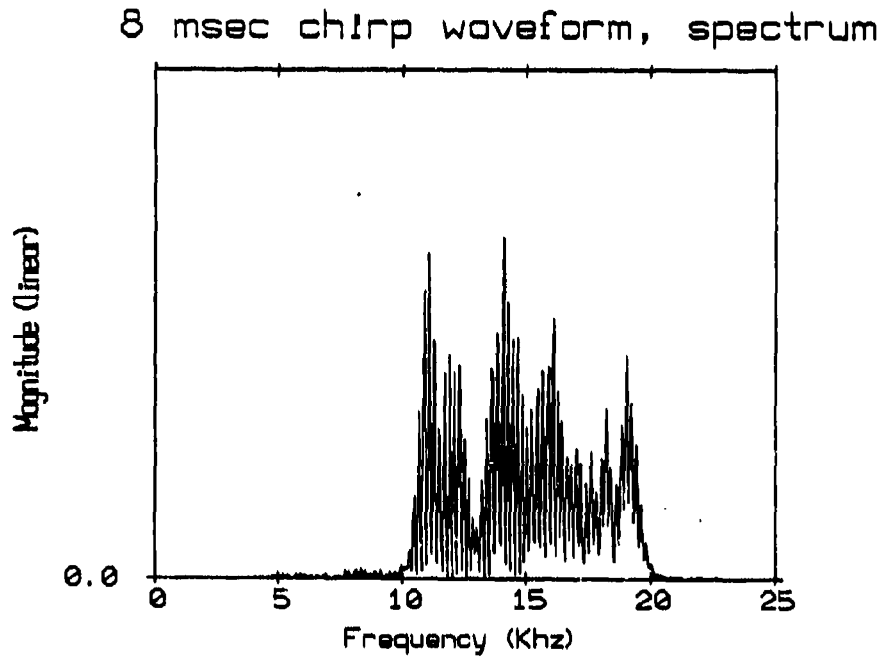

144543.1.ch4 , pulse No7

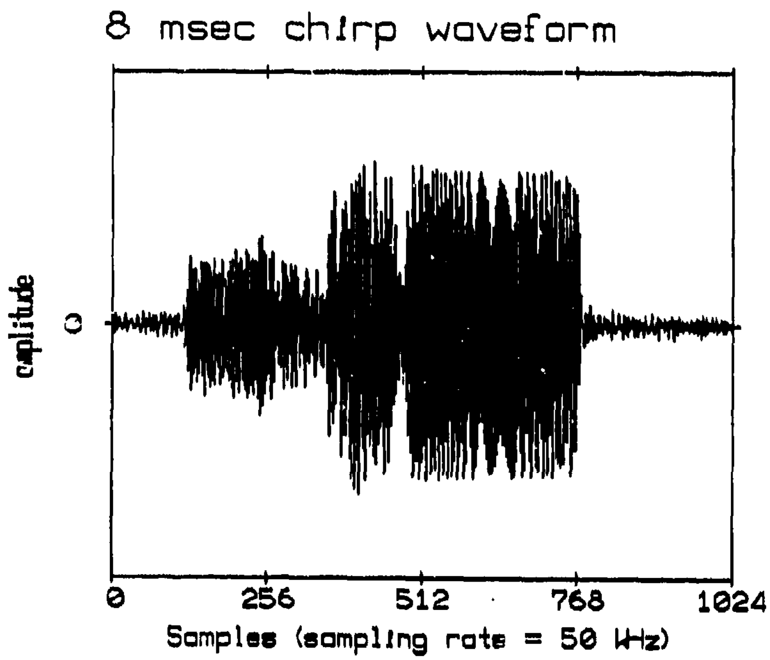

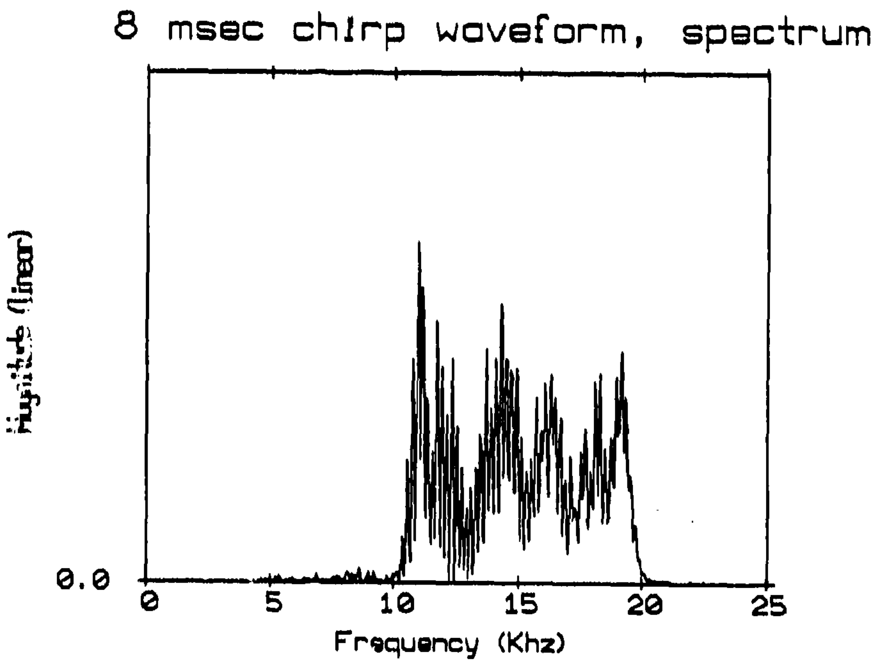

144543.1.ch4 , pulse No8

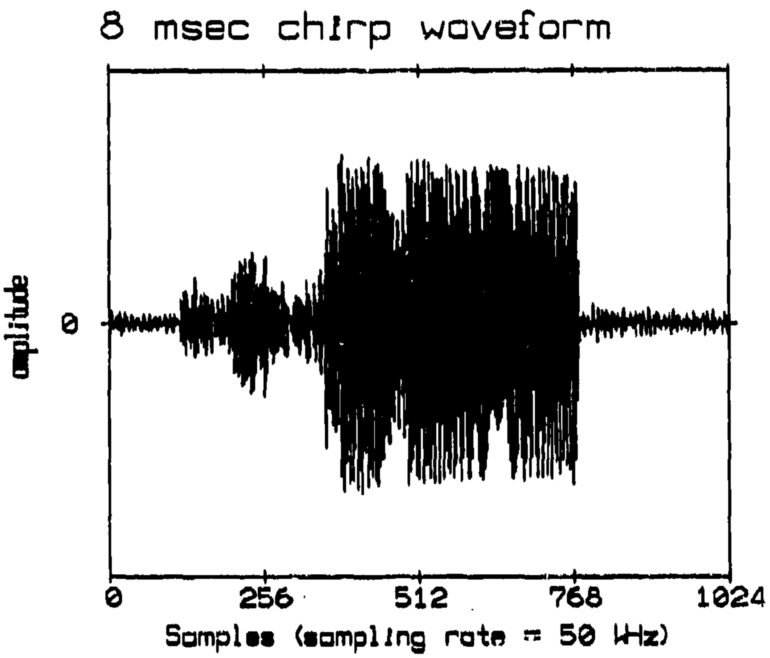

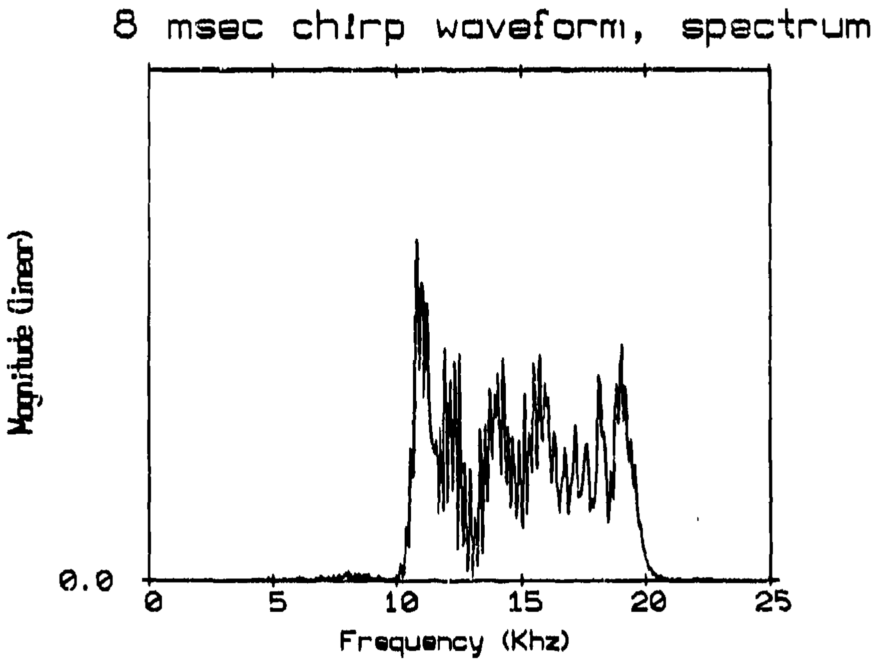

144543.1.ch4 , pulse No9

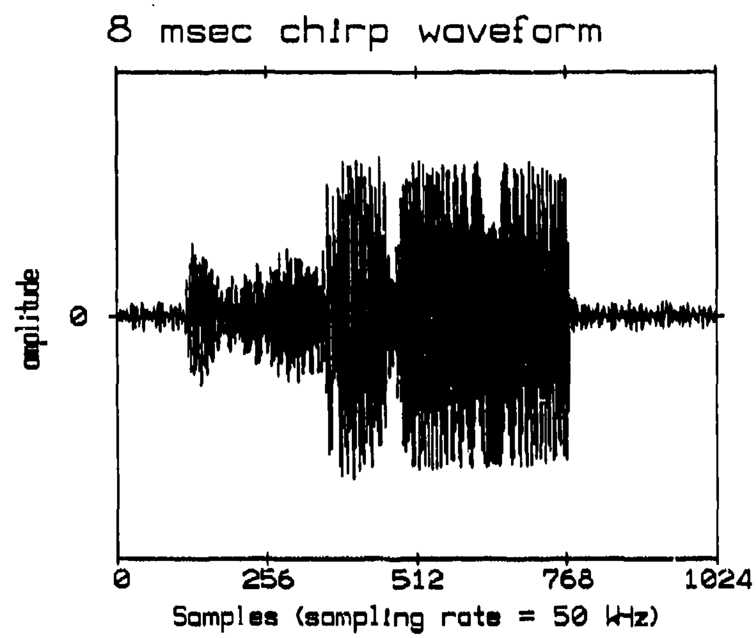

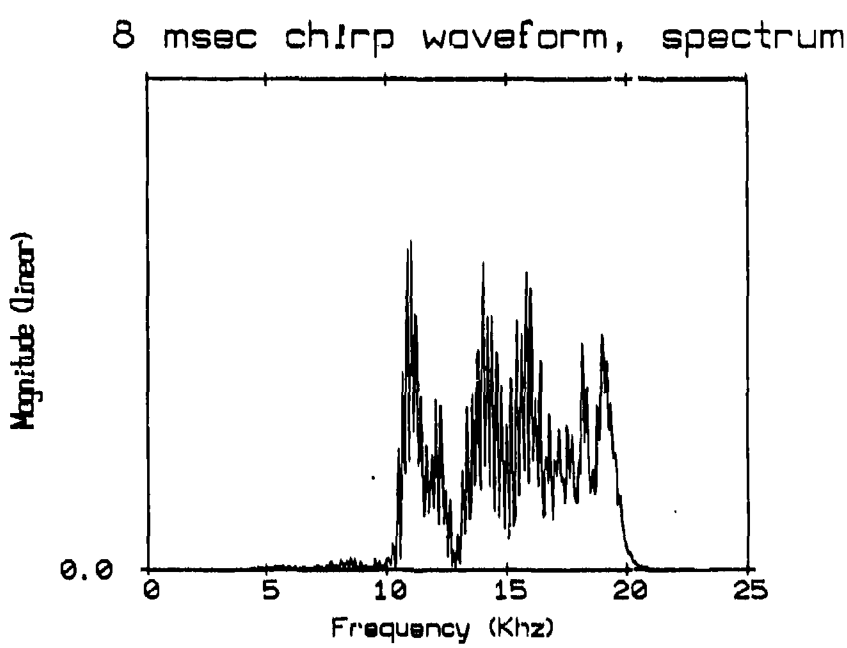

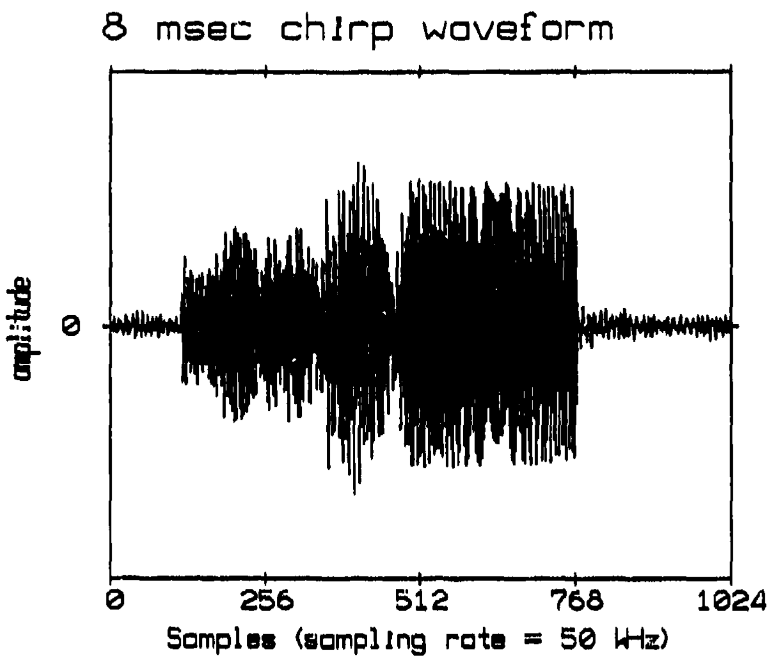
8 msec chirp waveform
amplitude
0
0
256
512
768
1024
Samples (sampling rate = 50 kHz)

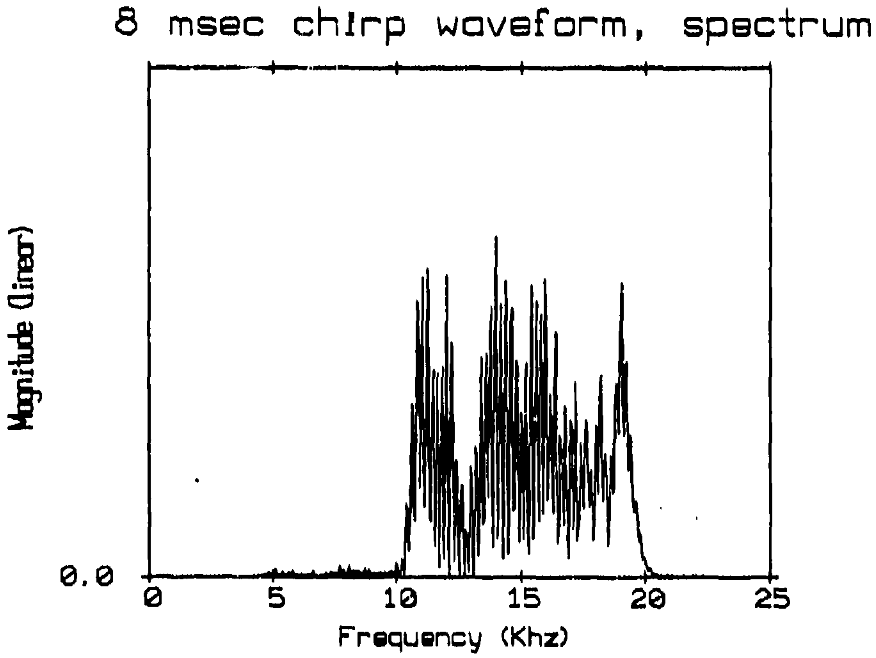
8 msec chirp waveform, spectrum
Magnitude (linear)
0.0
0
5
10
15
20
25
Frequency (Khz)

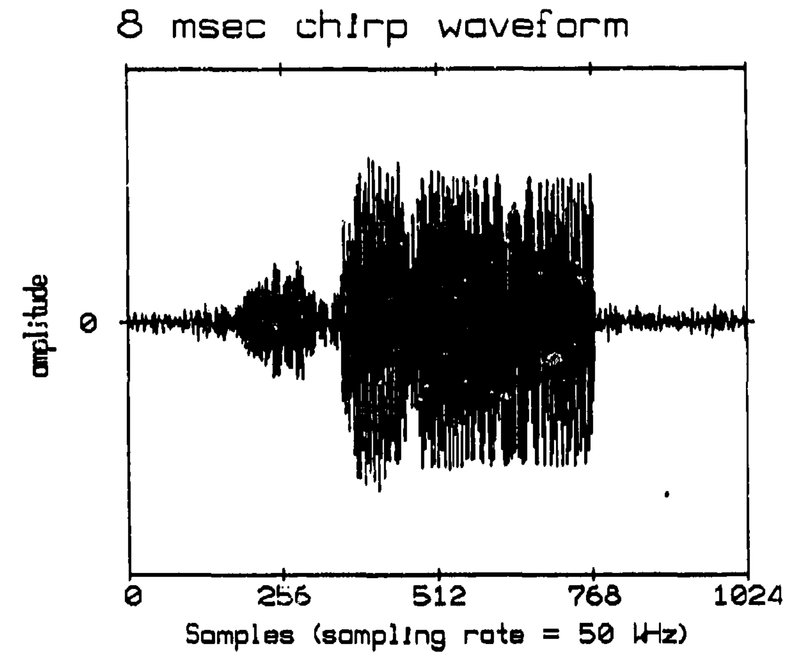
8 msec chirp waveform
amplitude
0
0
256
512
768
1024
Samples (sampling rate = 50 kHz)

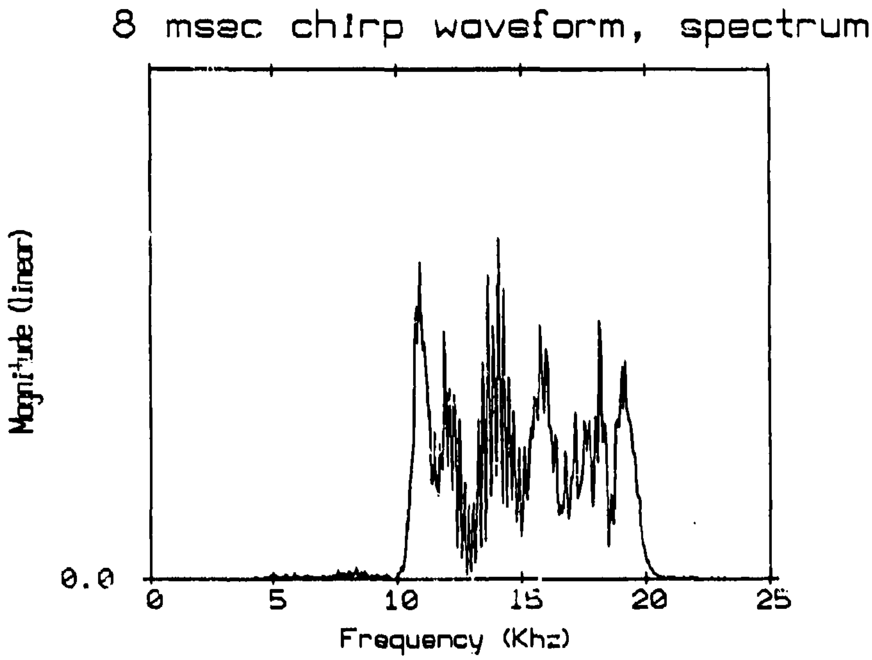
8 msec chirp waveform, spectrum
Magnitude (linear)
0.0
0
5
10
15
20
25
Frequency (Khz)

8 msec chirp waveform

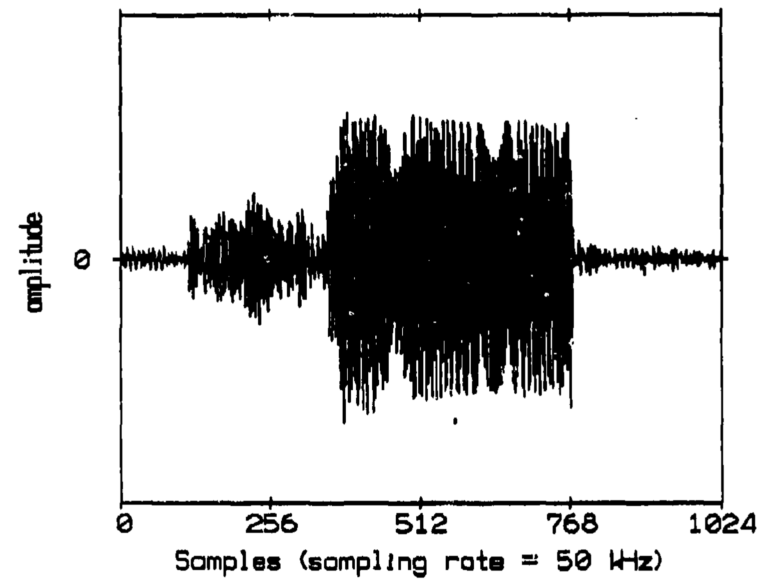

8 msec chirp waveform, spectrum

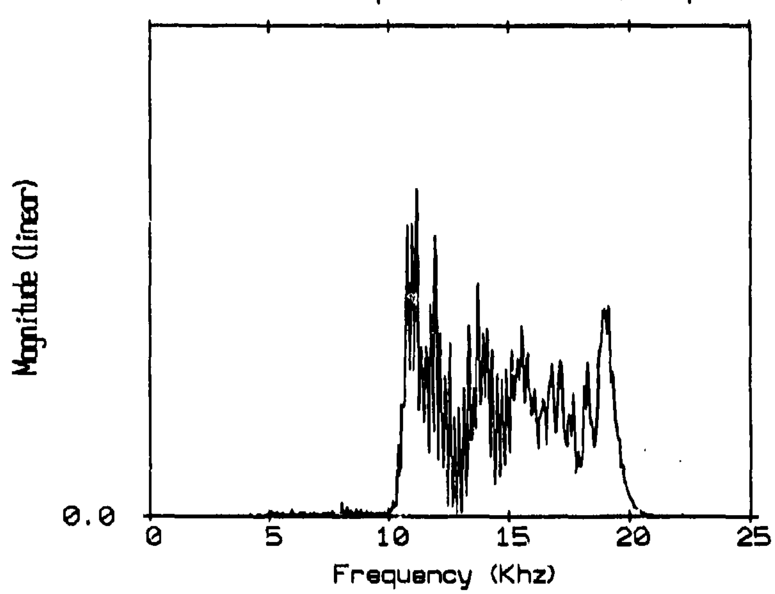

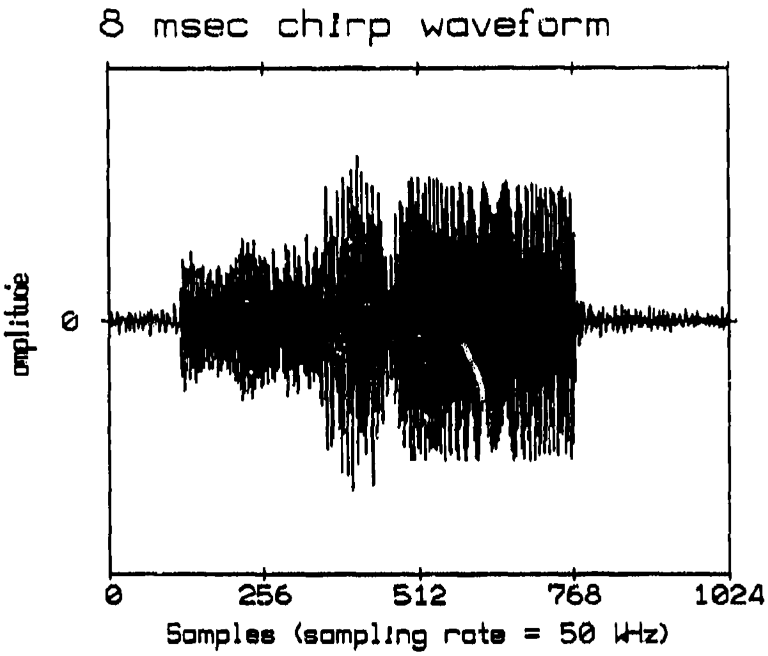
8 msec chirp waveform
amplitude
0
0
256
512
768
1024
Samples (sampling rate = 50 kHz)

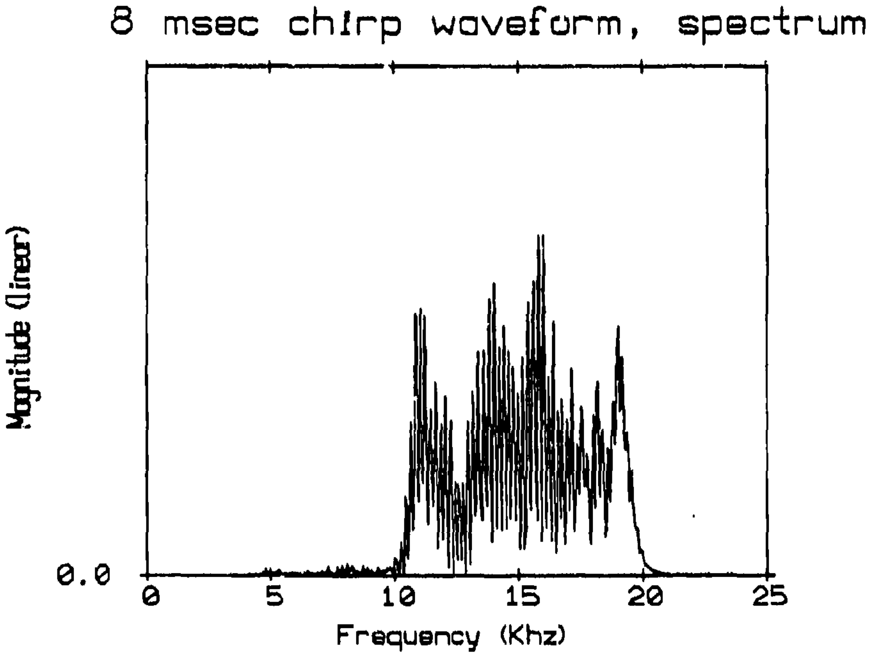
8 msec chirp waveform, spectrum
Magnitude (linear)
0.0
0
5
10
15
20
25
Frequency (Khz)

144543.1.ch4 , pulse No14

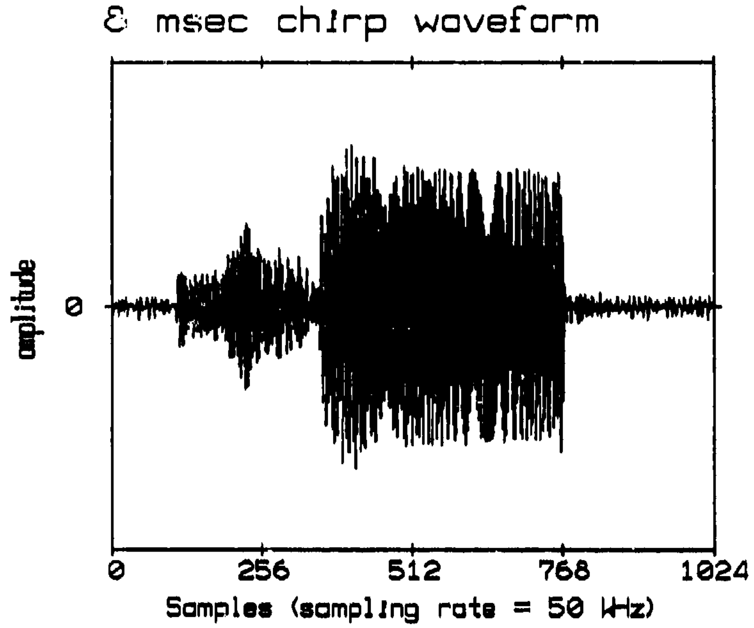

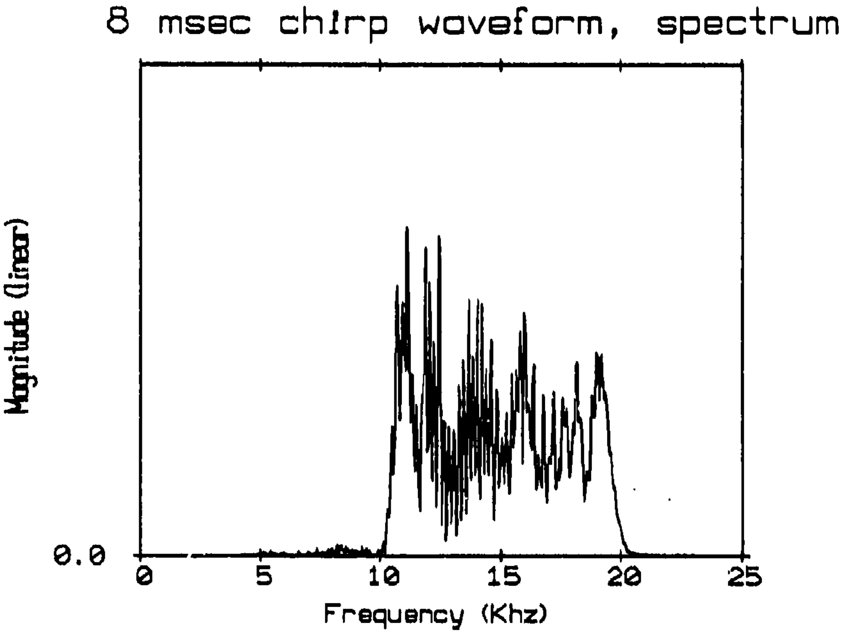

144543.1.ch4 , pulse No15

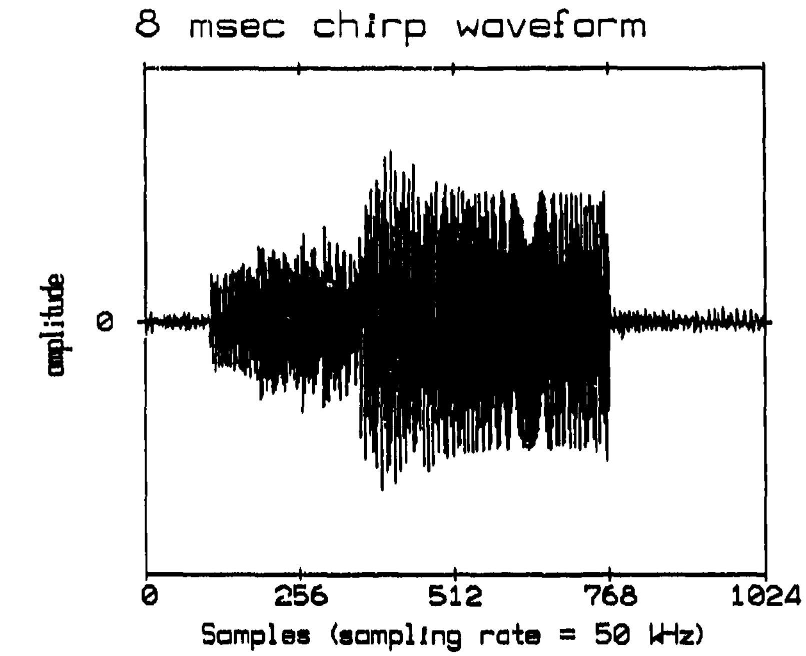

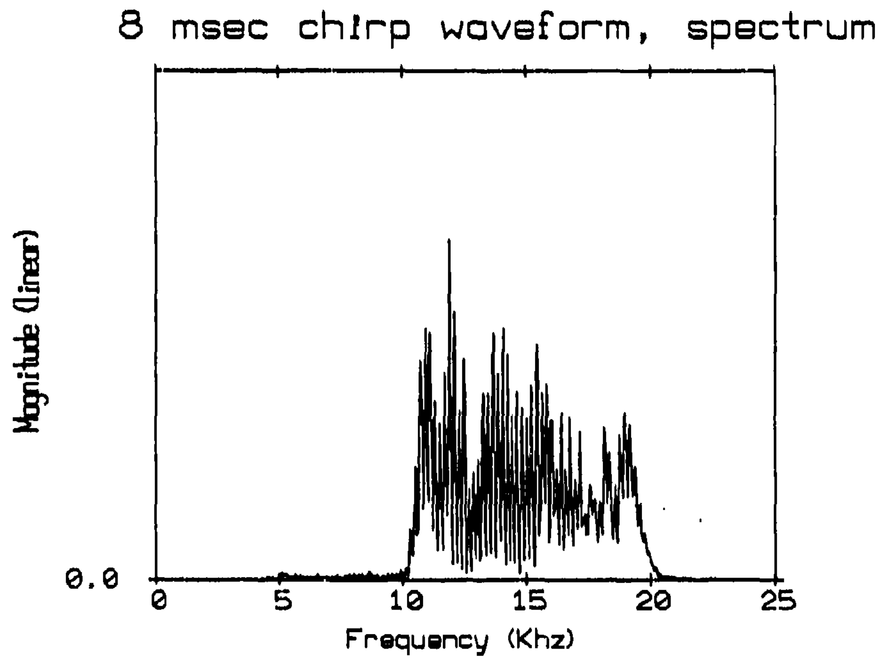

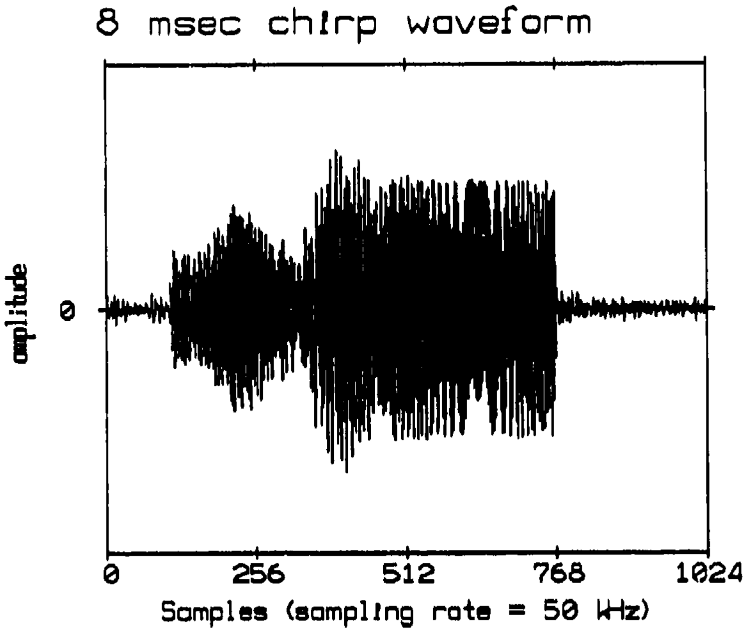
8 msec chirp waveform
amplitude
0
0
256
512
768
1024
Samples (sampling rate = 50 kHz)

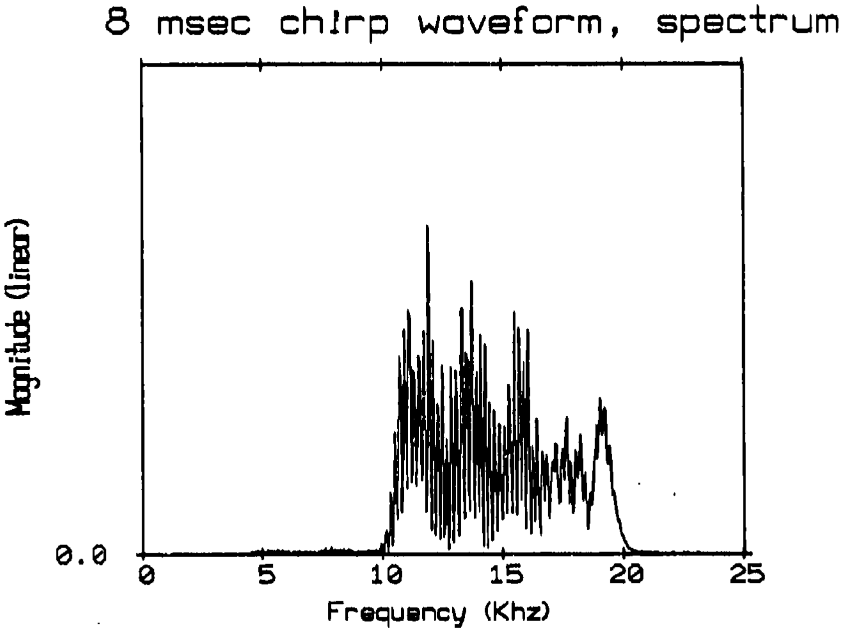
8 msec chirp waveform, spectrum
Magnitude (linear)
0.0
0
5
10
15
20
25
Frequency (Khz)

144543.1.ch4 , pulse No17

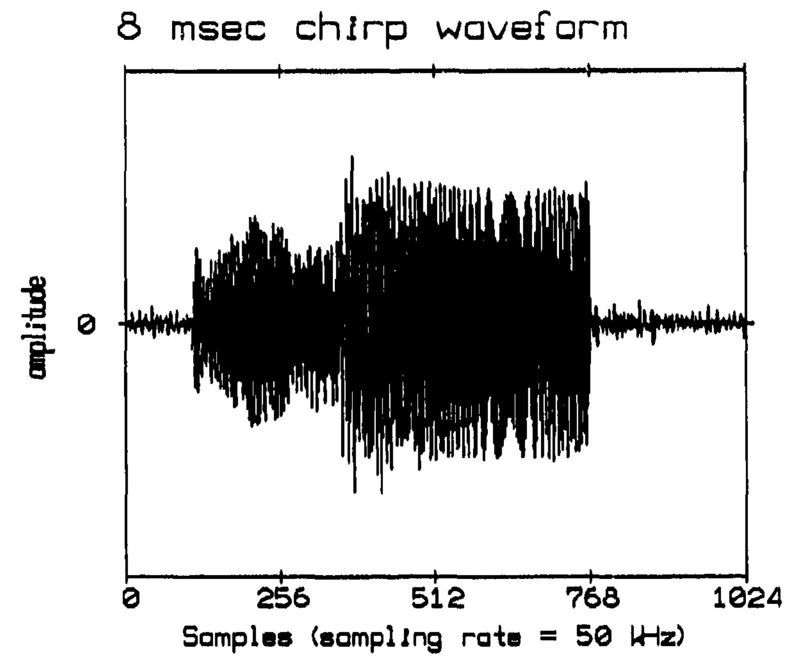

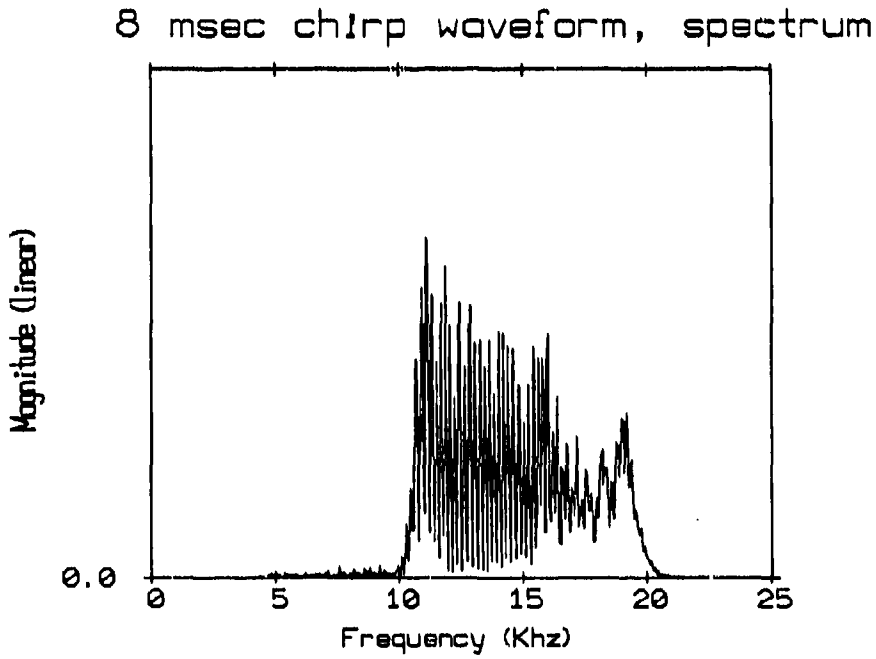

8 msec chirp waveform

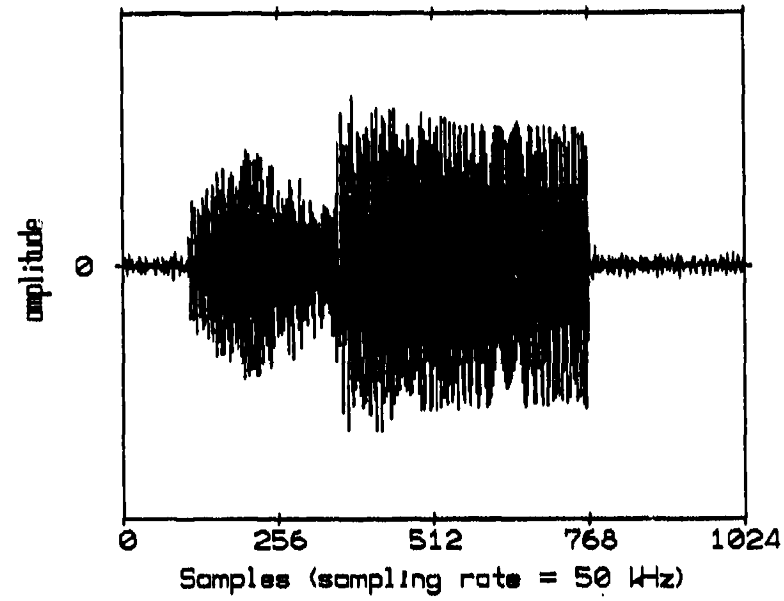

8 msec chirp waveform, spectrum

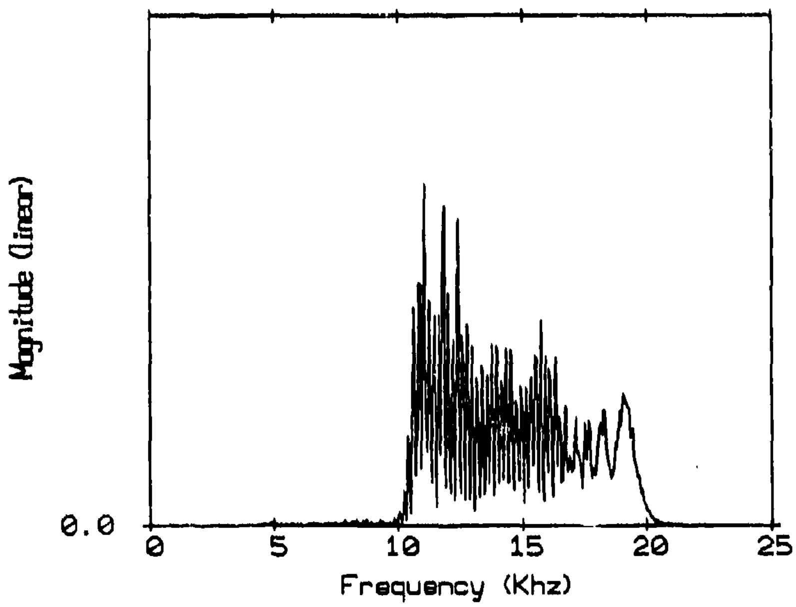

144543.1.ch4 , pulse No19

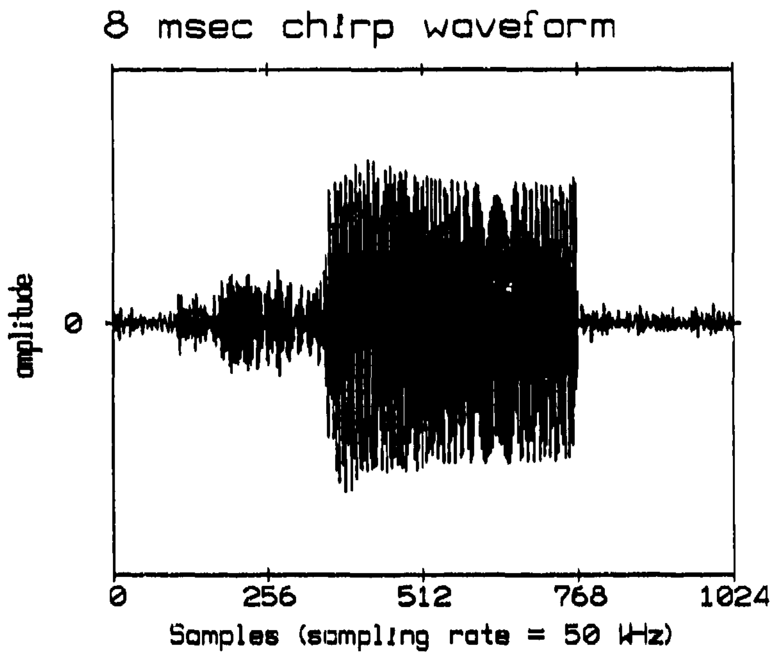

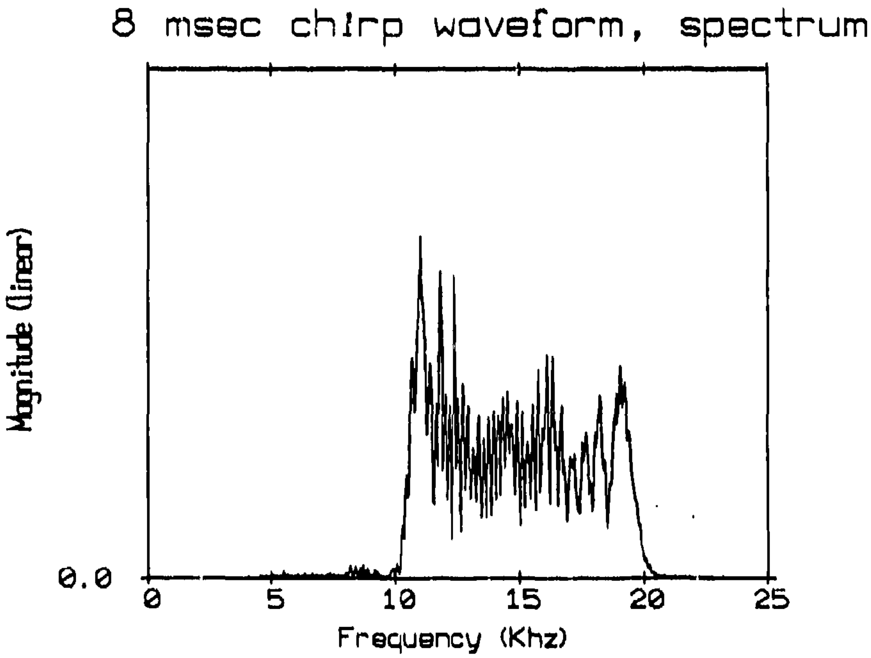

144543.1.ch4 , pulse No20

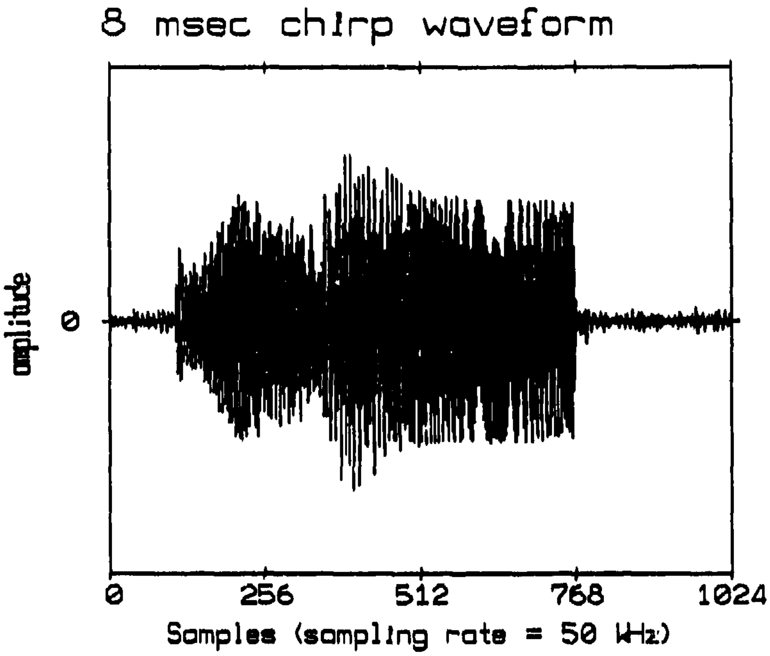

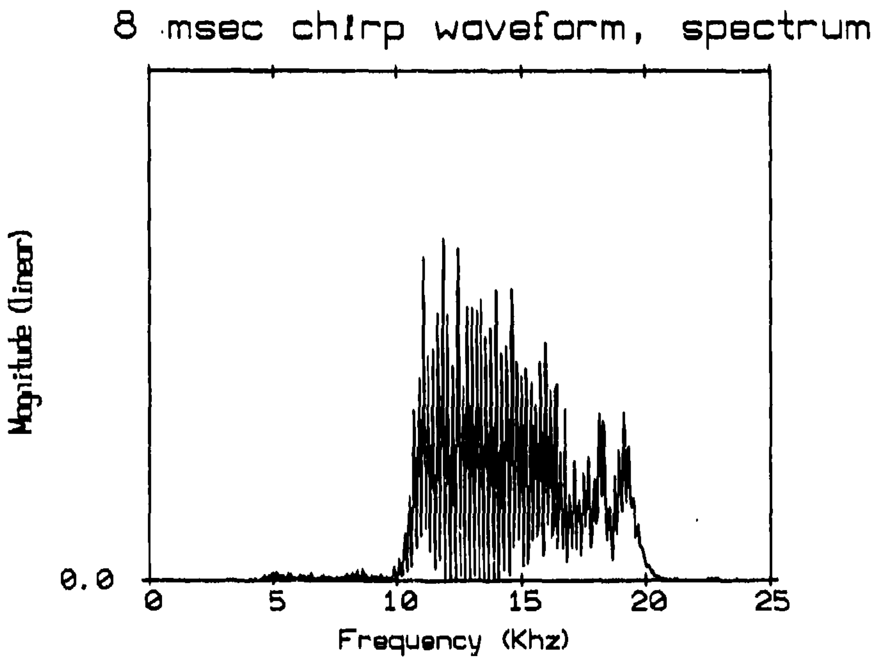

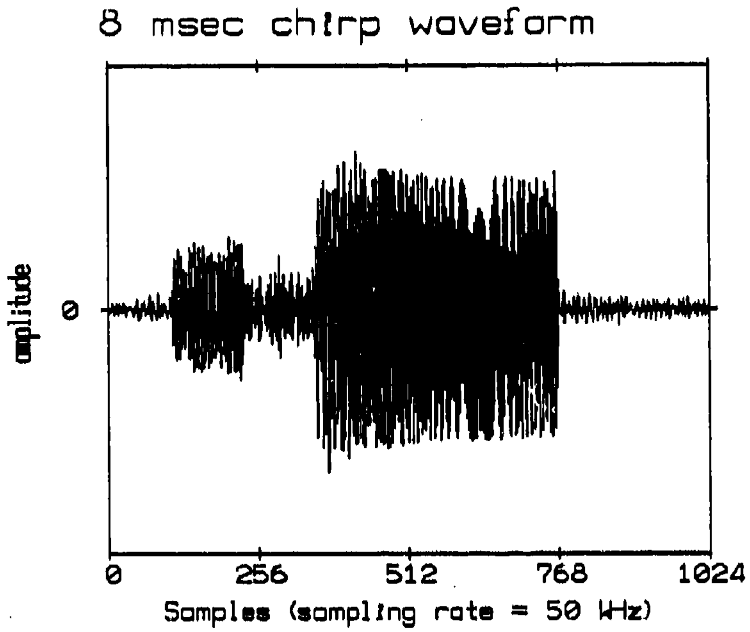
8 msec chirp waveform
amplitude
0
0
256
512
768
1024
Samples (sampling rate = 50 kHz)

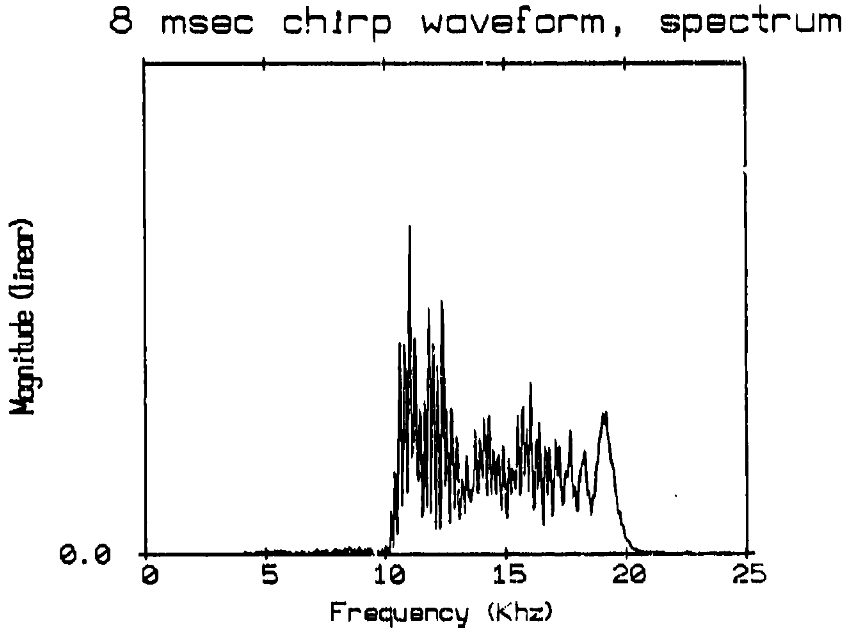
8 msec chirp waveform, spectrum
Magnitude (linear)
0.0
0
5
10
15
20
25
Frequency (Khz)

144543.1.ch4 , pulse No22

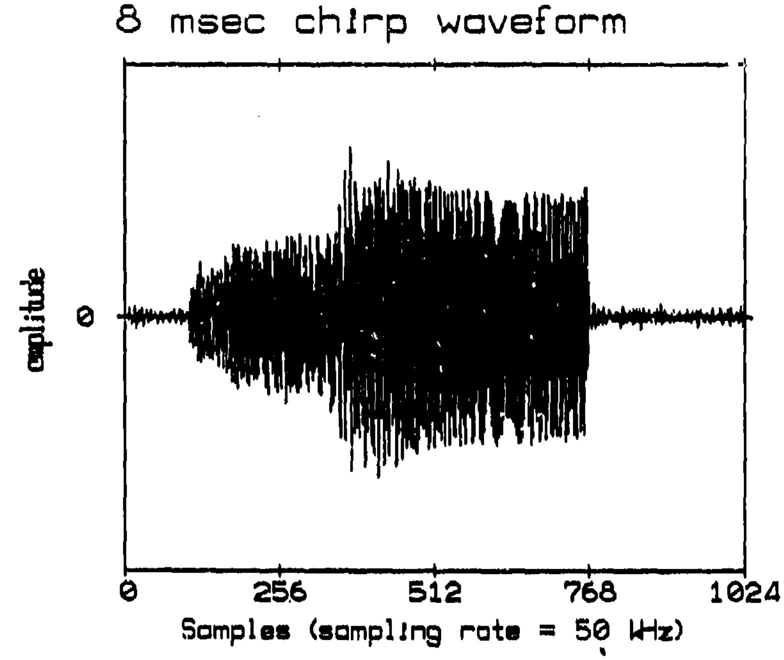

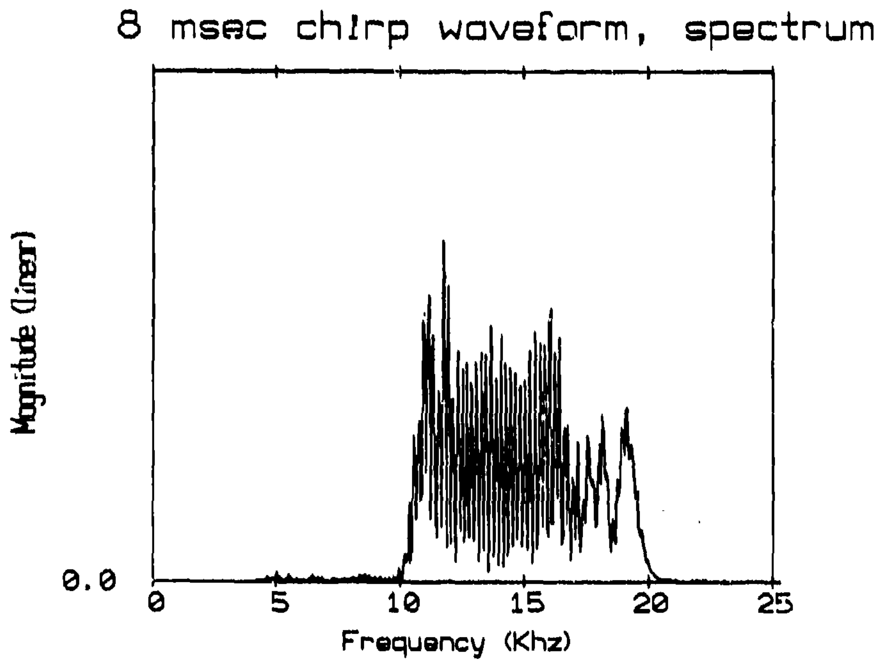

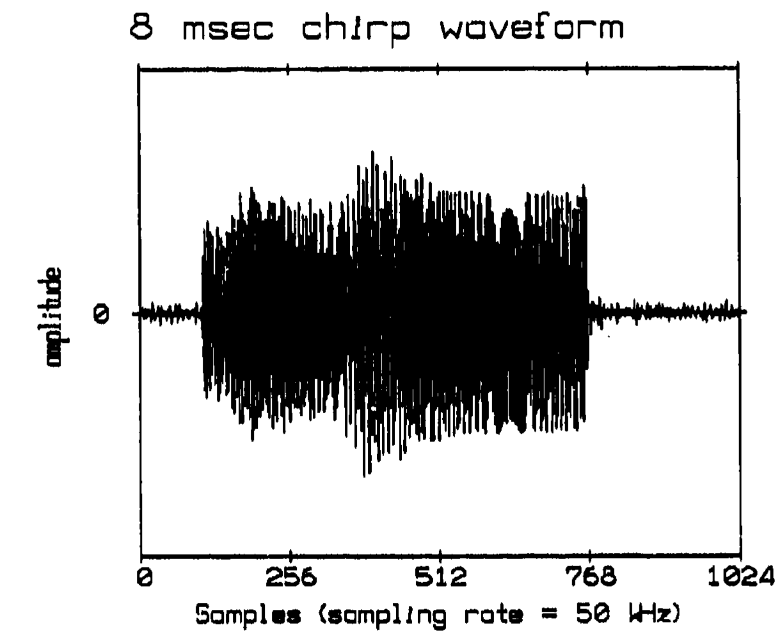
8 msec chirp waveform
amplitude
0
0
256
512
768
1024
Samples (sampling rate = 50 kHz)

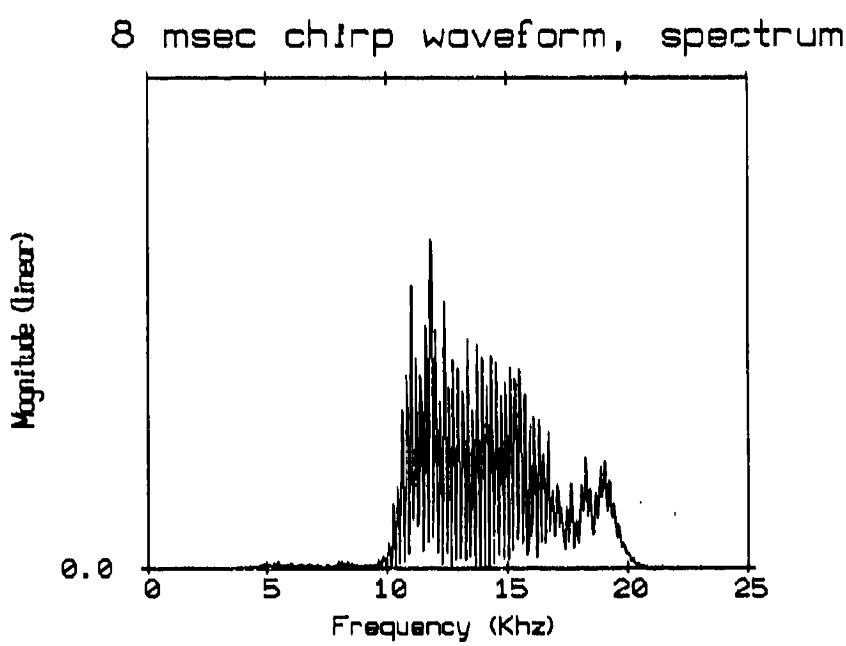
8 msec chirp waveform, spectrum
Magnitude (linear)
0.0
0
5
10
15
20
25
Frequency (Khz)

1444543.1.ch4 , pulse No24

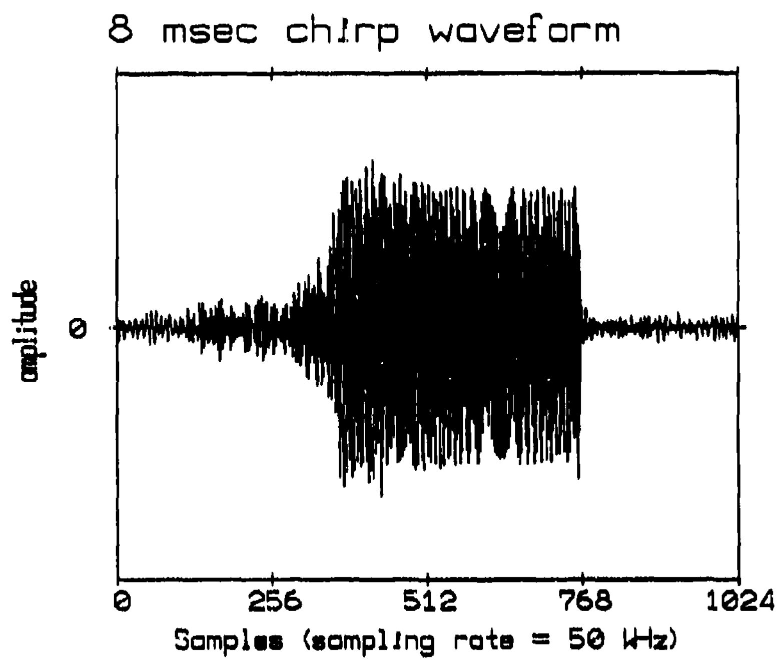

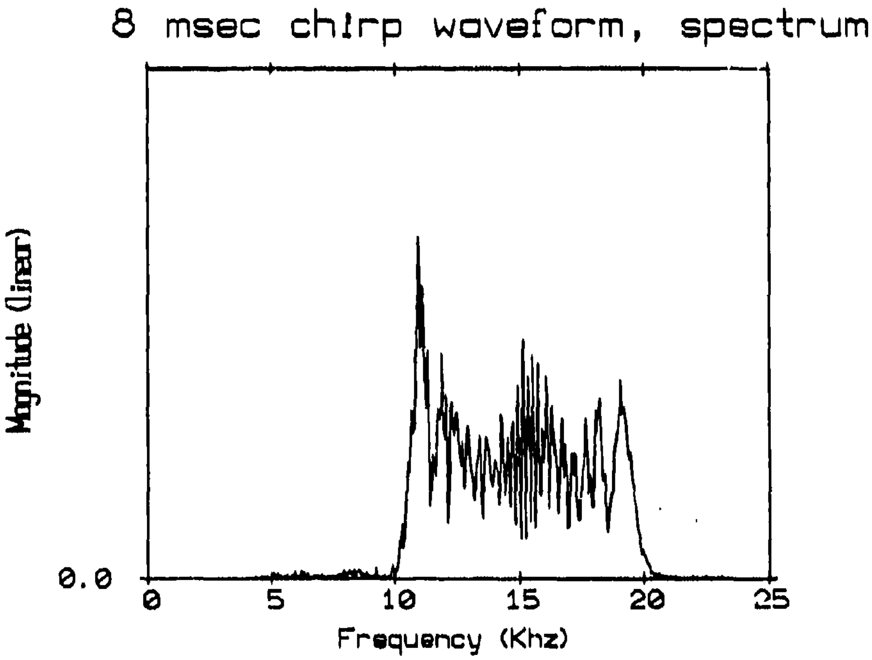

144543.1.ch4 , pulse No25

8 msec chirp waveform

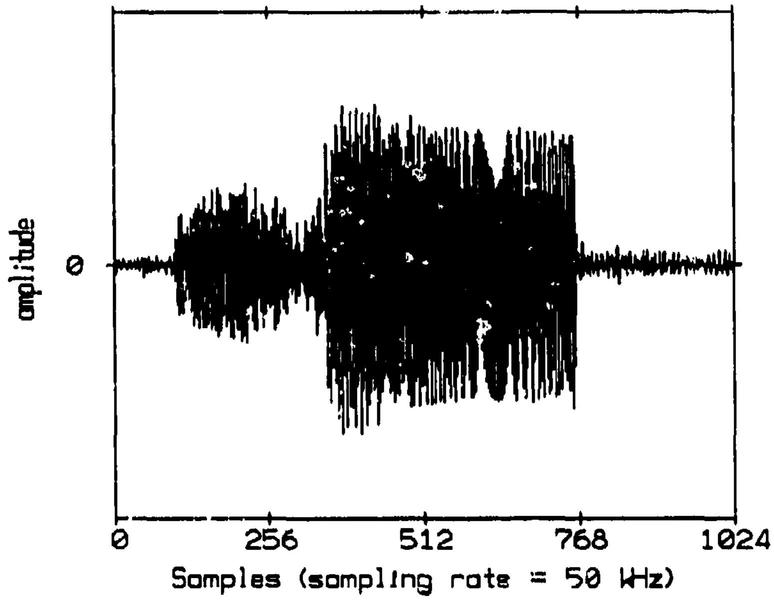

8 msec chirp waveform, spectrum

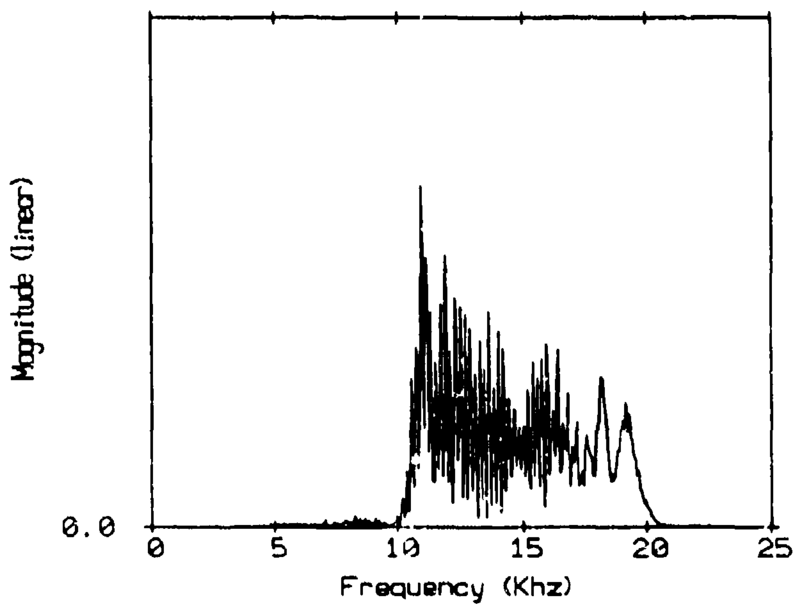

144543.1.ch4 , pulse No26

8 msec chirp waveform

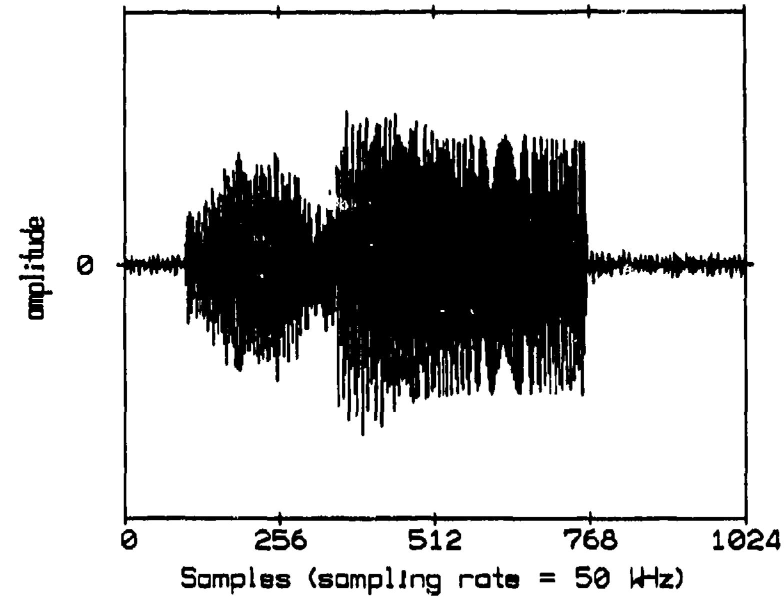

8 msec chirp waveform, spectrum

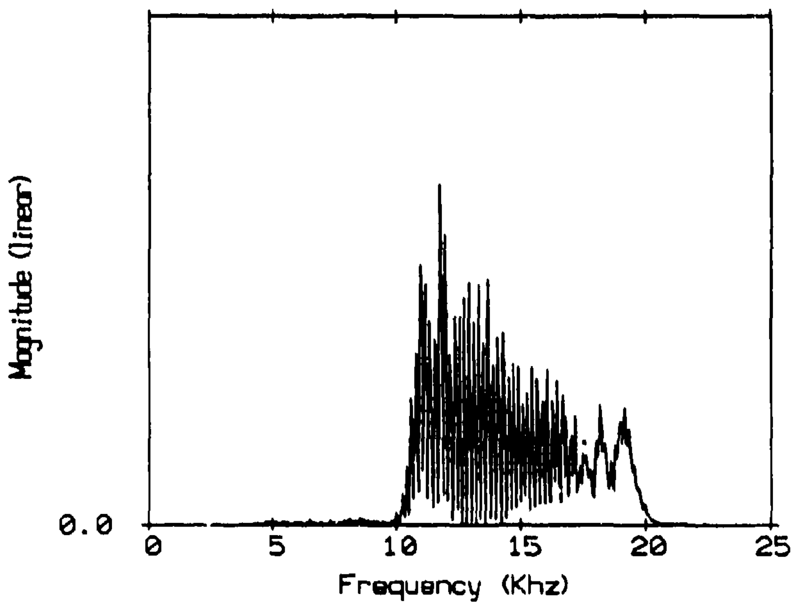

144543.1.ch4 , pulse No27

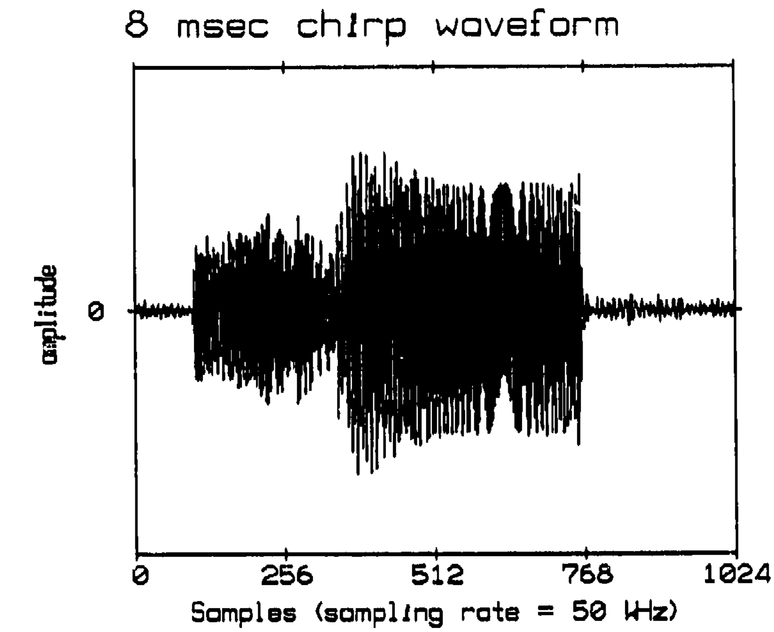

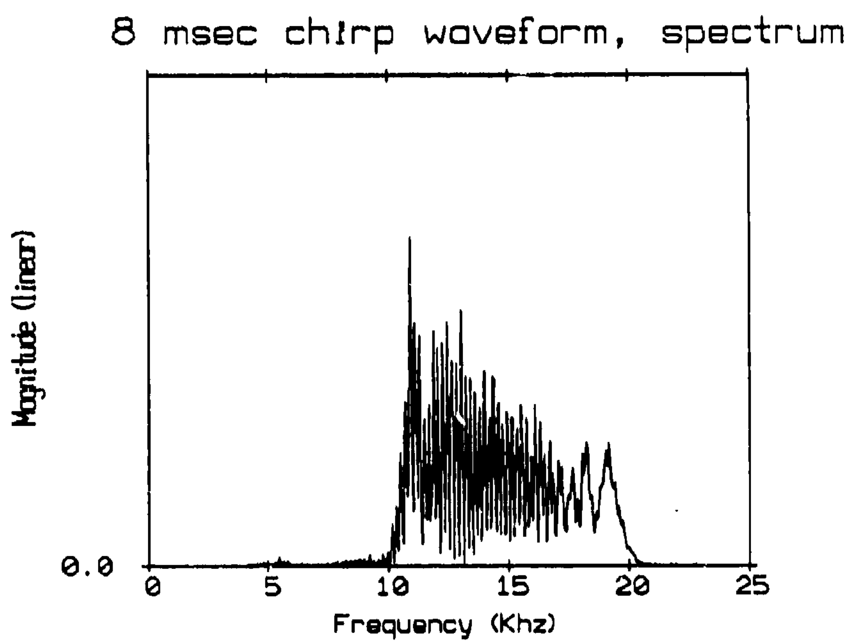

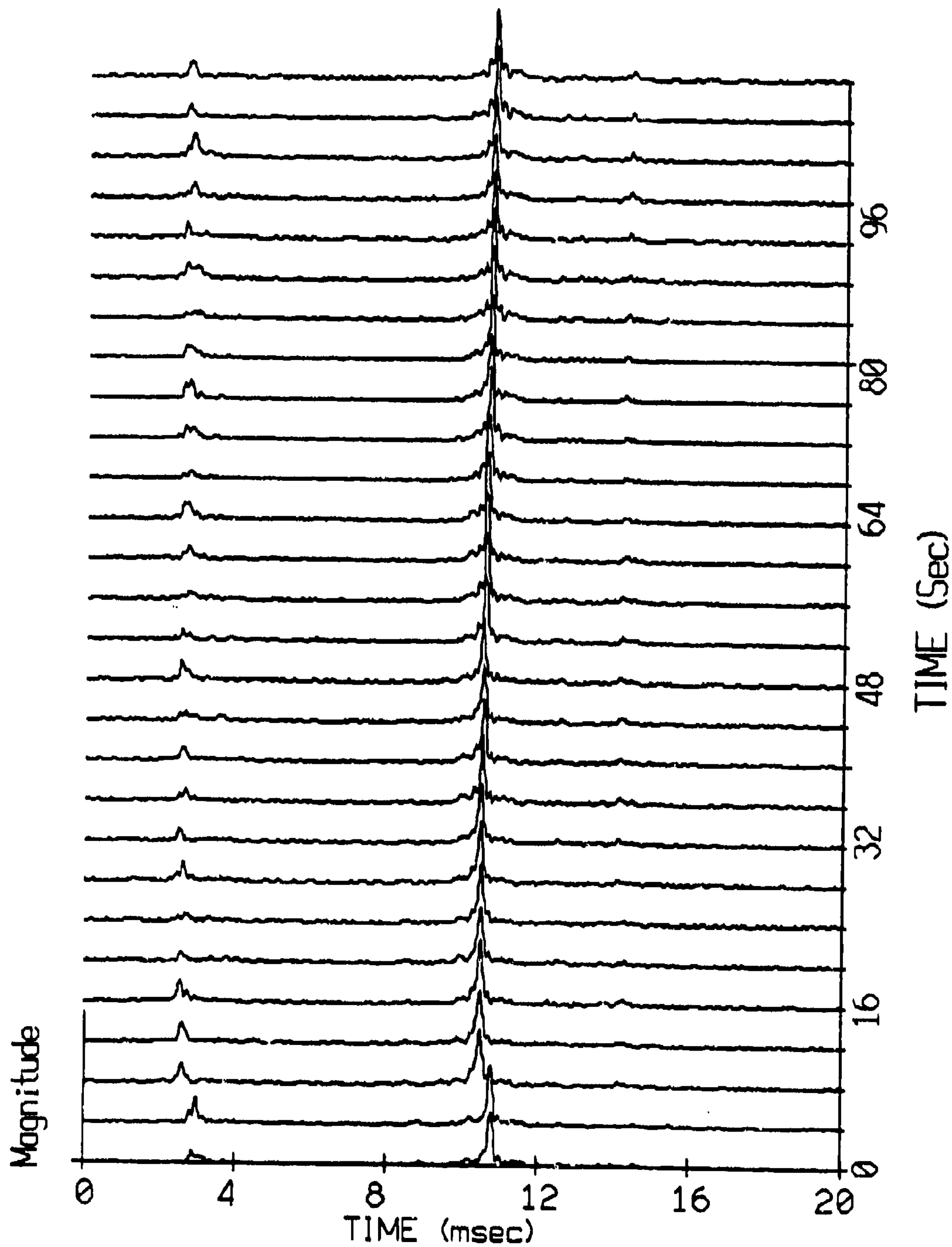

Figure 3.55. Time variation of channel direct path and first multipath character, (first 20 msec.) as calculated from sonobuoy No 2.

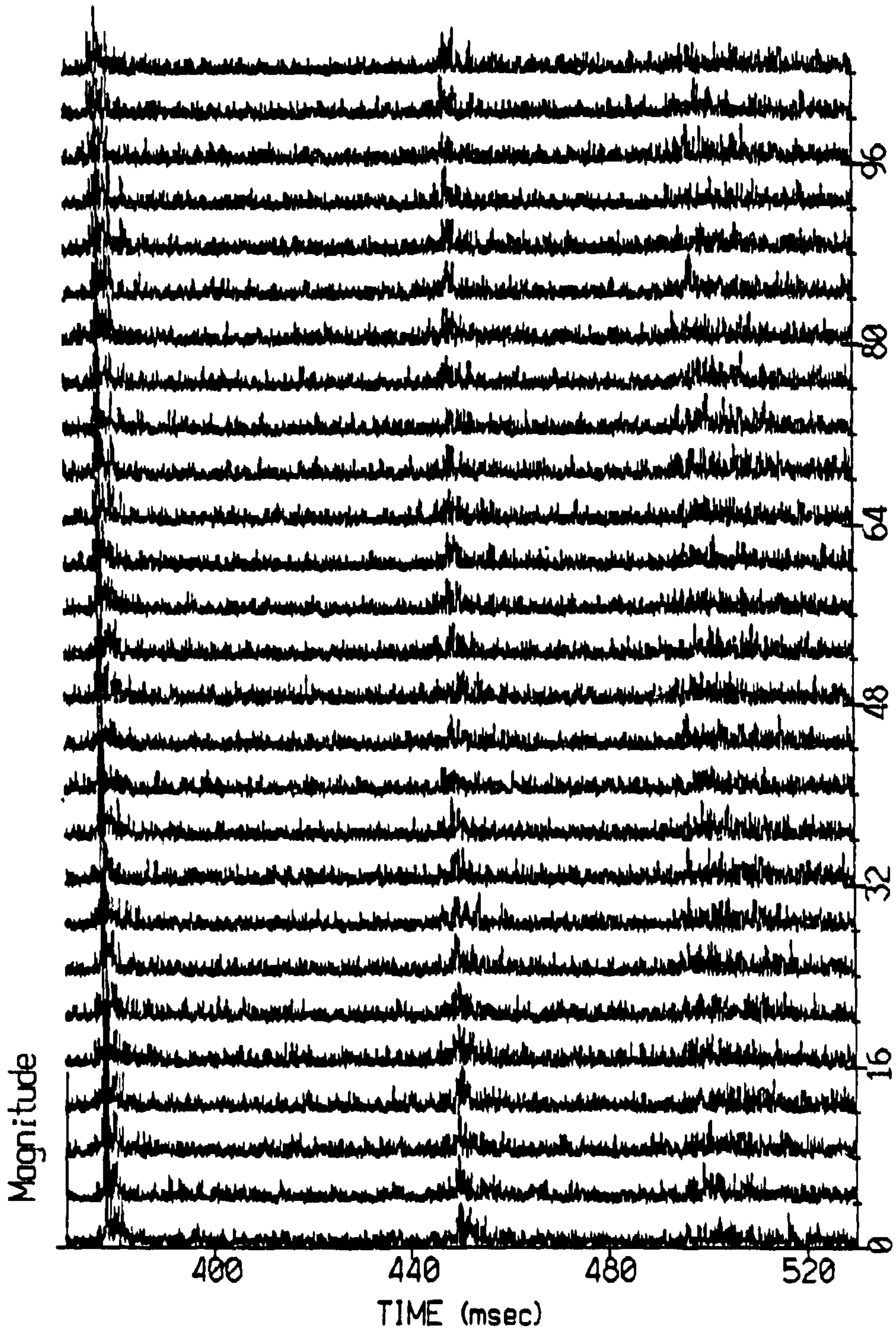

Figure 3.56. Time variaton of channel second third and fourth multipath character, as calculated from sonobuoy No 2 (time slice between 370 and 530 msec).

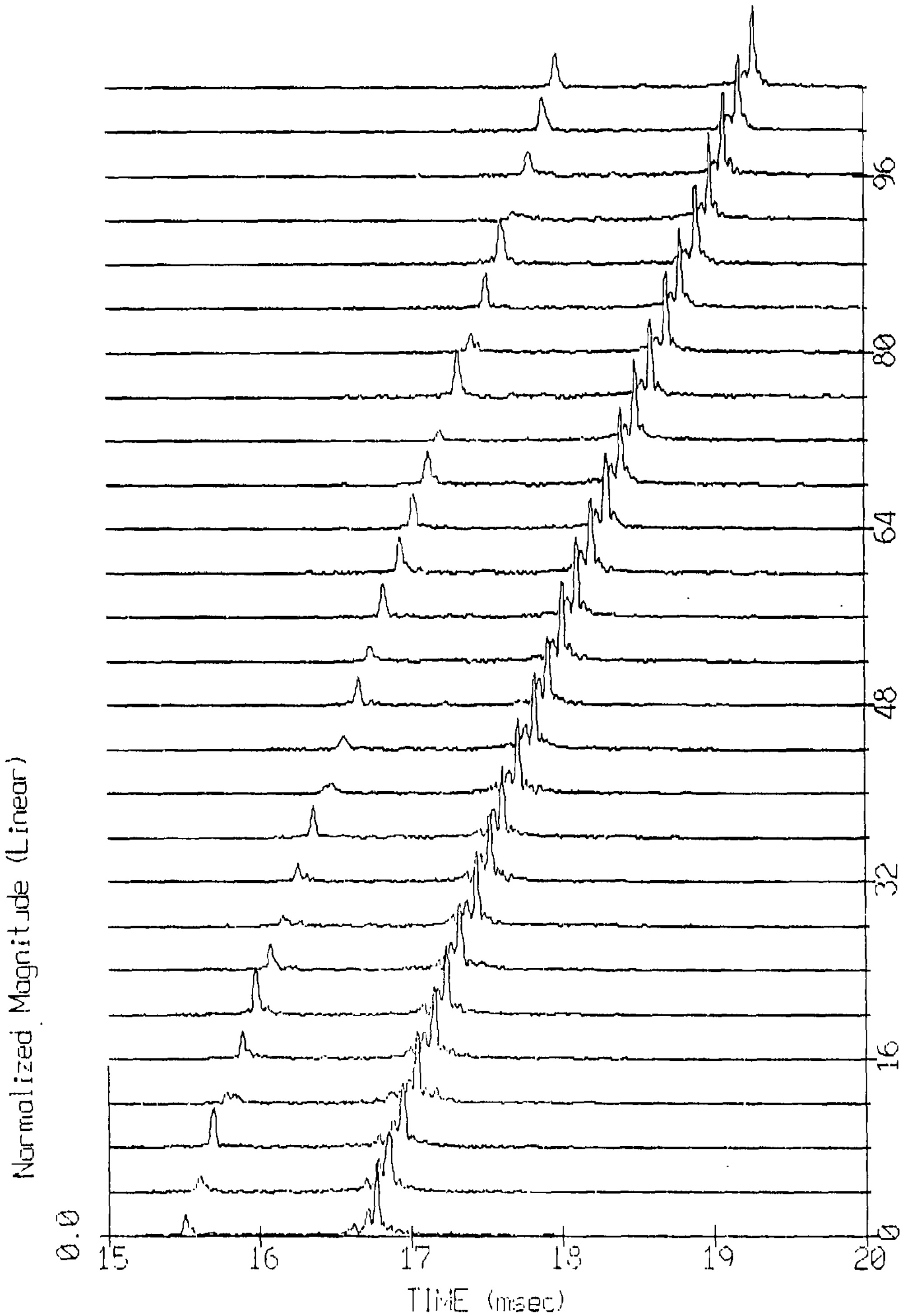

Figure 3.57. Time variation of channel direct path and first multipath character, (5 msec. interval) as calculated from sonobuoy No 4.

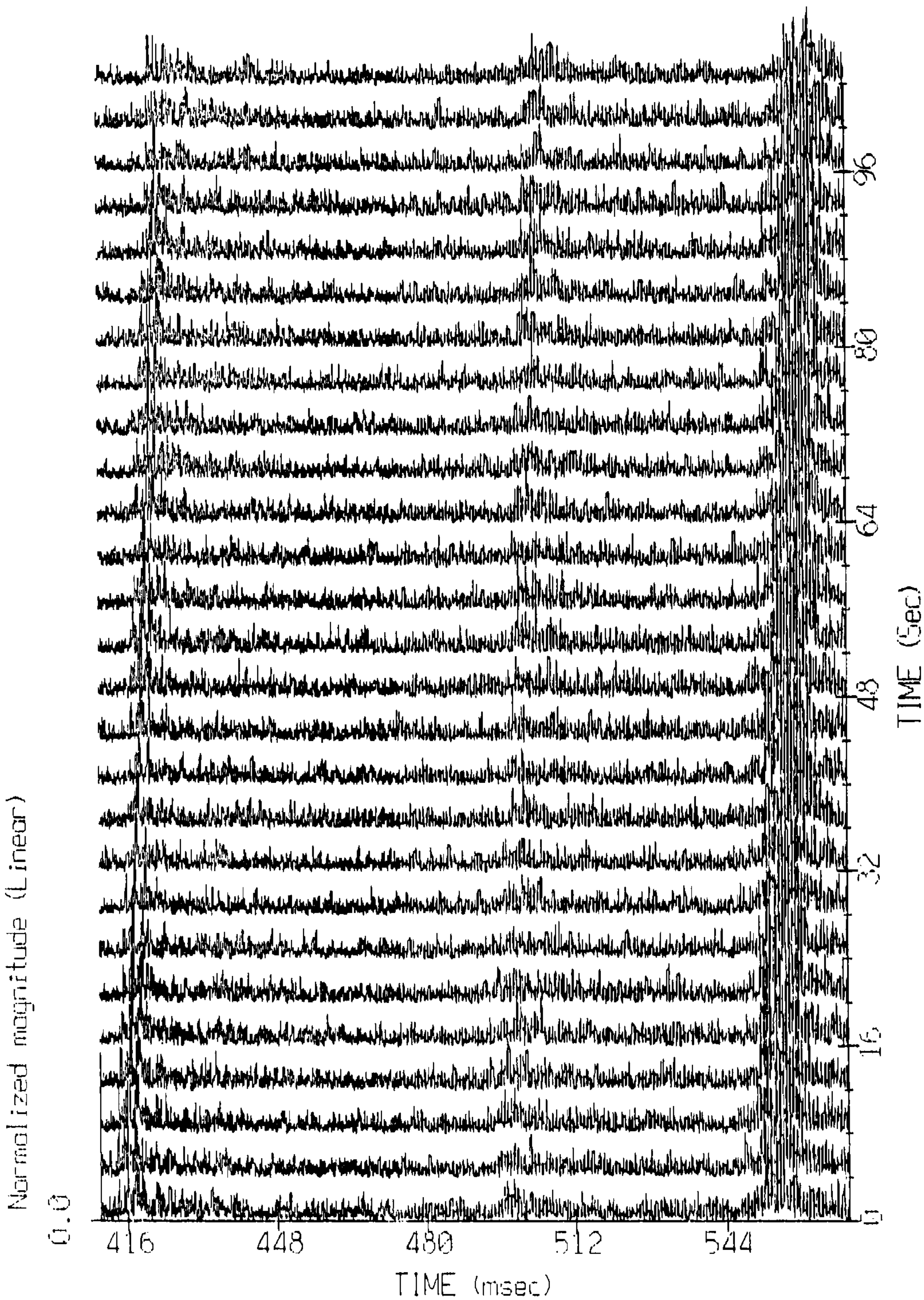

Figure 3.58. Time variaton of channel second third and fourth multipath character, as calculated from sonobuoy No 4.

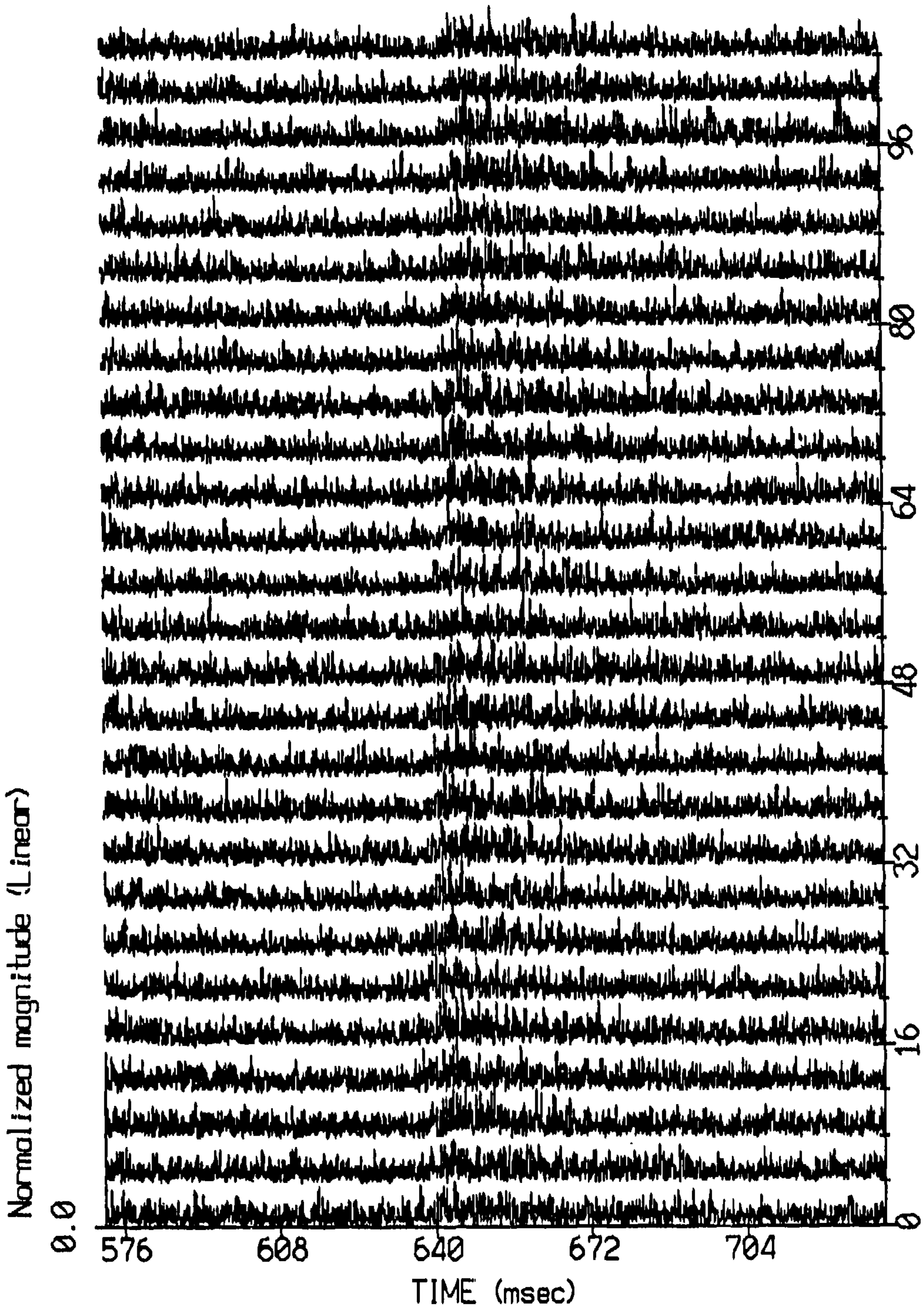

Figure 3.59. Time variaton of channel sixth multipath character, as calculated from sonobuoy No 4.

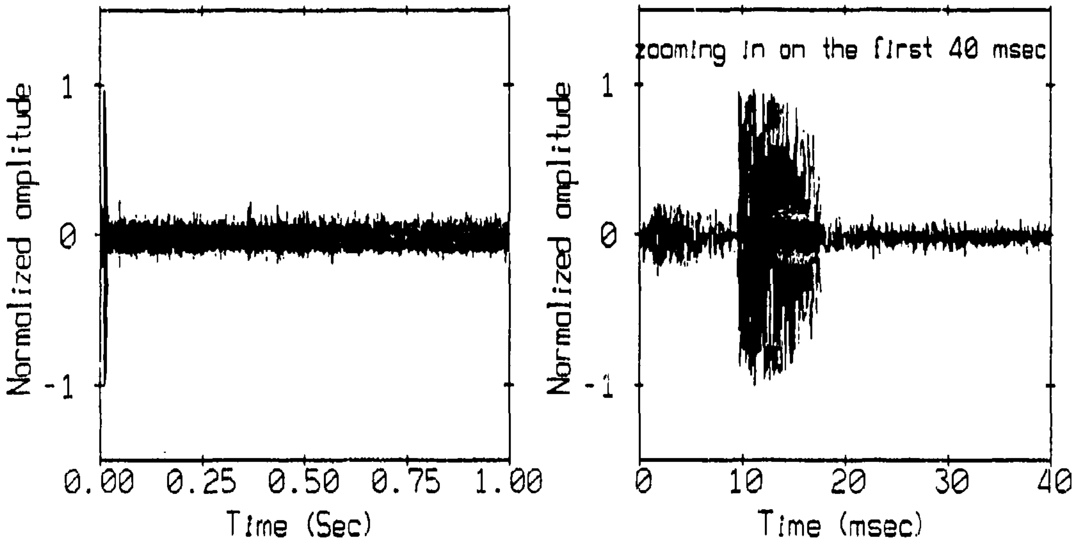

Figure 3.60. Typical received 8 msec chirp waveform.

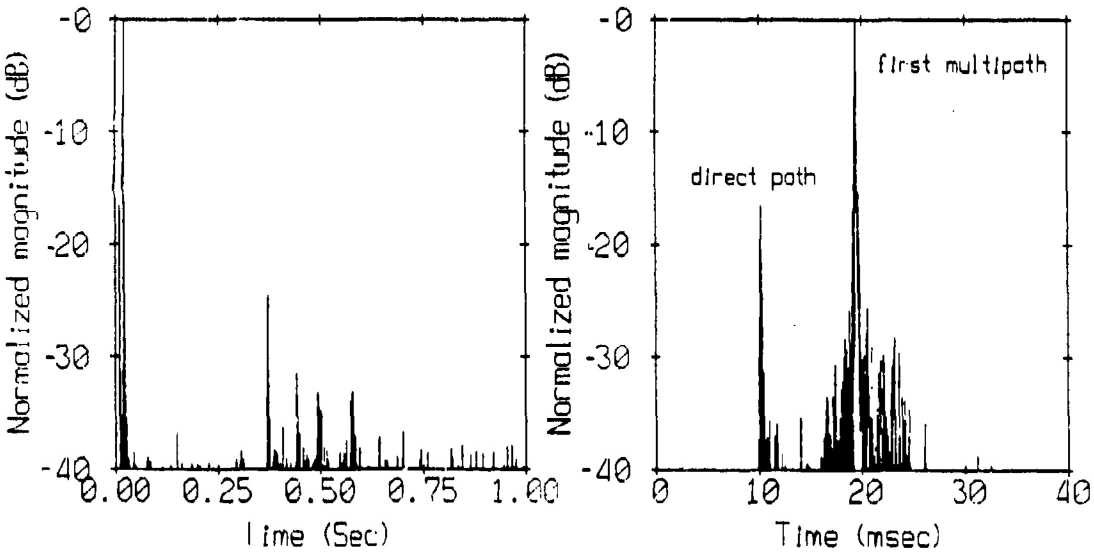

Figure 3.61. Typical channel multipath character.

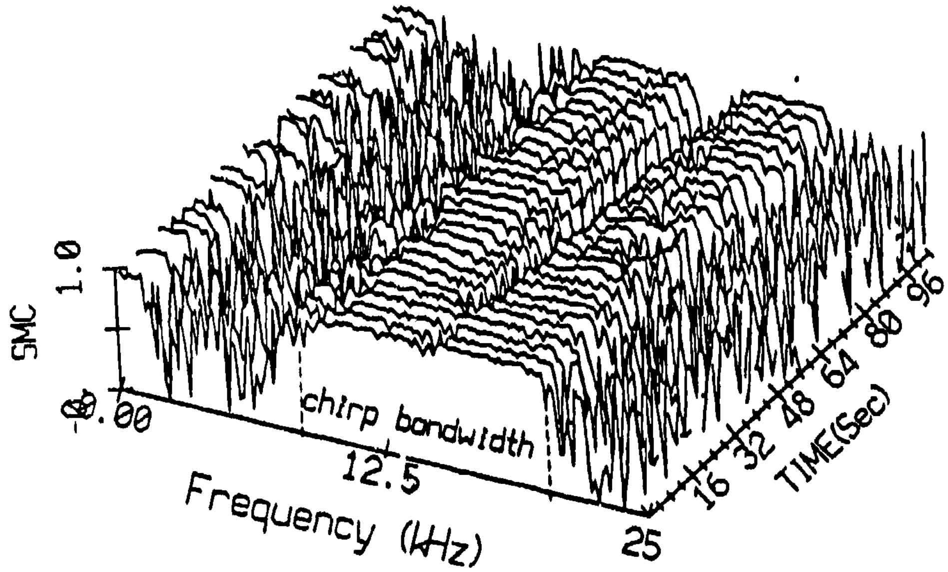

Figure 3.62. The square magnitude coherence function of the channel as a function of time, for waveforms received by sonobuoy No 2.

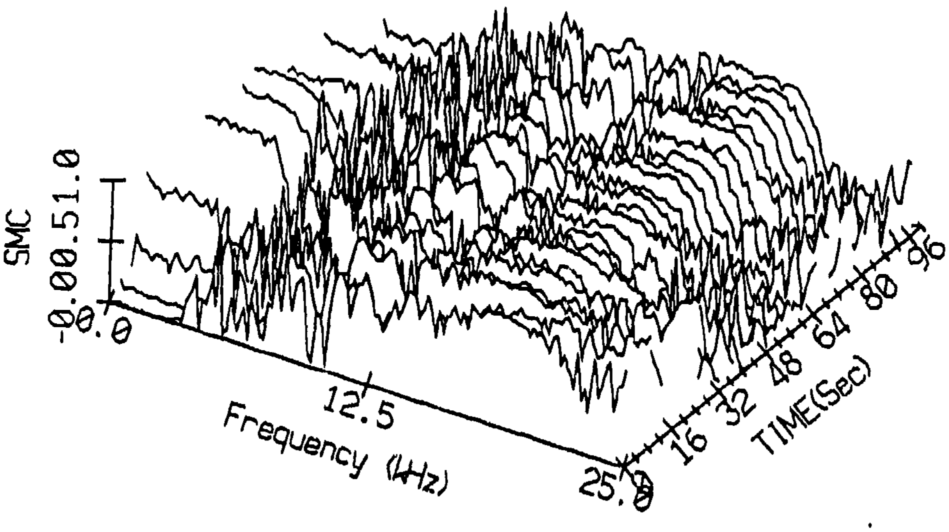

Figure 3.63. The square magnitude coherence function of the channel as a function of time, for waveforms received by sonobuoy No 4.

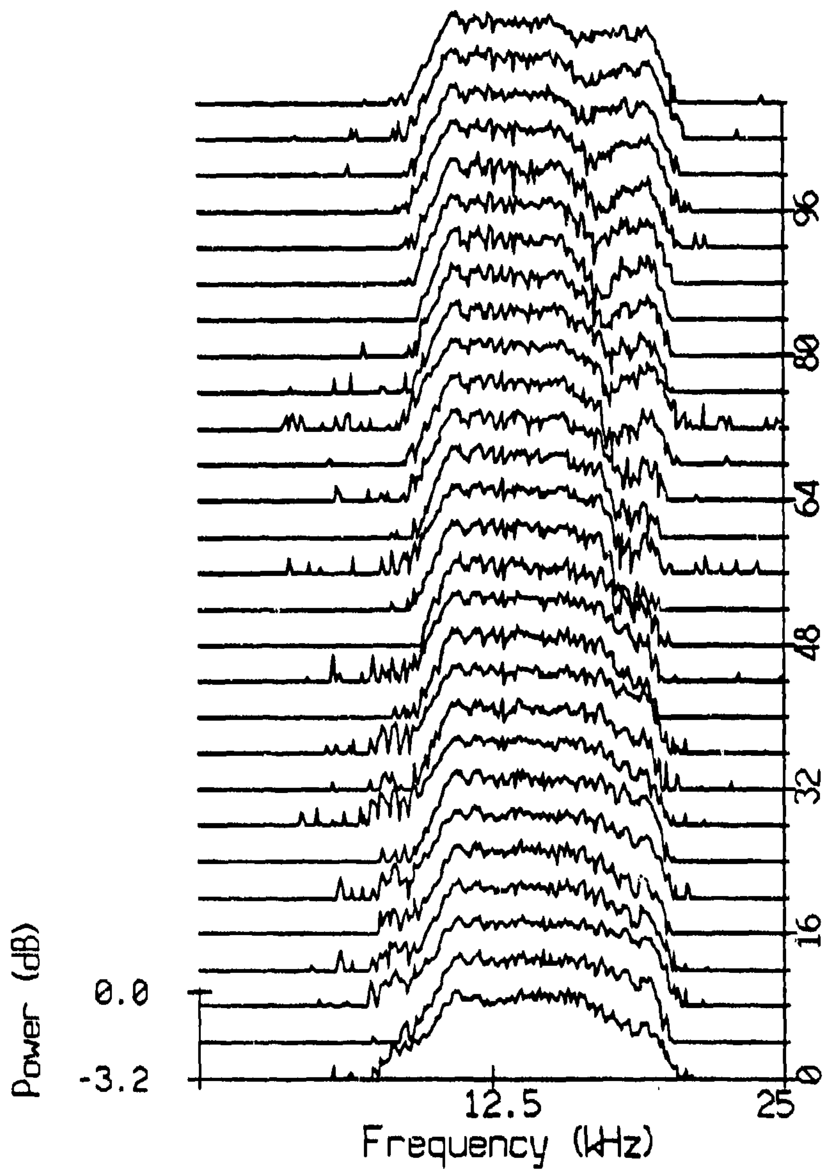

Figure 3.64. The spectra of 28 - 8 msec chirp waveform sequentially received by sonobuy No 2 (one every 4 sec.).

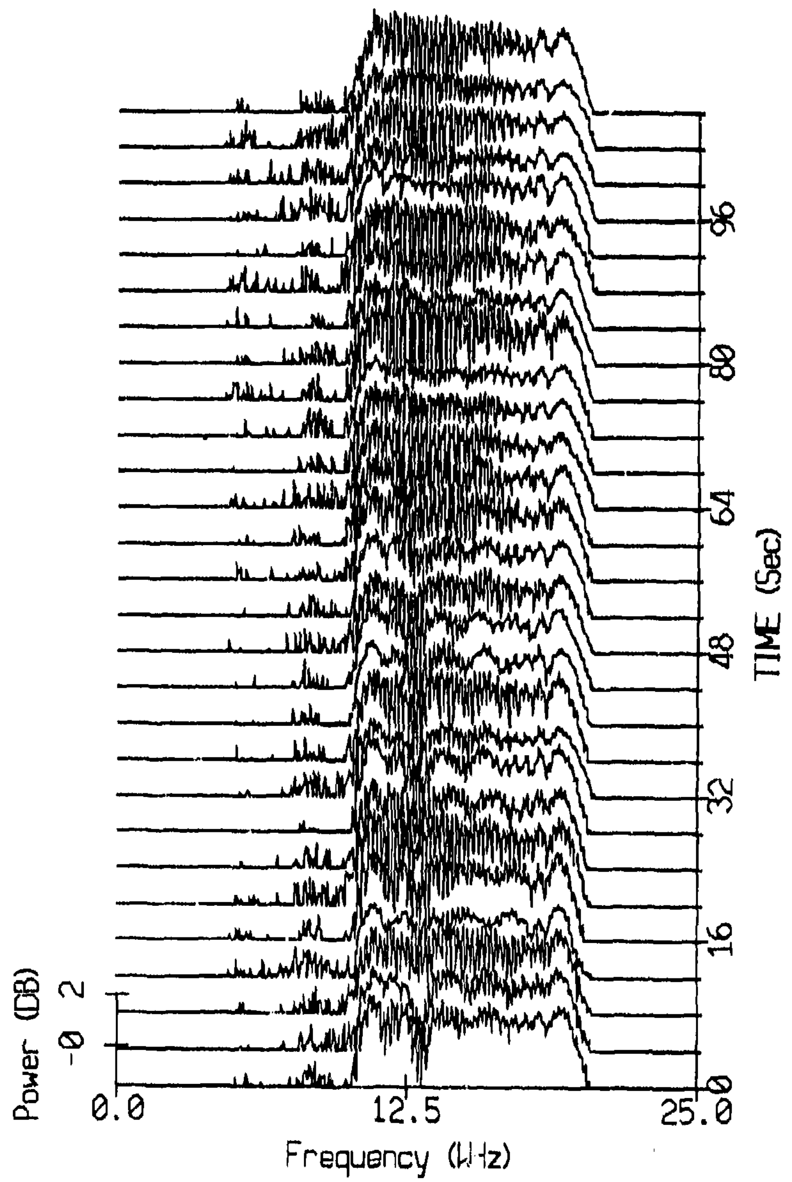

Figure 3.65. The spectra of 28 - 8 msec chirp waveform sequentially received by sonobuy No 4 (one every 4 sec.).

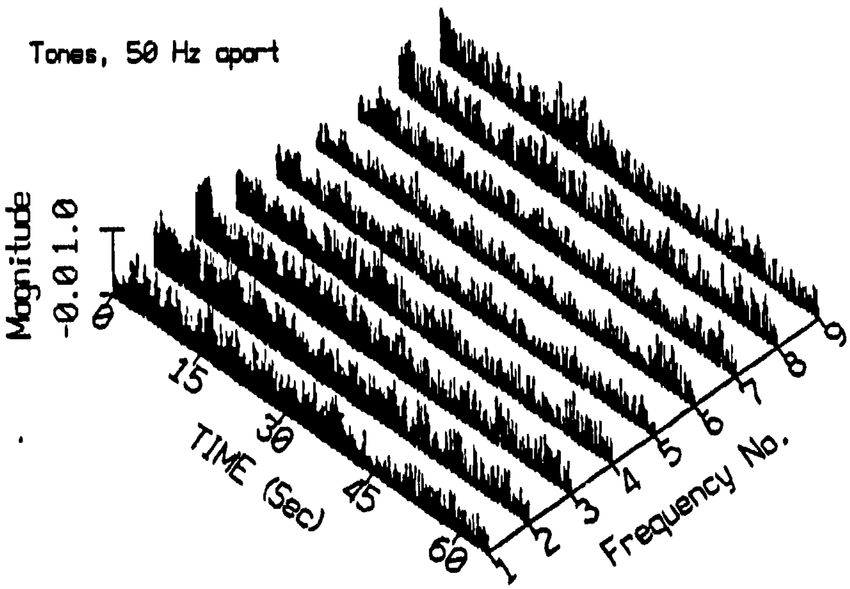

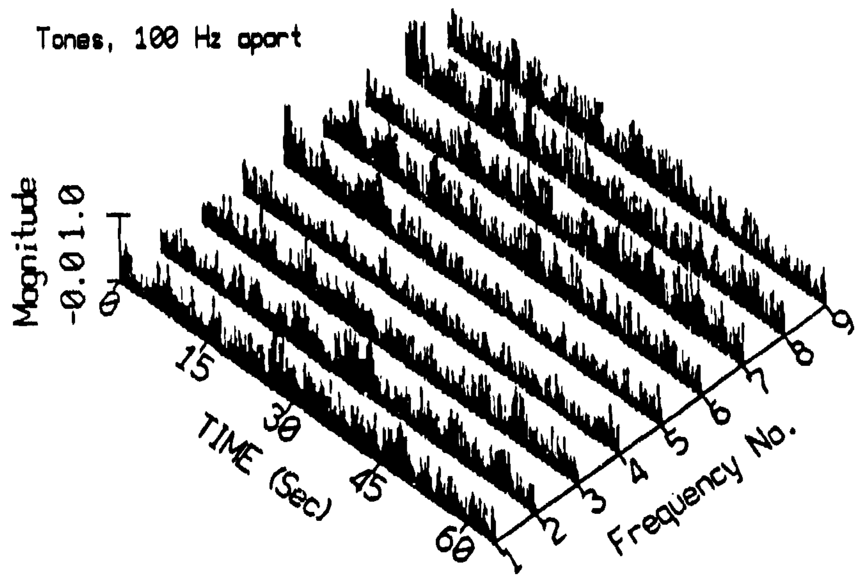

Figure 3.66. Amplitude variation of nine tones received by sonobuoy No 2, 50 and 100 Hz apart.

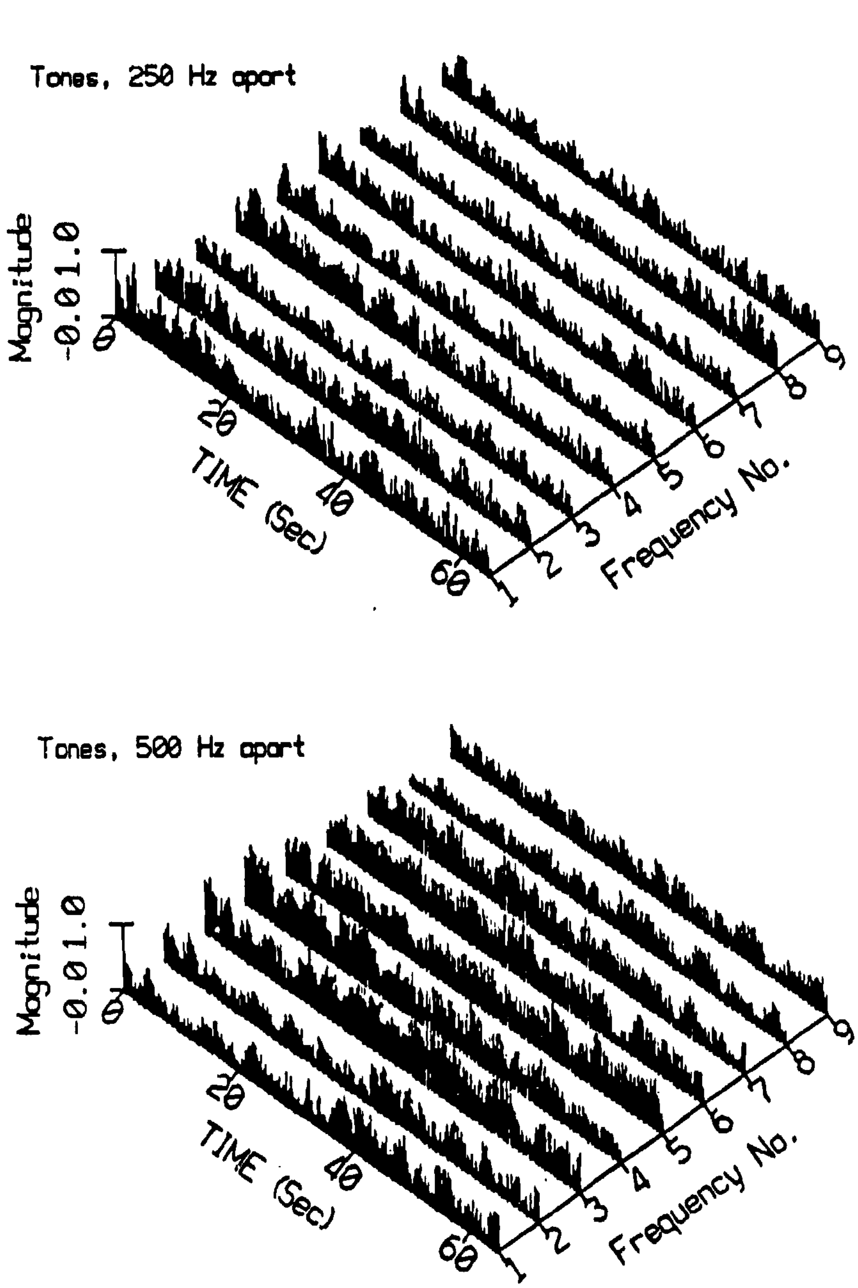

Figure 3.67. Amplitude variation of nine tones received by sonobuoy No 2, 250 and 500 Hz apart.

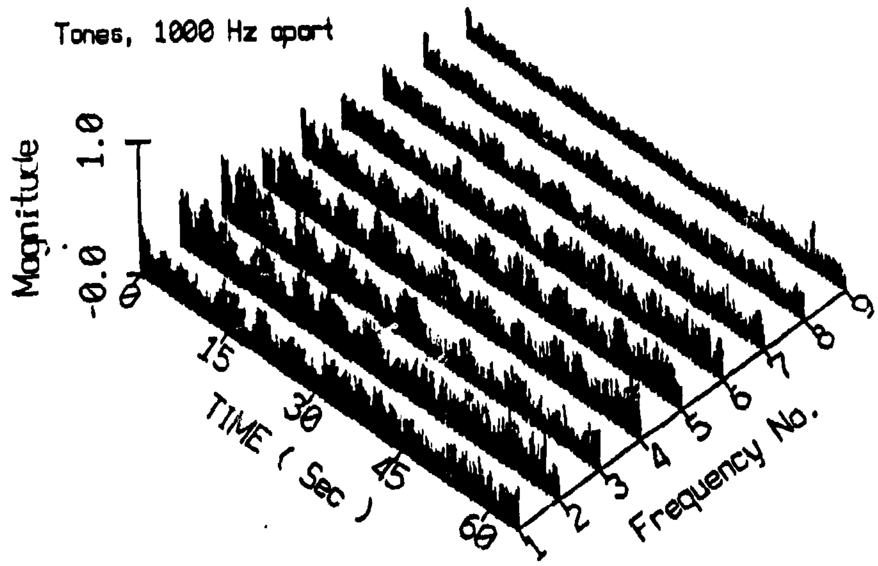

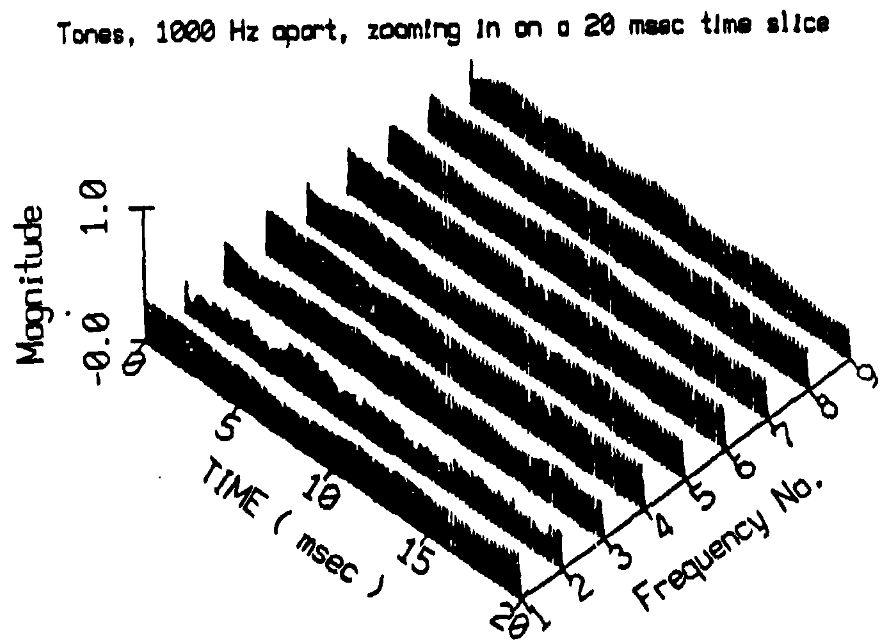

Figure 3.68. Amplitude variation of nine tones received by sonobuoy No 2, 1kHz apart.

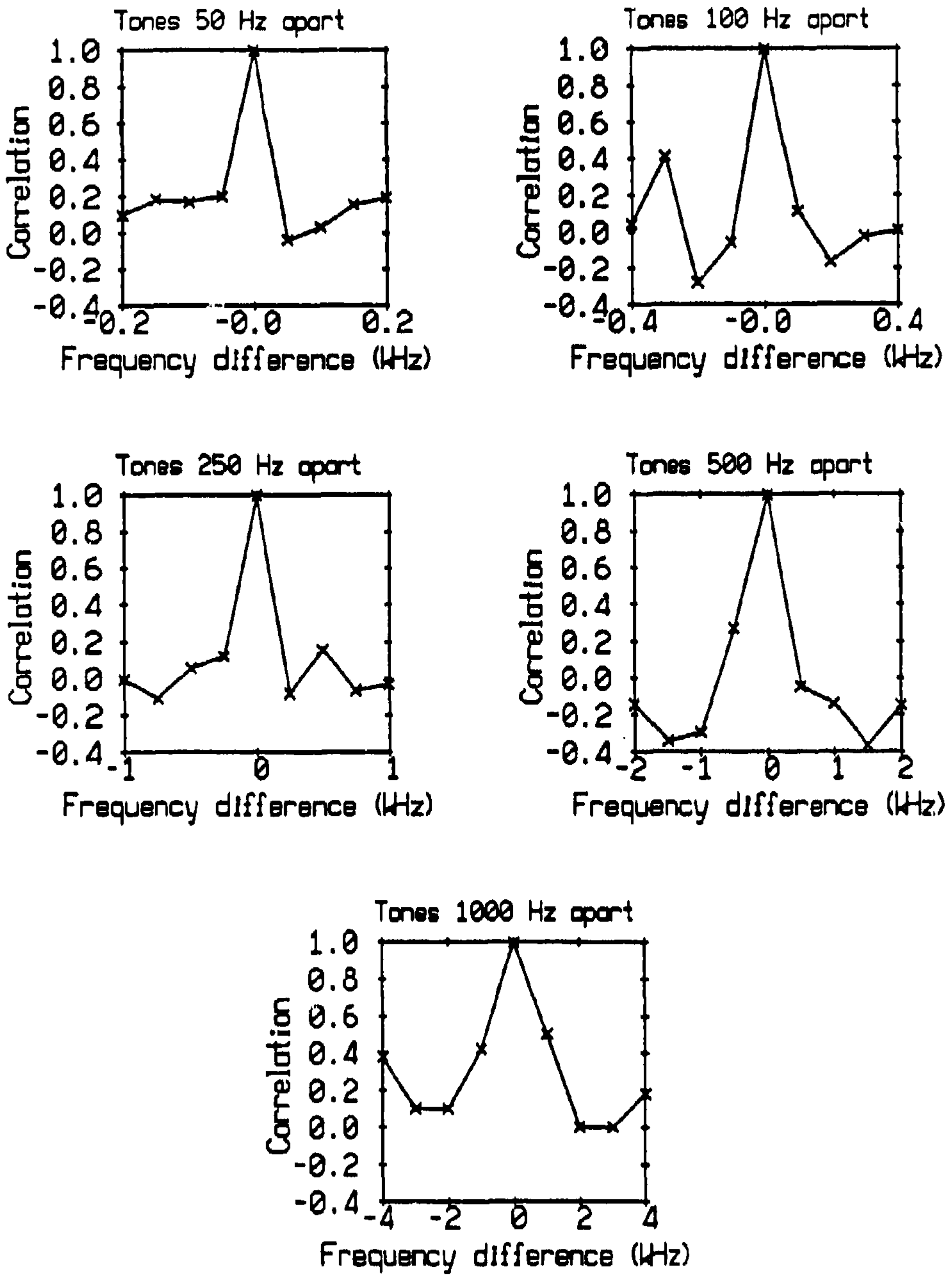

Figure 3.69. The correlation between the envelope of nine tones received by sonobuoy No 2 and the central tone for the five sets of tones.

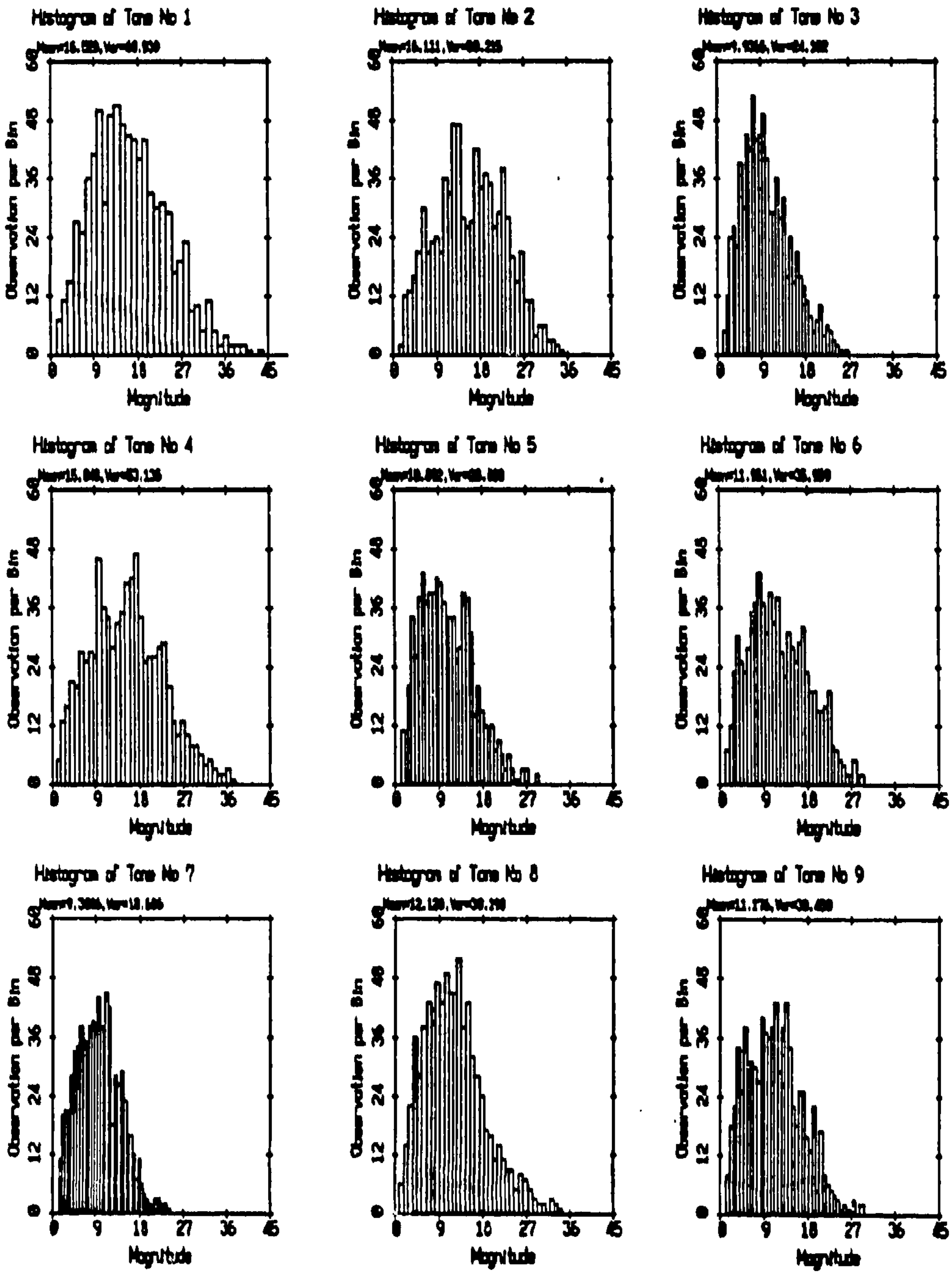

Figure 3.70. Histograms of the envelopes of the 250 Hz spaced tones, received by sonobuoy No 2.

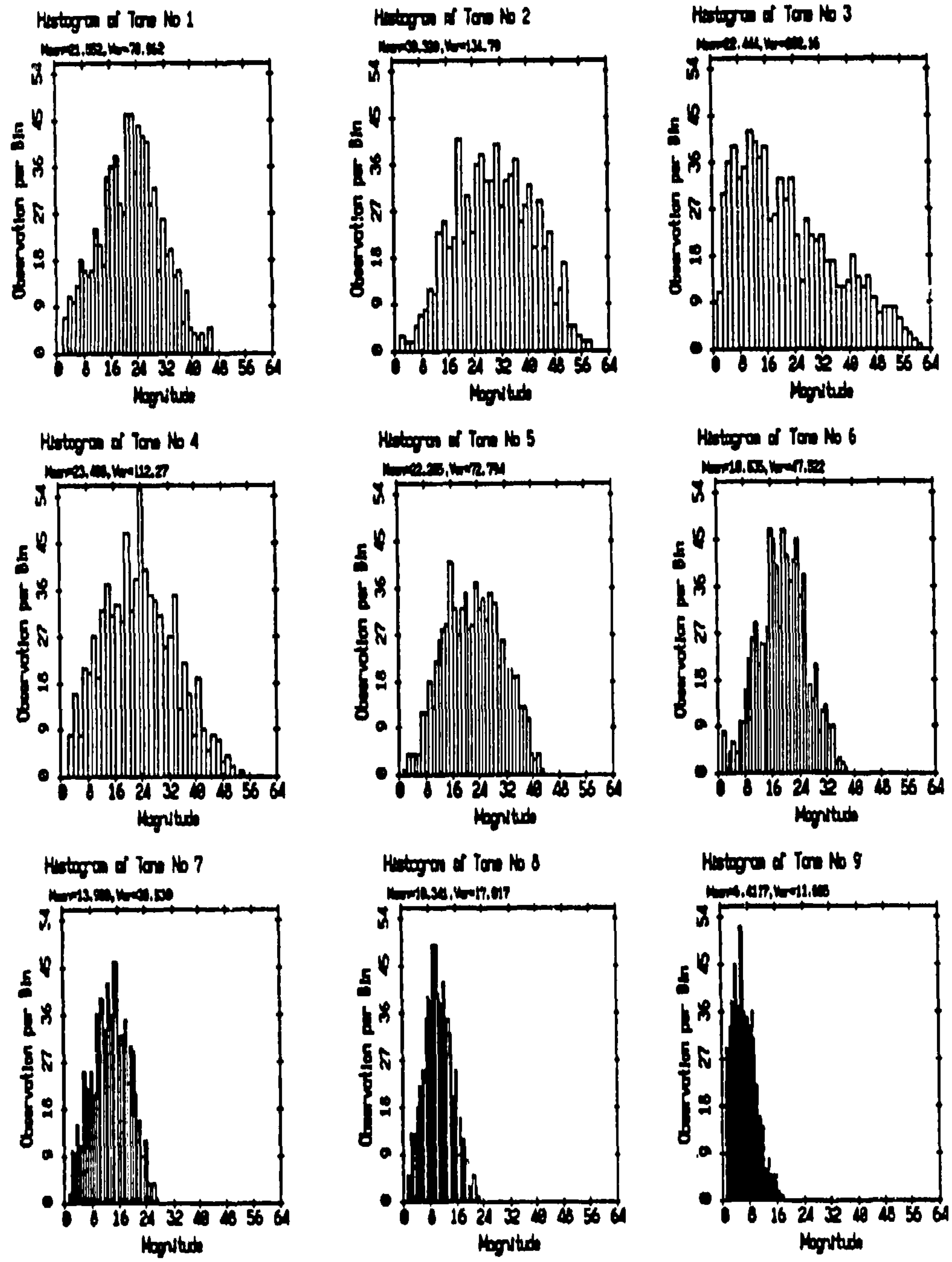

Figure 3.71. Histograms of the envelopes of the 1 kHz spaced tones received by sonobuoy No 2.

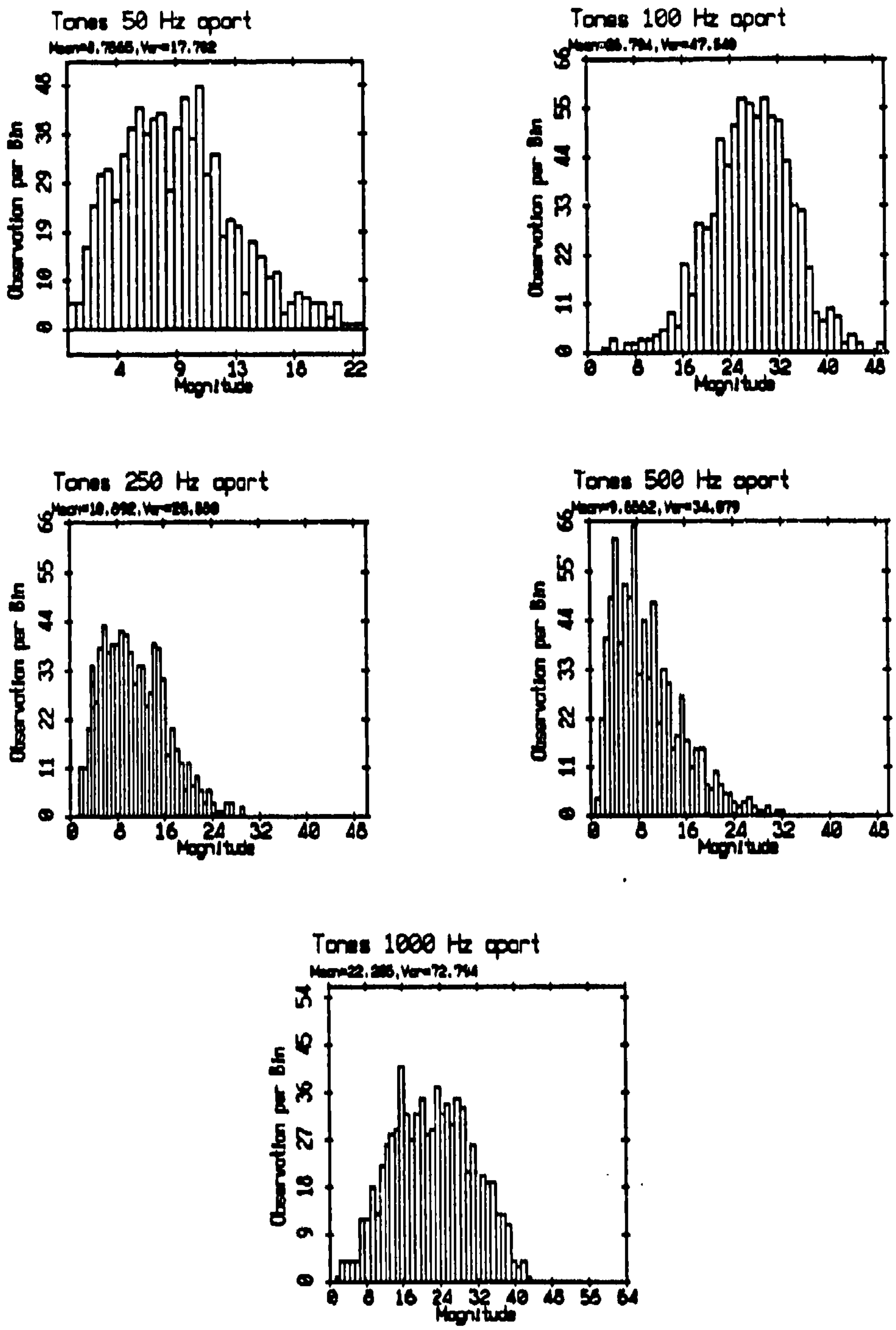

Figure 3.72. The histograms of the 15 kHz tone, at different time periods received by sonobuoy No 2.

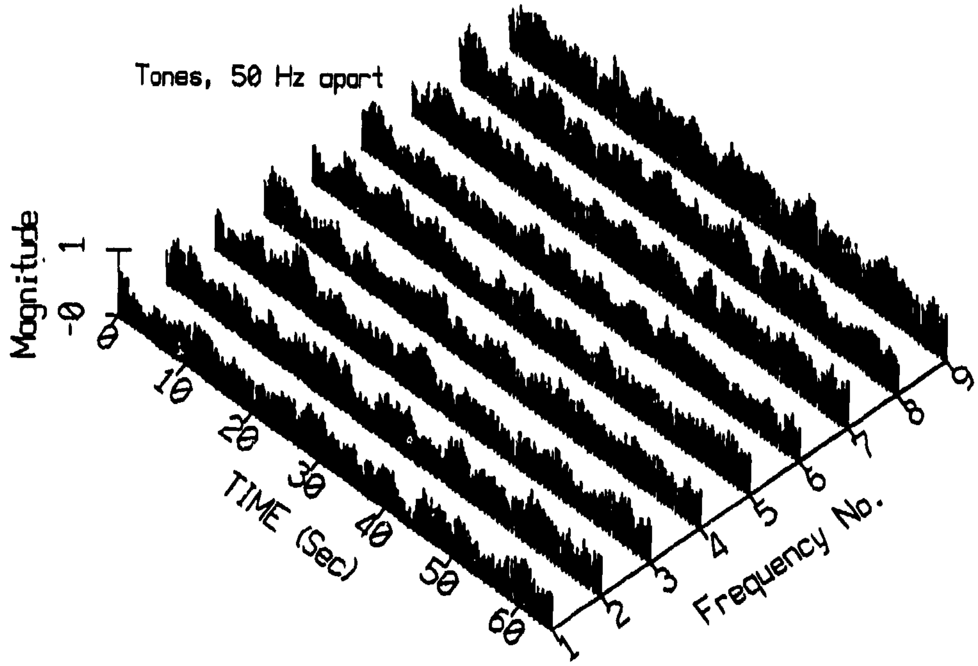

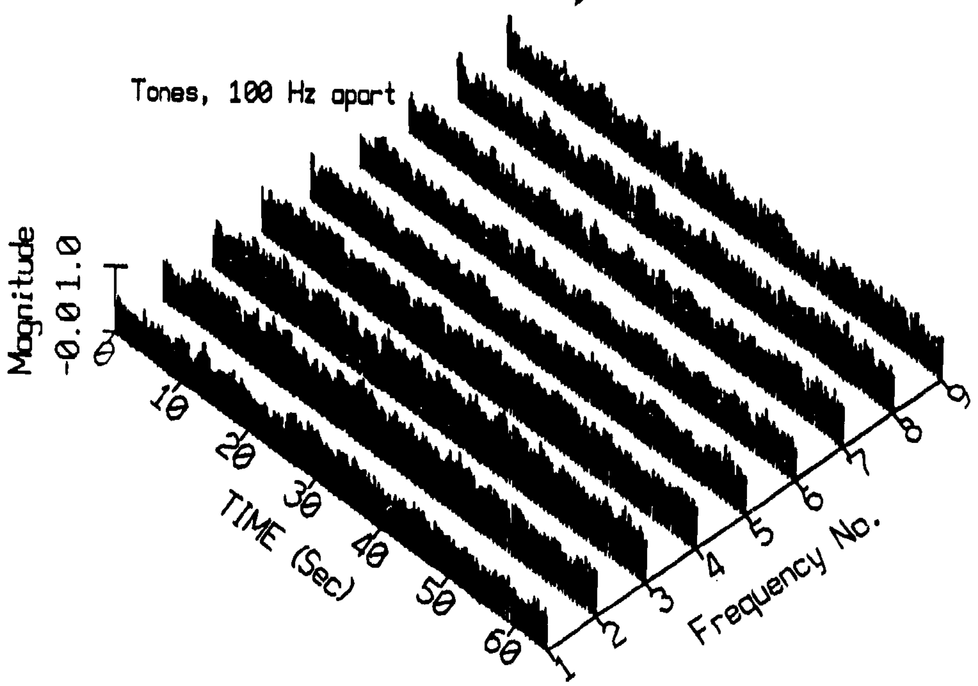

Figure 3.73. Amplitude variation of nine tones received by sonobuoy No 4, 50 and 100 Hz apart.

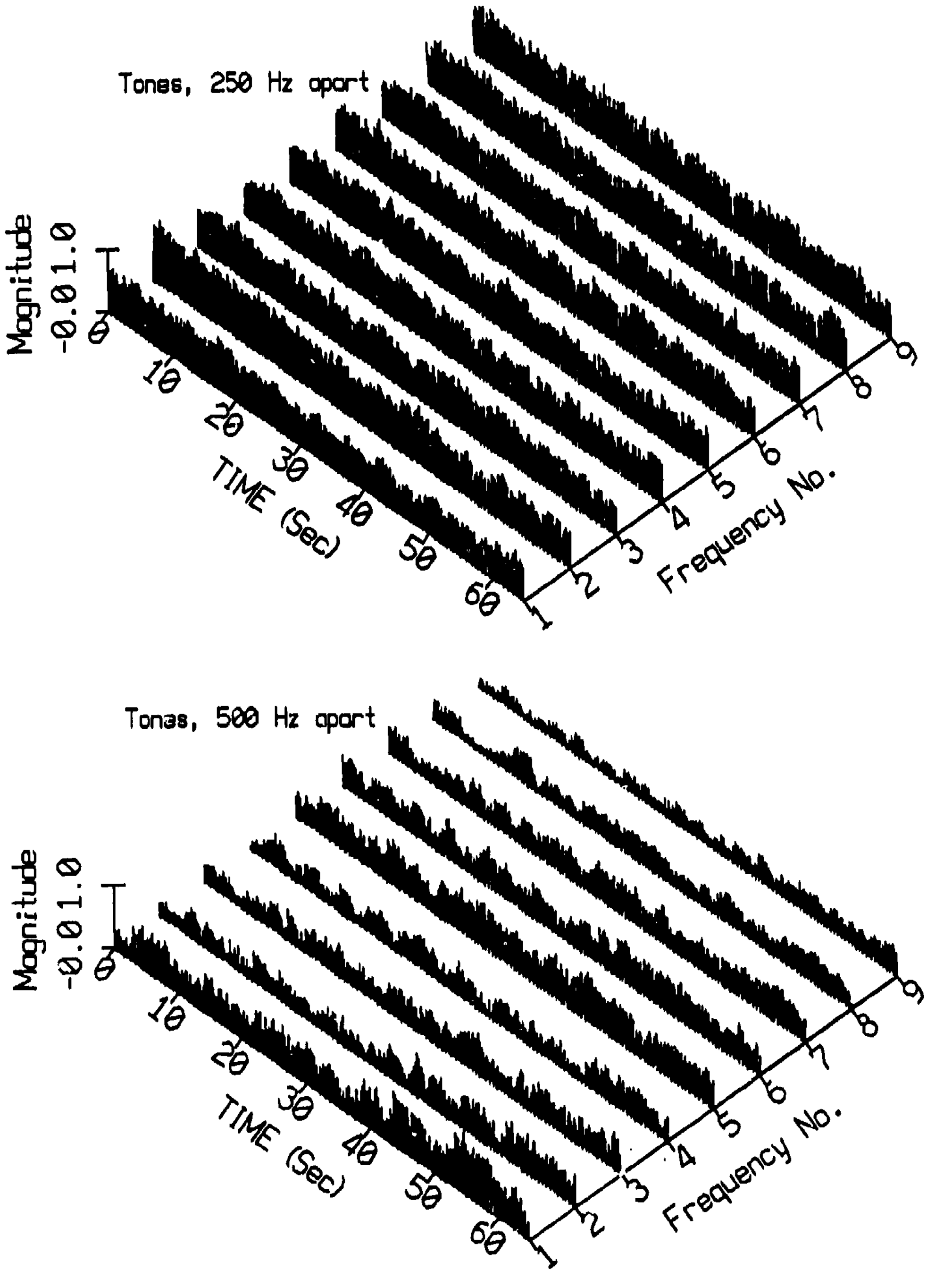

Figure 3.74. Amplitude variation of nine tones received by sonobuoy No 4, 250 and 500 Hz apart.

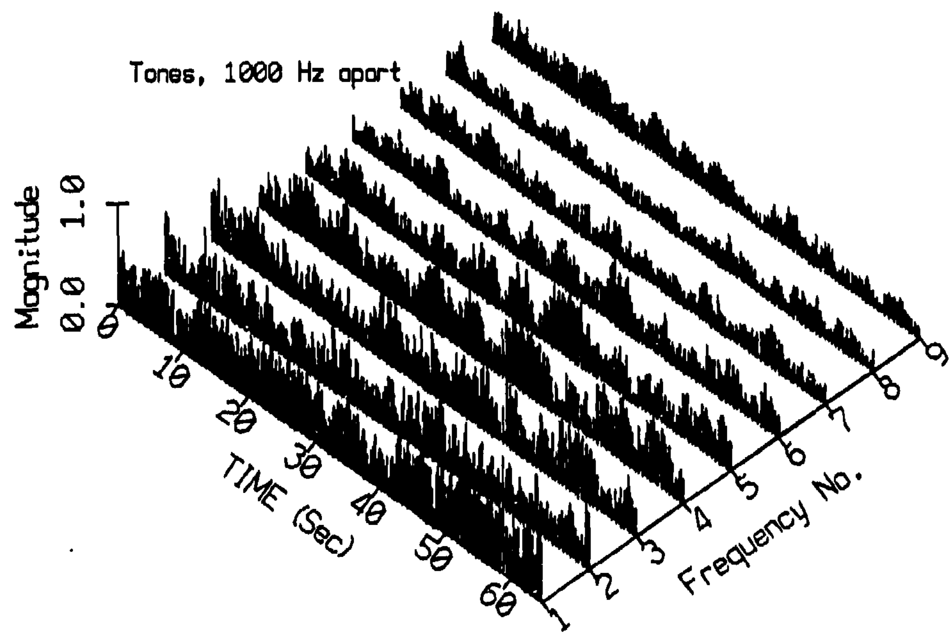

Figure 3.75. Amplitude variation of nine tones received by sonobuoy No 4, 1kHz apart.

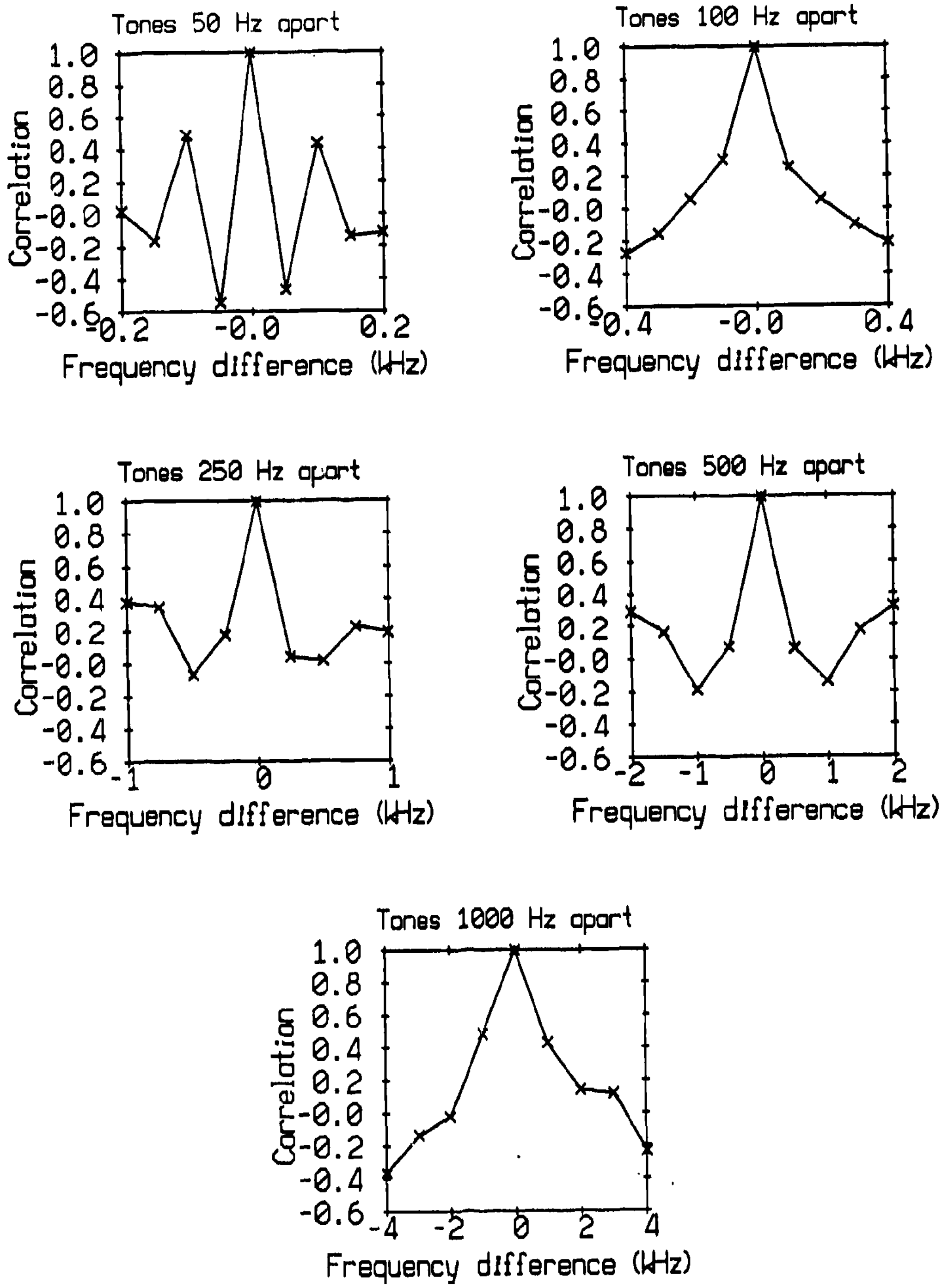

Figure 3.76. The correlation between the envelope of nine tones received by sonobuoy No 4 and the central tone for the five sets of tones.

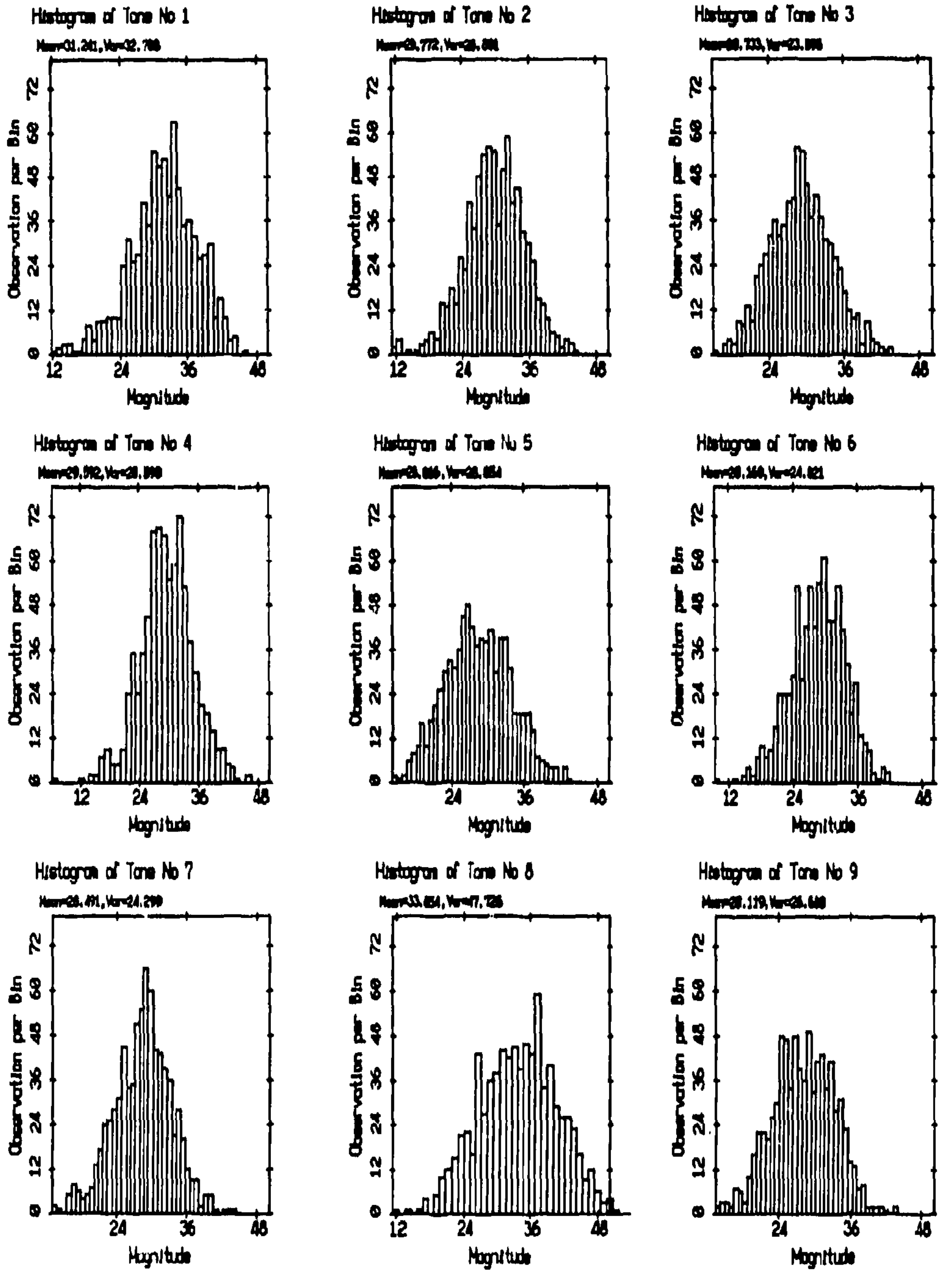

Figure 3.77. Histograms of the envelopes of the 250 Hz spaced tones, received by sonobuoy No 4.

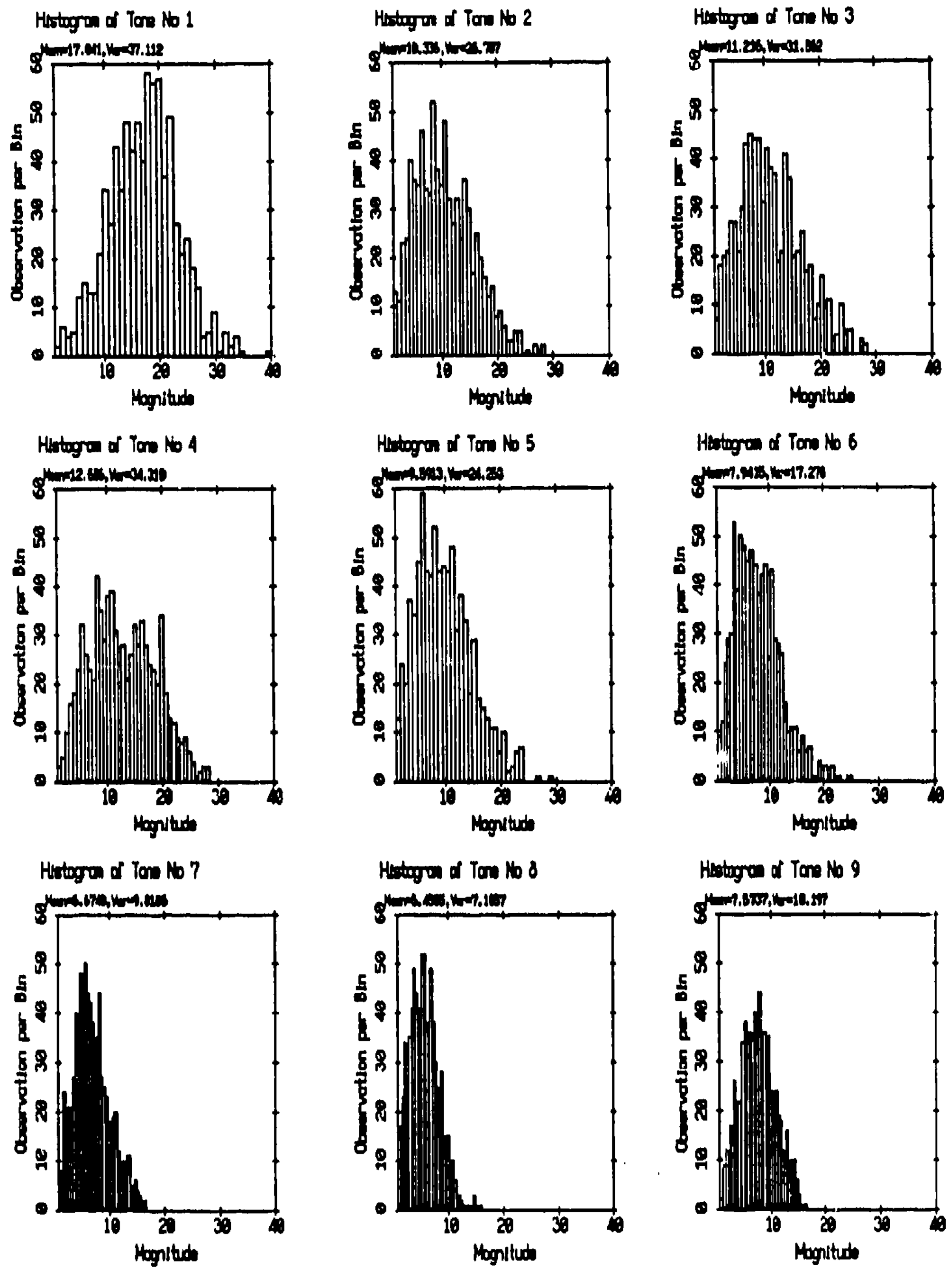

Figure 3.78. Histograms of the envelopes of the 1 kHz spaced tones received by sonobuoy No 4.

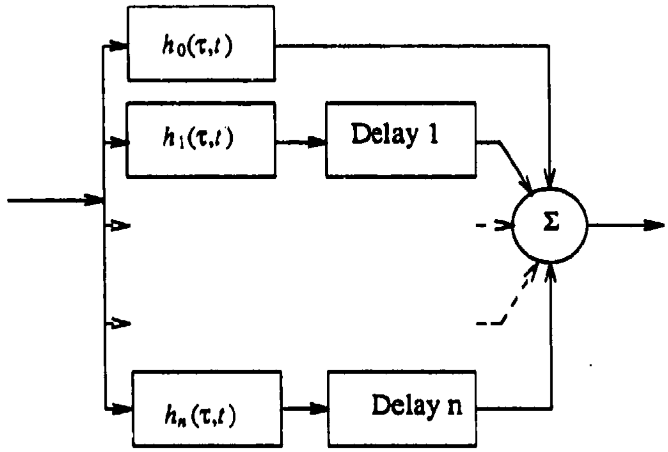

Figure 3.79. A simplified model of an underwater acoustic communication channel.

IV Real data analysis

A stream of pseudo randomly selected ones and zeros was differentially modulated by a chirp signal and transmitted as a part of the experiments. A receiver implemented in software processed the data. Figure 4.1 shows a block diagram of the receiver.

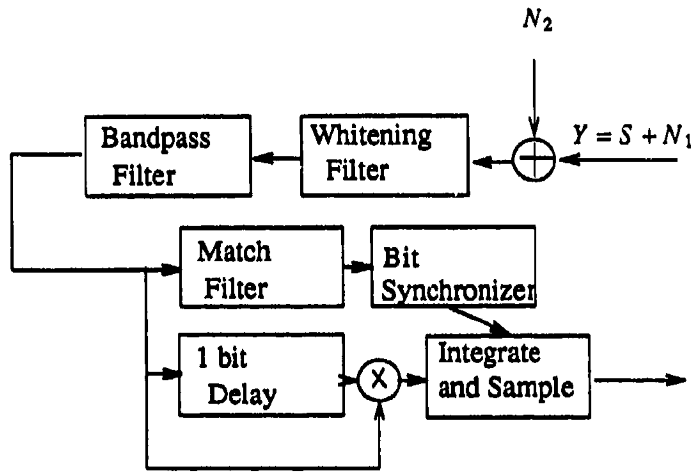

Figure 4.1. Implemented DPSK receiver - block diagram.

The ocean ambient noise is not white and has a power spectrum shown in Figure 4.2.

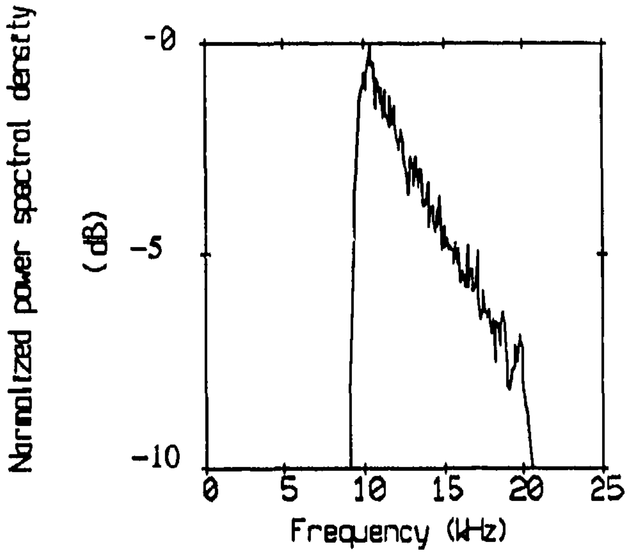

Figure 4.2. Power spectral density of the ambient noise (after bandpassing)

It can be approximated roughly as a single pole AR process. Therefore, the whitening filter was implemnted as a simple derivative. The received signal-to-noise ratio ($\overline{\gamma}_b$) was quite high (20 dB). In order to analyze the performance of the system, at several values of signal-to-noise ratio ambient noise (N_2 measured at different time interval which was clean from any signal) was added artificially to the received signal (Y).

A stream of 6×10^6 bits was analaysed. The achieved bit error and the theoretical bit error rate for DPSK modulation in the presence of AWGN are presented in Figure 4.3.

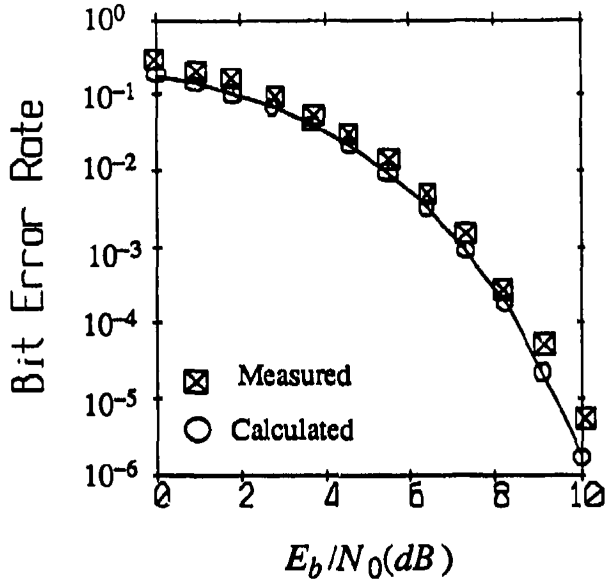

Figure 4.3. Comparison between theoretical and achieved bit error rate.

As shown in Figures 3.55 and 3.57, the first multipath is much stronger than the direct signal and the other multipath signals. Therefore, the bit synchronizer was locked onto the first multipath. Since the first multipath was so large relative to the other signals, in the range of bit error rate that was analyzed, the absence of the equalizer did not affect the achieved results.

Acknowledgements

This work was supported by the Naval Research Laboratory under contract N00014-88-K-2040.

References

1. Churgin, J. and S. J. Halminski, *Temperature, Salinity, Oxygen, and Phosphate in Waters off the United States*, 3, National Oceanographic Data Center, 1974.

2. Dotan, A. and W.S. Hodgkiss, "Coherence of transients," *MPL TM-422*, San-Diego, July 1990.

3. Lord, G. E. and T. D. Plemons, "Characterization and Simulation of Underwater Acoustic Signals Reflected from the Sea Surface," *J. Acoust. Soc. Am.*, vol. 63(2), pp. 378-384, Feb 1978.

4. Mackenzie, K. V., "Nine term equation for sound speed in the oceans," *J. Acoust. Soc. Am.*, vol. 70(3), 1981.

5. Urkowitz, H., *Signal theory and random processes*, p. 331, Artech House, 1983.